THE ADSORPTION OF NITROGEN AND ARGON

BY

EVAPORATED FILMS OF SODIUM CHLORIDE

A thesis submitted to

THE UNIVERSITY OF CAPE TOWN

in fulfilment of the requirements for the degree of

MASTER OF SCIENCE.

by

ALLEN L RODGERS B.Sc.(HONS.)

Department of Chemistry,
University of Cape Town,
Rondebosch, Cape,
South Africa.

October 1969.

A C K N O W L E D G M E N T S.

The author would like to express his sincere and grateful thanks to Dr. P.W. Linder, M.Sc. (Natal), Ph.d. (Cantab.), Senior Lecturer in the Department of Chemistry, University of Cape Town for his invaluable guidance, assistance and encouragement which was enthusiastically given throughout the period of the research and during the writing of this thesis.

The author is also indebted to Mr. S.G. Harris for the glassblowing, which was of a very high standard, and for his assistance in other technical aspects of the work.

Thanks are also due to Dr. A. Granville of the National Institute for Metallurgy for his advice concerning the evaporation procedure and to Mr. C. Firer for his general assistance and advice.

Finally, the author would like to thank his parents for their support and encouragement at all times.

SUMMARY.

An ultra-high vacuum apparatus has been designed and constructed. Pressures of the order of 1×10^{-8} torr have been attained routinely. The adsorption of nitrogen by Pyrex has been investigated and the results obtained have shown good agreement with those in the literature. Rigorously cleaned evaporated films of sodium chloride have been prepared and the adsorption of nitrogen and argon by them has been investigated. Isosteric heats and entropies of adsorption have been determined and theoretical entropies calculated. The appearance of a group of sites of uniform activity, hitherto unavailable owing to contamination of the surface, is postulated. The adsorption of nitrogen and argon has been found to be reasonably well represented by the immobile, localized model with indications of the adsorbed argon molecules occupying a different set of sites from the adsorbed nitrogen.

Two novel methods for the preparation of evaporated films of alkali halides are suggested.

TABLE OF FIGURES.

CHAPTER I.

INTRODUCTION

I.1. ELEMENTARY MODEL OF THE ADSORPTION OF A GAS BY A SOLID[1-4]

When a solid surface is in contact with a gas an interaction occurs which causes the concentration of the gas molecules to be greater in the immediate vicinity of the surface than in the gas phase. The process by which this surface excess concentration is formed is called adsorption. It is a dynamic process: gas molecules continuously strike the surface and either rebound specularly or remain on the surface for a finite time after which they leave in a direction and with a velocity which are independent of the direction and velocity of approach. The rate of collision with the surface depends upon the temperature, the pressure and the molar mass of the gas.

The fraction of the incident molecules which condense on the bare part of the surface is called the condensation coefficient α^*, (for meanings of symbols see Appendix 5) and it is a property of the surface and gas combined. The length of time any given molecule remains on the surface is called the residence time, τ. Equilibrium is attained when the rates of adsorption and desorption are equal.

Adsorption of a gas on a solid is a spontaneous process and is therefore accompanied by a decrease in the free energy of the system. The gas loses degrees of freedom in passing from the gas phase to the adsorbed state and thus there is also a decrease in entropy. It follows from the thermo-

(a) The heat of physical adsorption is of the same order of magnitude as the heat of liquefaction of the adsorbate whereas heats of chemisorption usually have values in the range of heats of ordinary chemical reactions.

(b) Desorption of adsorbate from a physically adsorbed layer can usually be accomplished under relatively mild conditions whereas desorption of chemisorbed species generally requires severe treatment such as application of high temperatures or positive ion bombardment.

(c) In physical adsorption the adsorption can, under appropriate conditions, proceed further than the formation of a monolayer and adsorbed layers several molecular diameters thick can be formed. The values of α^*, τ and Q (equation I.2.) for the second and higher molecular layers differ substantially from those for the first layer. In chemisorption the process is always restricted to monomolecular layers.

An ideal simple uniform surface consists of a number of adsorption sites all having the same potential energy and arranged in a regular pattern. The surface is still homogeneous, by definition, when the sites have different potential energies provided the potential energies occur in a regular pattern. If, however, the sites of different potential energies occur in a random fashion we have a heterogeneous surface.

When the molecules or molecular fragments are adsorbed and desorbed from specific sites corresponding to positions of minimum potential energy on the surface, we have localized adsorption. This can occur on both heterogeneous and homogeneous surfaces.

In contrast, non-localized adsorption occurs when the molecules are stable at all points on the surface and there are no favoured positions. The surface is not necessarily energetically uniform - there may indeed be regions of different energies - but the adsorbate molecules are not limited to specific points of attachment.

The surface of a solid is a two dimensional array of atoms that causes maxima and minima in the interaction energy as a molecule moves along the surface. If the activation energy to move from site to site is less than that required for desorption it is possible for a molecule to move laterally within the two dimensional phase while remaining in the adsorbed state. This is mobile adsorption, see Fig. I.1.(a). When the adsorbed molecule acquires sufficient thermal energy relative to χ it will translate freely inside the shaded area - that is the energetically continuous two dimensional phase. On the other hand, with non-mobile films the activation energy for surface diffusion exceeds the desorption energy, see Fig. I.1.(b). Thus molecules do not leave their adsorbed positions until returning to the gas phase.

The potential energy relation between P_e and χ thus determines whether the adsorbed film is mobile or immobile. These energies are characteristic of the adsorbate-adsorbent system.

Fig. I-1

I.2. PHYSICAL ADSORPTION FORCES[1]

If the interaction between an atom or molecule and a solid surface involves no transfer or sharing of electrons and the individuality of the interacting species is thereby maintained the forces are said to be of the physical or van der Waals type. The net interaction between an atom or molecule and a solid surface arises from the attractive van der Waals forces and the repulsive forces which occur when atoms come close enough for their electron clouds to overlap significantly. The attractive forces fall into several categories depending upon whether the adsorbate or solid surface possesses a permanent electric moment or not. If the adsorbed species has no permanent dipole or multipole moment then the attractive interaction with a non-polar surface is due to dispersion forces only. Additional attractive forces arise when both the adsorbate and the solid surface are polar owing to electrostatic interactions. When a non-polar adsorbate interacts with a polar surface or a polar adsorbate with a non-polar surface, contributions to the attractive energy arise from interactions between the permanent field of the polar solid and induced electric moments (usually dipole) in the adsorbate or from interactions between the permanent electric moments of the adsorbate and charge distributions induced in the adsorbent. With ionic crystals the high polarizing power of the electric field on the surface serves to enhance the electrostatic contributions to the attractive forces.

The work in this thesis deals mainly with the adsorption of nitrogen and argon on sodium chloride. Some preliminary work was also done on the adsorption of nitrogen

by glass in order to check experimental techniques. The appropriate forces involved in these examples are now discussed in further detail.

Dispersion Forces.[5]

Dispersion or London forces originate through the fact that in molecules and atoms of all kinds, the positively charged nuclei and the negatively charged electrons must be regarded as undergoing some kind of oscillations with respect to each other; as a result of this displacement of positive and negative charges every molecule behaves as an oscillating dipole. The electrostatic interaction between these dipoles and corresponding dipoles induced in adjacent molecules causes molecular attraction. These attractive forces, due to the oscillating dipole interactions are called dispersion forces.

The dispersion energy is given by

$$E_D = \frac{C'}{r'^6} \qquad \text{I.3.}$$

An expression for C' which has been used in calculations of interactions of molecules with solid surfaces is the Kirkwood-Müller[6] equation,

$$C' = 6\, m'.c^2 \,.\, \frac{\alpha'_1 \cdot \alpha'_2}{\left(\frac{\alpha'_1}{x_1}\right) + \left(\frac{\alpha'_2}{x_2}\right)} \qquad \text{I.4.}$$

Repulsive Forces.

The repulsive energies at close seperations between pairs of inert gas atoms can be calculated from the equation[1],

$$E_R = B' . e^{(-ar')} . \qquad \text{I.5.}$$

(For alkali halides $a = 2{\cdot}90\text{Å}^{-1}$).

Mason and Rice[7] suggest that the potential parameters, a and B' in equation I.5., between a pair of unlike molecules 1 and 2 can be calculated from the equations,

$$a_{12} = \tfrac{1}{2}(a_{11} + a_{22}) \qquad \text{I.6.}$$

$$B'_{12} = (B'_{11} \; B'_{22})^{\frac{1}{2}} \qquad \text{I.7.}$$

Forces between non-polar molecules and ionic crystals.[1]

If a non-polar molecule is in the neighbourhood of an ionic crystal it experiences an attractive force due to the dipole induced in the molecule by the electrostatic field of the crystal in addition to dispersion and repulsive forces. The induced attractive potential, E_i, is given by the expression,

$$E_i = -\tfrac{1}{2}\alpha' F_e^{\,2} . \qquad \text{I.8.}$$

The equation holds if F_e does not change rapidly over the volume occupied by the molecule. This is seldom the case and it is necessary therefore to perform an integration over the volume V of the molecules assuming some charge distribution. The induced attractive potential is then given by the expression,

$$E_i = \int \frac{E - E_c}{J} . \rho . \, dV \qquad \text{I.9.}$$

Forces between molecular quadrupoles and the field gradients adjacent to ionic or polar surfaces.

There is yet another interaction energy which must be taken into account known as the quadrupole interaction energy.[8]

Just as the dipole moment of a polar molecule may be regarded as being composed of two centres of charge, one positive and the other negative, seperated by a definite distance within the molecule, so a quadrupole may be pictured as arising from the seperation of equal and opposite dipoles, eg. $\overset{-}{O} - \overset{++}{C} - \overset{-}{O}$. The magnitude of the quadrupole moment is proportional to the product of the dipole moment and the seperation between the charges of either dipole. For a "linear" molecule, i.e. with an axis of symmetry, Drain[9] used the following expression for the quadrupole moment η which is due to Greenhow and Smith[10]:

$$\eta = \tfrac{1}{2} \int \rho\,(r^*,\theta^*)\,(3\cos^2\theta^* - 1)\,r^{*2}.dr \qquad \text{I.10.}$$

The net energy of interaction between a linear quadrupole and a uniform electric field is zero because the effects of the two oppositely oriented component dipoles balance each other exactly. With a non homogeneous field, however, the field strength in general varies over the entire length of the molecule and the component interactions of the constituent dipoles therefore have different energies. Thus quadrupole interactions arise only in non homogeneous fields. The interaction energy energy E_Q of a quadrupole with an unhomogeneous field is given by[9]

$$E_Q = \tfrac{1}{2}\,\eta\,\frac{\partial^2 E_L}{\partial W^2} \qquad \text{I.11.}$$

Although the electric field at a particular point within the quadrupole may actually be zero the field gradient is such that the quadrupole interaction is finite.

I.3. PREVIOUS WORK ON THE INTERACTION OF NON-POLAR MOLECULES WITH IONIC CRYSTALS.

The heat of adsorption may be calculated from the dispersion energy (equations I.3 and I.4), the repulsive energy (equations I.5, I.6 and I.7), the induced attractive potential energy (equations I.8 and I.9) and the quadrupole interaction energy (equation I.11). Many workers, cited by Young and Crowell[1] have compared calculated heats of adsorption with experimentally determined values.

Lenel[11] calculated the dispersion and induced dipole interaction energies for the following systems: argon with potassium chloride, potassium iodide, lithium fluoride and caesium chloride; krypton with potassium chloride; carbon dioxide with potassium chloride and potassium iodide. For carbon dioxide he included effects due to the quadrupole moment. Lenel's calculated heats showed good agreement with his own experimental values the biggest discrepancy being $0{\cdot}42$ k.cal mole^{-1}.

Orr[12,13] calculated dispersion, electrostatic interaction and repulsive (with a = $2{\cdot}9$Å^{-1}) energies for the adsorption of argon, nitrogen and oxygen by potassium chloride and caesium iodide. He found good agreement between calculated and observed heats except for the case of argon on caesium iodide where the calculated value was found to be higher than the experimental heat by about $0{\cdot}6$ k.cal mole^{-1}. This experimental value was confirmed by Tompkins and Young[14] who concluded that the discrepancy was due to the fact that the caesium iodide was exposing a different crystal face (110) to Orr's model (100). This variation in surface properties with crystal face is called the 'crystal face' effect. Alkali halide crystals

are ideal for studies of this effect. Young[15] found that the interaction of an argon atom with the (111) planes of potassium chloride exceeds the interaction with the (100) planes. This he attributed to the lower density of ions on the (111) face allowing the argon atoms to penetrate more deeply into this face. Young regarded the difference between the calculated and experimental heats of adsorption as a measure of surface heterogeneity. This difference was found to be 0·3 kcal.mole^{-1} for both the (111) and (100) faces of potassium chloride and thus Young concluded that the octahedral and cubic crystals were of comparable uniformity.

Hayakawa[16-20] has done a tremendous amount of work on the interaction of non-polar gases with alkali halides. The systems he has investigated are the adsorption of argon, oxygen, nitrogen and carbon dioxide on crystals of sodium chloride[16], cubic potassium chloride[17], potassium bromide[18] and octahedral potassium chloride[19]. In the calculation of heats of adsorption corrections were made for hindered rotation. Experimental values of the initial heats of adsorption were determined by extrapolating the heat curves to zero coverage. The differences between these and the corresponding calculated values were regarded as a qualitative measure of the surface heterogeneity. Since the differences were greater for the (111) face of octahedral potassium chloride than for the (100) faces of cubic potassium chloride, he concluded that the octahedral surfaces were less perfect. On the whole, good agreement was obtained between the calculated and experimental values for argon but less satisfactory results were obtained for nitrogen and carbon dioxide. The larger discrepancies in the latter cases were due, according to Hayakawa, to inadequate

knowledge of the quadrupole moments of nitrogen and carbon dioxide and to the approximate nature of the calculations of the effects of hindered rotation of these molecules.

Hayakawa[20] points out that there are two types of surface heterogeneity. The first is due to the distribution of different sites on the crystal surface eg. on the (100) plane of an alkali halide crystal there are the following sites:

(i) the centre of a lattice cell;
(ii) the mid point of a lattice edge;
(iii) an alkali ion and
(iv) a halogen ion.

The second is due to lattice imperfections. The maximum difference between calculated heats for the different sites was regarded as a qualitative measure of the surface heterogeneity due to the first factor.

The difference between the experimentally determined initial heats and the heats associated with the strongest of the calculated interactions were taken as a crude measure of the surface heterogeneity of the other type. For sodium chloride and potassium bromide the heterogeneity was found to be due to the distribution of sites. For cubic potassium chloride, argon gave the same result, but nitrogen and carbon dioxide gave results indicating that the heterogeneity was due to lattice imperfections. It was also found that the heterogeneity due to lattice imperfections was greater for the octahedral than for the cubic crystals.

Both types of surface heterogeneity give rise to a decrease in the heat of adsorption with increasing coverage in the low coverage region. Hayakawa found that with

increasing coverage the isosteric heats of adsorption for argon, oxygen and nitrogen on cubic sodium chloride, cubic potassium chloride and cubic potassium bromide fell initially, rose to a maximum and then fell steadily to the value of the latent heat of vaporization or sublimation of the adsorbate. For carbon dioxide the heat fell initially and then began to rise but did not reach a maximum. For octahedral potassium chloride the isosteric heats fell linearly at low coverage and after two abrupt changes of slope fell gradually to the value of the latent heat of sublimation or evaporation of the adsorbate. For carbon dioxide, the heats decreased steadily. The initial decrease in the heat of adsorption in all cases was attributed to the non uniformity of the surface. In the cases where adsorption maxima occurred in the subsequent regions of the heat curves, the increasing heats were interpreted as arising from mutual attractive forces between adsorbed molecules. Adsorption on octahedral potassium chloride is complicated by the fact that two faces, both (111), predominate on the crystals, namely, one composed entirely of chloride ions and the other potassium ions. Moreover, because the crystal habit was modified by adding lead chloride, the potassium faces are somewhat contaminated by lead ions. The presence of this impurity results in an increase in the heat of adsorption on the potassium ion faces. Adsorption at low coverage proceeds exclusively on the chloride faces and when these faces are almost covered, adsorption also occurs on the potassium ion faces. Thus the range of surface heterogeneity is greatly extended on this type of crystal thereby masking the effect of mutual interactions between adsorbed molecules.

Granville and Hall investigated the adsorption of nitric oxide on an evaporated film of cubic potassium chloride[22]

and the adsorption of krypton and nitric oxide on evaporated films of lithium chloride, sodium chloride, potassium chloride and caesium iodide[23]. Nitric oxide was chosen since its quadrupole moment is almost the same as that of nitrogen. This was of great interest since Hayakawa[17] had postulated that the higher heats of adsorption obtained with nitrogen on sodium and potassium chloride as compared with argon and oxygen were due to the quadrupole interaction with the surface. Their aim was to determine whether the contribution of the quadrupole interaction of nitric oxide was also significant or not.

Granville and Hall calculated the heats of adsorption for nitric oxide and krypton by the following approximate method. A form of the repulsive interaction energy which is somewhat simpler than equation I.5. is the formula[1]

$$E_R = B'(r')^{-u} \qquad \text{I.12.}$$

Combination of equations I.3. and I.12. gives the expression,

$$E_s = \frac{B'}{(r')^u} - \frac{C'}{(r')^6}. \qquad \text{I.13.}$$

A value of 9 is assigned to u for the interaction of two identical simple molecules[24] eg. the interaction of one nitrogen molecule with another. If the values of the constants in equation I.13. are known, the equilibrium seperation energy, E_s, for any pair of like interacting molecules may be calculated. Now, the molecules of different substances will experience interactions of different magnitudes with a given surface. Granville and Hall[22,23] suggest that the ratio of the interaction energies is in the same ratio as the seperation

energies of the different molecules. For example, the value of E_s for argon[24] is 1.46×10^{-14} ergs. Suppose the value for another molecule B is $(E_s)_B$. The interaction energy of the species B with a given surface is then given by

$$Q_B = \frac{(E_s)_B}{1.46 \times 10^{-14}} \times Q_{argon} \qquad \text{I.14.}$$

where Q_{argon} refers to the heat of adsorption of argon with the same surface. This method of estimating the heat of adsorption does not include the contribution of the quadrupole interaction. Granville and Hall used equation I.14. to calculate the heats of adsorption for nitric oxide and for krypton on several of the adsorbents mentioned above. The values of E_s for these two gases were obtained from Moelwyn-Hughes[24] while the heats of adsorption of argon used were those calculated by Hayakawa for the various adsorbents. Isosteric heats of adsorption were determined experimentally and the value at the lowest coverage considered (not extrapolated) was taken as the initial heat of adsorption. These values were compared with the calculated heats. With both gases on the (100) face of potassium chloride and also with krypton on lithium fluoride good agreement was found. Heats for the two caesium chloride films prepared agreed with heats calculated for the (110) face of caesium chloride but not the (100) face. However, the calculated heats for both krypton and nitric oxide on the (100) face of sodium chloride were found to be about 1.0 kcal.mole^{-1} lower than the experimental values. Since the ratios of the experimental heats $\frac{Q(NO)}{Q(Kr)}$ for all the films, with the exception of lithium chloride (which was high), were all in good agreement with the ratio, 1.38, of the

equilibrium seperation energies[24] of nitric oxide and krypton, the discrepancy between the observed and calculated heats for sodium chloride could not have been due to the potential method being invalid. Granville and Hall concluded that it was probably due to the fact that that the sodium chloride was exposing some crystalline face other than (100). Shulz[25] has observed the predominance of the (110) plane in evaporated films of sodium chloride.

Granville and Hall attributed the small differences between experimental and calculated heats for nitric oxide on cubic potassium chloride, lithium chloride and sodium chloride to surface heterogeneity arising from both surface imperfections and the presence of different crystal faces. They reached this conclusion since the magnitude of the differences were of the same order as those found by the Hayakawa[19] who attributed the discrepancies to heterogeneity effects. Thus Granville and Hall concluded that since the differences could be explained, the contribution of the quadrupole interaction of nitric oxide which had not been included in the calculated heats, had no significant effect. However, the high ratio of experimental heats obtained for lithium chloride indicated that the quadrupole effect may be important possibly because of the small size of the lithium ion.

The heat curves for the two caesium chloride films showed a sharp increase at values of the coverage $\theta = 0{\cdot}50$. This effect was also reported by Orr[13] for argon adsorbed on the (100) face of potassium chloride and by Hayakawa[16, 17] for argon, oxygen and nitrogen. Dube[26] has associated an increase in heat of adsorption with completion of the monolayer and thus Granville and Hall have interpreted their results

on caesium chloride as indicating completion of the monolayer.

The heat curves of nitric oxide on the lithium, sodium and potassium chloride films showed a gradual decrease in the heat of adsorption with increasing coverage. This as has been mentioned was also found by Hayakawa[19] with argon on octahedral potassium chloride powder. This type of variation of heat with coverage occurs when the effect of surface heterogeneity completely overshadows the effect of lateral interactions.

I.4. THERMODYNAMICS OF ADSORPTION

Young and Crowell[1] cite workers who have emphasized the importance of determining the thermodynamic properties of adsorbed layers in order that effectual comparisons between experimental situations and physical models may be made. The practice of comparing a single isotherm with the predictions of a model is nearly worthless, since it has been shown that there are usually several models, which, with the appropriate choice of a few parameters, can give an isotherm of a particular shape at one temperature. It is therefore important to obtain isotherms at several temperatures from which comparisons can be made with various models through the thermodynamic functions. This enables a much more intimate experimental test of adsorption theories to be made.

The Adsorption Isotherm.

Experimental measurements of the amount of gas adsorbed, N, as a function of the pressure and temperature may be conveniently represented by adsorption isotherms, $N = f(P)_T$, the form of which can yield qualitative information about the adsorption process.

Brunauer et al[27] have classified the isotherms that are obtained for systems at temperatures below the critical temperature of the gas. There are five basic isotherm shapes shown in Fig.I.2. Type I are associated with systems where adsorption does not proceed beyond a unimolecular layer. The other four types represent multilayer adsorption, types IV and V being characteristic of highly porous adsorbents. A very large number of theoretical isotherms $N = f(P)_T$ have been proposed to explain the various types of experimental result.[1]

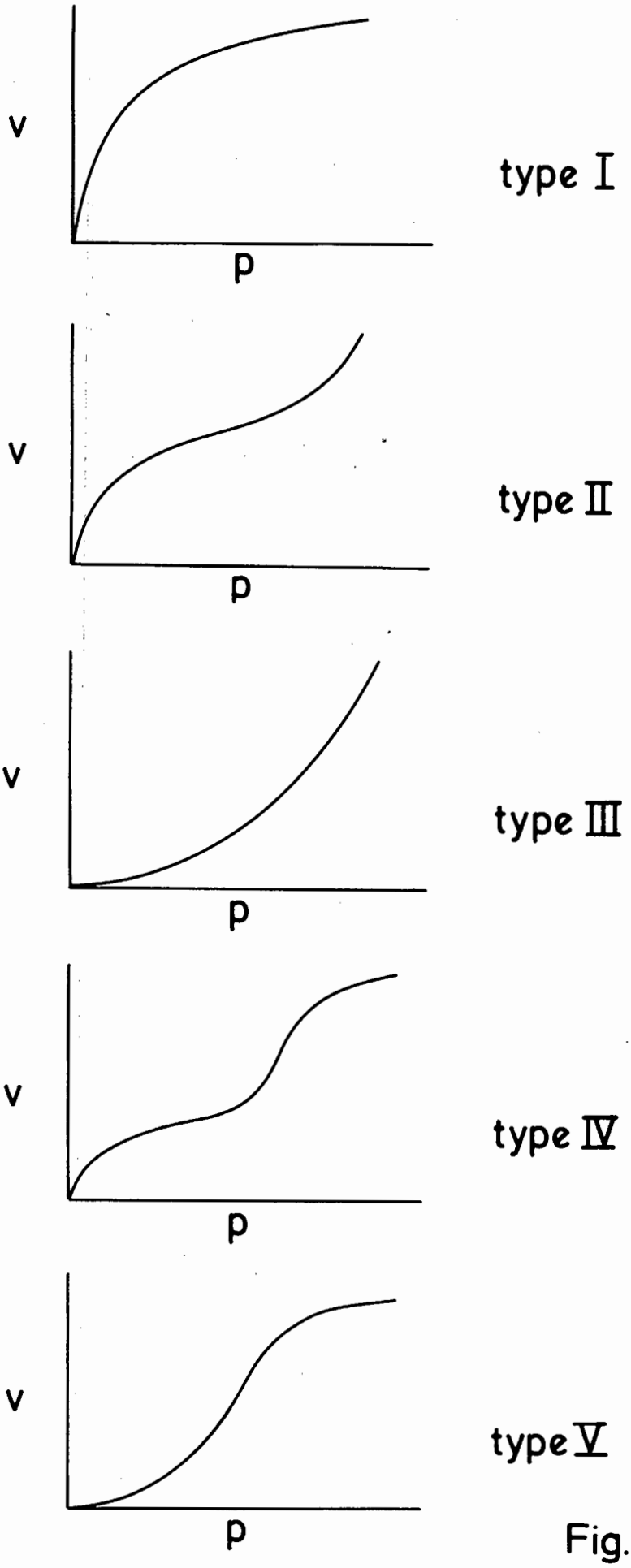

Fig. I-2

The isosteric heat of adsorption varies with the degree of surface coverage. Plots of Q against N are called heat curves and are useful in determining the thermodynamic functions of the system, in characterizing the nature of the adsorbent surface and in indicating the degree of lateral interaction of adsorbed molecules. The application of the heat curves in the latter two cases has been illustrated in section I.3.

Entropy of Adsorption.[28]

If information regarding the movement and arrangement of adsorbed molecules is required, a knowledge of the entropy change, ΔS, is necessary.

Consider the transfer of one mole of an ideal gas from a standard state of one atmosphere and temperature T to an adsorbed state. The free energy change is given by the expression,

$$\Delta G = RT \ell n \frac{P}{1} = RT \ell n P. \qquad \text{I.16.}$$

Provided that ΔS and Q are independent of the temperature we have from equation I.1. that

$$\Delta S = - \frac{d(\Delta G)}{dT} \qquad \text{I.17.}$$

By applying equation I.16 it is possible to determine ΔG for a fixed coverage at several temperatures and hence ΔS (equation I.17.). In particular if isotherms are available at two neighbouring temperatures T_1 and T_2, it follows that ΔS at a particular coverage, θ, may be evaluated from the following

expression,

$$\Delta S_\theta = R \frac{T_1(\ell n\ P_1)_\theta - T_2(\ell n\ P_2)_\theta}{T_2 - T_1} . \qquad \text{I.18.}$$

Thus, both the isosteric heat of adsorption and the differential entropy can be found directly from isosteric plots of log P against $\frac{1}{T}$ (equations I.15. and I.18.).

To derive useful information from experimental results a comparison must be made with theoretical values of the entropy change.

Theoretical Calculation of Entropy.

The entropy of a polyatomic molecule is expressed as the sum of four separable contributions arising respectively from translation, rotation, internal vibration and electronic configuration.

(i) Mobile non-localized adsorption.

For a mobile non-localized ideal two dimensional gas in the adsorbed state the translational entropy may be calculated by the following expression[3],

$$S_t = R\ell nM + 2R\ell nT - 4{\cdot}61. \qquad \text{I.19.}$$

The vibrational entropy normal to the surface is given by Halford's expression,[30]

$$S_v = 1{\cdot}987 \left[\frac{h}{kT} \left(e^{\frac{h\nu}{kT}} - 1\right)^{-1} - 2{\cdot}303 \log \left(1 - e^{\frac{-h\nu}{kT}}\right)\right] \qquad \text{I.20.}$$

On the surface of an adsorbent the rotation of an adsorbed molecule is somewhat

restricted. The two degrees of rotational freedom possessed by a molecule in the gas phase are converted into one degree of freedom of planar rotation in the plane parallel to the surface and one degree of rocking vibration.[31] The entropy associated with the one degree of planar rotation may be calculated from the following expression also due to Halford[30],

$$S_r = R \ln \frac{1}{\pi\sigma'} \left[\frac{8\pi^3 \left(A^{*a'} B^{*b'} \ldots\ldots G^{*g'}\right)^{\frac{1}{n^*}} kT}{h^2} \right]^{\frac{n^*}{2}} + \frac{Rn^*}{2} \quad \text{I.21.}$$

For a mobile non-localized adsorbed film the entropy is usually obtained by summing S_t, S_v and S_r; electronic contributions to the entropy are usually negligible.

(ii) Immobile localized adsorption.

For an immobile localized film there will be no translational entropy. The vibrational and rotational terms may or may not be important. In all cases it is necessary, however, to include a configurational term associated with the number of ways of distributing the molecules over the surface. The treatment is as follows. Entropy is related to the thermodynamic probability W' by the well known expression[5],

$$S = k \ln W'. \quad \text{I.22.}$$

W' is given by the number of ways in which n molecules may be arranged on n_0 sites on the surface of the adsorbent,

$$W' = \frac{n_0 (n_0 - 1)(n_0 - 2) \ldots\ldots [n_0 - (n - 1)]}{n!} \qquad \text{I.23.}$$

which can be rearranged to give the expression,

$$W' = \frac{n_0 !}{(n_0 - n)!\ n!} \qquad \text{I.24.}$$

From equation I.22. it follows that the configurational entropy is given by the expression,

$$S_c = k\ \ell n \frac{n_0 !}{(n_0 - n)!\ n!} \qquad \text{I.25.}$$

To make the expression tractible Stirling's approximation may be applied. Equation I.25. then simplifies to

$$S_c = -k \left[n\ \ell n \frac{n}{n_0} + (n_0 - n)\ \ell n\ (n_0 - n)/n_0 \right] \qquad \text{I.26.}$$

Equation I.26. applies to the Langmuir model which ignores surface heterogeneity and mutual interactions between adsorbed molecules. Consequently when these effects are significant equation I.26. is not valid. Drain and Morrison[32] have determined experimental values

of the configurational entropy for systems in which the non uniformity of the surface was taken into account but in which the effects of mutual interactions were ignored. From this, Hayakawa[16] has developed the following approximate expression,

$$S'_c = 1{\cdot}987 \frac{\pi^2}{3} \frac{d \ell n\ N}{d \ell n\ P} \qquad \text{I.27.}$$

To obtain the total entropy for an immobile localized film either equation I.26. or I.27. may be used. It may also be necessary to include vibrational and/or rotational contributions (I.20. and I.21.) but electronic contributions are usually negligible.

(iii) Three dimensional ideal gas.

The translational entropy may be calculated from the Sackur-Tetrode equation[33],

$$S'_t = \frac{3}{2} R\ \ell n\ M + \frac{5}{2} R\ \ell n\ T - 2{\cdot}30. \qquad \text{I.28.}$$

The entropies for each vibrational and rotational degree of freedom may be calculated from equations I.20. and I.21. respectively. Electronic contributions are usually negligible.

Interpretation of Entropy.

The total experimentally calculated entropy obtained from equation I.18. represents the entropy change which occurs when a three dimensional gaseous adsorbate is adsorbed. It

has been shown that it is possible to calculate the entropy associated with a three dimensional gas. It is also possible to calculate the entropy of the adsorbed molecules. The differences between the theoretical entropy of the three dimensional gas and various combinations of the entropies S_t, S_v, S_r, S_c and S'_c of the adsorbed molecules must be compared with the experimental value until a particular combination gives good agreement. In this way it is possible to determine, by trial and error, which of the entropies S_t, S_v, S_r, S_c and S'_c are significant and consequently a good insight into the nature of the adsorbed film may be obtained.

I.5. PREVIOUS WORK ON ALKALI HALIDE CRYSTALS - ENTROPIES

Hayakawa[16-19] in his investigations of the adsorption of nitrogen, argon and oxygen on cubic sodium chloride, cubic potassium chloride, cubic potassium and octahedral potassium chloride used an equation equivalent to equation I.18. to calculate experimental entropies of adsorption. The theoretical values of the entropy changes were calculated using the principles outlined in section I.4.

The variation of the experimentally determined entropy with coverage for all three gases on all the adsorbents with the exception of octahedral potassium chloride was very similar to the respective heat curves. The variation for argon and oxygen and their respective magnitudes were comparable while the values for nitrogen showed different features in the range of $0{\cdot}5 \leqslant \theta \leqslant 1$. The experimental values for the three gases were found to be in good agreement with the values calculated for the two dimensional gas in the range $0{\cdot}3 \leqslant \theta \leqslant 0{\cdot}9$ and the discrepancies at lower values of the coverage were attributed to entropy changes of the adsorbent.

Hayakawa also calculated the entropies of solid argon, solid and liquid oxygen and solid nitrogen. The entropy curve for localized adsorption was obtained by adding the configurational entropy as calculated from equation I.27. to the entropy of the solid. The resultant curve was compared with the experimental curve. This was done for all adsorbents except octahedral potassium chloride. At a coverage of about $\theta = 0{\cdot}9$ the experimental curves for argon and oxygen shifted from the curve of the two dimensional gas to the curve for localized adsorption. This was attributed to a phase change

from a gaseous film to a condensed film. This treatment contains considerable uncertainties however due to the fact that equation I.27. ignores the effects of mutual interactions which, as indicated by the heat curves, was strongly evident.

I.6. PREVIOUS WORK ON THE ADSORPTION OF NITROGEN AND OTHER GASES ON PYREX

Since in this project the work on glass was undertaken merely to check experimental techniques, the discussion that follows is limited.

Several workers[34-37] have found that their experimental results for the adsorption of various gases on Pyrex may be represented by the Dubinin and Radushkevich adsorption isotherm equation. This equation may be written in the form[36],

$$\ell n\, \sigma = \ell n\, \sigma_M - B(-RT\, \ell n\, \frac{P}{P_0})^2 \qquad \text{I.29.}$$

The term $-RT\, \ell n\, \frac{P}{P_0}$ is usually represented by a single symbol (ε) and is commonly known as the adsorption potential.

The Dubinin and Radushkevich equation is developed from the Polanyi potential theory which predicts for systems following the theory that a characteristic curve independent of temperature is obtained when the coverage is plotted as a function of the potential. No specific form of this curve is predicted however. The theory states that when gases are adsorbed near their boiling points those regions of the adsorbent surface for which adsorption energies $E \geqslant \varepsilon$ are fully covered by an adsorbed film in a liquid-like state. Regions for which $E \leqslant \varepsilon$ make an unimportant contribution to the adsorption. The distribution of values of E on the surface of the adsorbent, therefore, determines the form of the characteristic curve.

For system which may be described by the Dubinin and Radushkevich equation, a plot of $\log \sigma$ against ε^2 yields

the close agreement of the value of σ_M with the accepted monolayer coverage for nitrogen suggested that Pyrex is non porous for nitrogen.

Hobson and Armstrong[36] found that the adsorption of nitrogen and argon by a Pyrex spherical flask fitted the Dubinin and Radushkevich theory. The values of the constants for nitrogen were found to be $B = 3.61 \times 10^{-7}$ and $\sigma_M = 6.4 \times 10^{14}$. For argon the values were $B = 7.20 \times 10^{-7}$ and $\sigma_M = 7 \times 10^{13}$. The accepted number of argon atoms per $cm.^2$ in a monolayer on a flat surface is 5.5×10^{14} molecules/$cm.^2$, so that a large difference between the theoretical and experimental monolayer coverages was found. This discrepancy was not found for nitrogen. Henry's law was not obeyed. The isosteric heats of adsorption for both gases were found to increase as the coverage was lowered, a property normally associated with a heterogeneous surface.

Ricca et al[37] found that for the adsorption of argon, krypton and xenon, Henry's law was not followed even at the lowest pressures. Some of the Dubinin and Radushkevich plots were found to deviate from linearity at high coverage. The experimentally determined ratios of σ_M for the three different gases were found to be greatly in excess of the values calculated from the generally accepted[1] molecular areas. Ricca et al postulated that this was due to the fact that some parts of the glass exhibit the "superactivity" found by Ross and Roberts[38]. This "superactivity" arises from a partial devitrification of the glass giving a highly porous molecular sieve like structure.

I.7. OBJECTIVES OF THE RESEARCH

All the alkali halide samples investigated by Hayakawa[16-19] were crystals obtained from aqueous solutions. The apparatus used was of the conventional volumetric type with pressures being measured on a mercury manometer. Thus the overall contamination in the system was probably quite high.

The samples of Granville and Hall[22,23] were certainly cleaner since they were deposited from the vapour phase in vacuo but the apparatus incorporated mercury cut-offs and contamination from this source seems likely.

The objectives of this project may now be clearly defined:

(a) to design and construct an ultra-high vacuum apparatus suitable for the measurement of the adsorption of non-polar gases on rigorously cleaned ionic surfaces;

(b) to determine adsorption isotherms of nitrogen on Pyrex in order that experimental techniques may be checked;

(c) to prepare evaporated films of alkali halides under ultra-high vacuum conditions;

(d) to determine adsorption isotherms of non-polar gases on these films;

(e) to determine the heat of adsorption at very much lower coverages than Hayakawa or Granville and Hall in order that a more precise estimation of the initial heat of adsorption might be made;

(f) to compare the results obtained with those of Hayakawa and Granville and Hall and to test whether there are any significant differences as a result of having used a cleaner sample.

C H A P T E R II.

APPARATUS SUITABLE FOR THE DETERMINATION OF ADSORPTION ISOTHERMS AT VERY LOW PRESSURES.

II.1. PRINCIPLES OF DESIGN

An adsorption isotherm shows the variation of the amount of gas adsorbed with the equilibrium pressure. Basically adsorption isotherms may be determined in the following way. A sample of the adsorbent under investigation is first degassed at as high a temperature as is practicable, in a good vacuum, in order to remove adsorbed gases. Then, while the adsorbent is maintained at a constant known temperature a measured quantity of the adsorbate is introduced into the system. The adsorption of the gas by the solid results in a decrease in pressure above the adsorbent. When the pressure remains constant, equilibrium has been attained. The amount of gas unadsorbed is determined and subtraction from the quantity originally admitted gives the amount of gas adsorbed. This value, plotted against the equilibrium pressure, gives the first point on the adsorption isotherm. Now in the design of an apparatus for the determination of adsorption isotherms, two possible principles exist for the evaluation of the amount of gas admitted to the adsorbent. They are:

(i) the pipette method whereby a dose of gas is measured in a calibrated volume prior to its exposure to the adsorbent;

(ii) the gas is admitted to the adsorbent through a capillary of known conductance for a measured time.

These are now discussed in detail.

(i) *The Pipette Method.*

The apparatus is shown in Fig.II.1.(a). Adsorbate is bled through the first valve into the doser (bound by valves 1 and 2) in successive aliquots, the pressure of each being measured before being exposed to the adsorbent by the opening of valve 2. Once opened the valve is left open until the equilibrium pressure of the adsorbate has been measured. It is then shut and the second dose let into V_c. The pressure here is measured and the valve opened again. The adsorbent cell is surrounded by a thermostating liquid.

Number of molecules admitted.

It follows that the number of molecules in the doser before the i^{th} dose of adsorbate is admitted to the adsorbent is given by the expression,

$$(n_c)_i = 9{\cdot}6575 \times 10^{18} \times \frac{(P_c)_i \cdot V_c}{T_r} \quad . \qquad \text{II.1.}$$

The pressure in the doser before admitting the i^{th} dose is $(P_a)_{i-1}$. Thus the residual number of molecules in the doser is given by the equation,

$$(n_r)_i = 9{\cdot}6575 \times 10^{18} \times \frac{V_c}{T_r} \times (P_a)_{i-1} \quad . \qquad \text{II.2.}$$

It follows that the total number of molecules admitted to the adsorption cell in i aliquots is equal to

$$9{\cdot}6575 \times 10^{18} \frac{V_c}{T_r} \left[\Sigma (P_c)_i - \Sigma (P_a)_{i-1}\right]. \qquad \text{II.3.}$$

Number of molecules unadsorbed.

After the admittance of the i^{th} dose to the adsorbent, the equilibrium pressure, corrected for thermal transpiration (see Appendix 1) is given by the expression,

$$P_{corrected} = (P_a)_i \left(\frac{T_a}{T_r}\right)^{\frac{1}{2}} .$$

This expression is only valid within the limits discussed in Appendix 1. The number of molecules not adsorbed in the volumes V_c and V_d which are at room temperature (see Fig. II.1.(a).) and in the volume V_a which is at the temperature of the thermostat is given by the equation,

$$(n_d)_i = 9{\cdot}6575 \times 10^{18} (P_a)_i \left[\frac{(V_c + V_d)}{T_r} + \frac{V_a}{T_a}\left(\frac{T_a}{T_r}\right)^{\frac{1}{2}}\right]. \quad \text{II.4.}$$

Number of molecules adsorbed.

The number of molecules adsorbed after the admission of i aliquots is given by the equation,

$(n_a)_i$ = (total number of molecules admitted to the system) - (total number of molecules not adsorbed).

Using equations II.3. and II.4. and simplifying gives the following equation,

$$(n_a)_i = \frac{9{\cdot}6575 \times 10^{18}}{T_r}\left[V_c\{\Sigma(P_c)_i - \Sigma(P_a)_i\} - (P_a)_i\{V_d + \left(\frac{T_r}{T_a}\right)^{\frac{1}{2}} . V_a\}\right]$$

II.5.

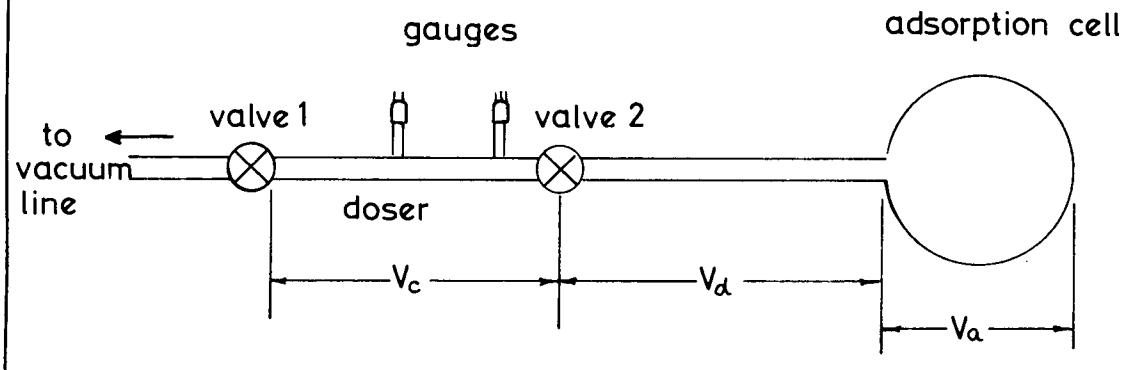

(a) METHOD (i)

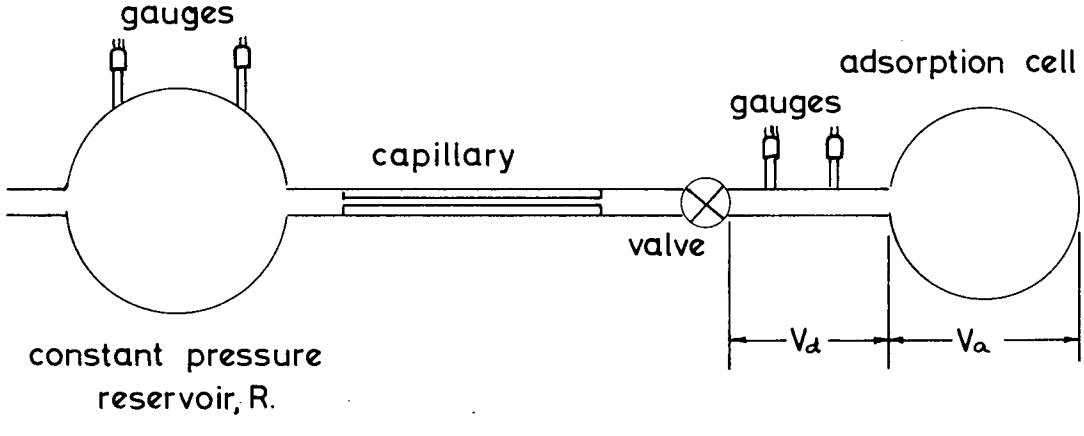

(b) METHOD (ii)

Fig. II-1

(ii) *The Capillary Method.*

The apparatus is shown in Fig. II.1.(b). A flow system (discussed in detail in section II.3.) is used to maintain the pressure in the reservoir, R, at a constant value which is not perturbed when the valve is opened or closed. Gas reaches the adsorbent through a capillary which is interposed between the gas reservoir and the adsorption cell. The measuring principle is then simply the well known one of evaluating the gas flow through the capillary by continuously monitoring the pressure at its ends and is due to Wagener[39,40]. The quantity of gas admitted to the adsorbent is obtained from the product of the flow rate through the capillary and the length of time for which the valve is kept open. Alternatively if adsorption is extremely rapid, equilibrium may be attained instantaneously thereby allowing the valve to be kept open all the time. In this case the pressure gauge reading gives a continuous measure of the amount of gas unadsorbed.

After t_i seconds the true equilibrium pressure in the adsorbent bulb is given by

$$(P_a)_i \left(\frac{T_a}{T_r}\right)^{\frac{1}{2}} .$$

Expressions for the evaluation of the total number of molecules admitted and total number of molecules unadsorbed are now developed.

Total number of molecules admitted.

It is important to distinguish three regimes of gas flow[41,42] specified by a dimensionless parameter called the Knudsen number. This is defined as the ratio of the mean free path of a molecule to a characteristic dimension of the channel through which the gas is flowing (for example, the radius in the case of a cylindrical tube).

At high pressures collisions between molecules occur more frequently than collisions of molecules with the container walls. The mean free path is small compared with the characteristic dimension of the vessel. In this range of small Knudsen numbers intermolecular collisions predominate in determining the characteristics of the flow. Consequently the gas behaves as a viscous fluid.

At low pressures on the other hand the mean free path is large compared to the characteristic dimension and most of the collisions which a molecule makes are with the walls of the containing vessel and not with other gas molecules. The analysis of the flow is primarily a geometrical problem of determining the restrictive effect of the walls on the free flight of a molecule. Since there are comparatively few intermolecular collisions each molecule acts independently of the others. Flow at large Knudsen numbers is therefore called free molecule flow or simply molecular flow.

At intermediate pressures and values of the Knudsen number, both types of collision are influential in determining the flow characteristics.

In the type of apparatus described here flow through the capillary is associated with large Knudsen numbers. Turnbull et al[41] give the following expression for the mass flow rate of gas through a long cylindrical tube of any shaped cross-section

$$\frac{dG_m}{dt} = K' \frac{8}{3} \left(\frac{2m}{\pi kT}\right)^{\frac{1}{2}} \frac{A_r^2}{bL} (P_1 - P_2) \quad g.sec.^{-1} \qquad II.6.$$

For a long tube of circular cross section where $\frac{L}{2r} \geq 100$, $K' = 1$, $A_r = \pi r^2$, $b = 2\pi r$. Expressing the flow rate in terms of molecules.sec.$^{-1}$ rather than g.sec.$^{-1}$ gives the expression,

$$\nu_f = \frac{4\pi}{3} \left(\frac{2}{\pi R}\right)^{\frac{1}{2}} \frac{r^3}{L} \frac{(P_1 - P_2)}{\sqrt{MT}} \times \mathcal{N} \qquad II.7.$$

Substituting the numerical values of π, R and $\mathcal{N}$ in equation II.7. and expressing pressures in torr rather than dynes.cm.$^{-2}$ gives the following general expression for the flow rate, in molecules.sec.$^{-1}$.

$$\nu_f = 2{\cdot}943 \times 10^{23} \times \frac{r^3}{L} \times \frac{(P_1 - P_2)}{\sqrt{MT}} \text{ molecules.sec.}^{-1} \qquad II.8.$$

If the pressure at one end of the capillary is very much greater than the pressure at the other end (say 1000 times) then with reference to Fig. II.1.(b)., the approximation $P_R - P_a = P_R$ can be made.

If we assume that adsorption equilibrium is attained instantaneously (as is the case with nitrogen on sodium

chloride[16]), the valve may be kept open all the time in which case the pressure of the gas in the adsorption cell is a continuous measure of the amount of gas unadsorbed.

After t_1 seconds the total number of molecules admitted is equal to

$$2{\cdot}943 \times 10^{23} \times \frac{r^3}{L} \times \frac{(P_R)_1 \; t_1}{\sqrt{MT}} \quad . \qquad \text{II.9.}$$

On the other hand if equilibrium is not instantaneous the adsorbate is admitted in a succession of aliquots. In this case the total number of molecules admitted after i doses is given by

$$\frac{2{\cdot}943 \times 10^{23} \times \frac{r^3}{L}}{\sqrt{MT}} \sum_{j=1}^{i} (P_R)_j \; t_j \; . \qquad \text{II.10.}$$

Number of molecules unadsorbed.

Similar arguments to those used in deriving equation II.4. yield the expression,

$$(n_d)_i = \frac{9{\cdot}6575 \times 10^{18}}{T_r} (P_a)_i \left[V_d + \left(\frac{T_r}{T_a}\right)^{\frac{1}{2}} V_a \right] \; . \qquad \text{II.11.}$$

Expression for the amount adsorbed.

It follows that that the number of molecules adsorbed is given by the expression,

$$(n_a)_i = \frac{2{\cdot}943 \times 10^{23} \times r^3}{\sqrt{MTr} \times L} \sum_{j=1}^{i} (P_R)_j \; t_j \; -$$

$$\frac{9{\cdot}6575 \times 10^{18}}{T_r} (P_a)_i \left[V_d + \left(\frac{T_r}{T_a}\right)^{\frac{1}{2}} V_a \right] . \qquad \text{II.12.}$$

II.2, CHOICE OF BASIC DESIGN

In deciding which of the two principles to adopt two main factors were taken into consideration -

(i) the precision of the respective methods and

(ii) simplicity of design and operation.

For estimating the precision of the two methods expressions were derived for evaluating the error in the number of molecules adsorbed. (The derivations are given in Appendix 2).

For the pipette method we have,

$$\partial(n_a)_i = \frac{9{\cdot}6575 \times 10^{18}}{T_r}\left[V_c^2 E_v^2\left(\sum_{j=1}^{i}(P_c)_j - \sum_{j=1}^{i}(P_a)_j\right)^2\right.$$

$$+ V_c^2 E_P^2\left\{\sum_{j=1}^{i}\{(P_c)_j\}^2 + \sum_{j=1}^{i}\{(P_a)_j\}^2\right\} + \left[(E_P^2 + E_v^2)\left\{V_d^2 + (\frac{T_r}{T_a})V_a^2\right\}\right.$$

$$\left.\left.+ 2E_P^2\left\{V_c V_d + V_a(\frac{T_r}{T_a})^{\frac{1}{2}}(V_c + V_d)\right\}\right]\left\{(P_a)_i^2\right\}^2\right]^{\frac{1}{2}} \qquad \text{II.13.}$$

and for the capillary flow method,

$$\partial(n_a)_i = \left[\left(\frac{2{\cdot}943 \times 10^{23} \times r^3}{\sqrt{MT_r}\cdot L}\right)^2\left[\left(9\frac{\delta^2 r}{r^2} + \frac{\delta^2 L}{L^2}\right)\left(\sum_{j=1}^{i}(P_R)_j t_j\right)^2\right.\right.$$

$$\left.+ E_P^2\sum_{j=1}^{i}\{(P_R)_j t_j\}^2 + \delta t^2\sum_{j=1}^{i}\{(P_R)_j\}^2\right]$$

$$\left.+\left(\frac{9{\cdot}6575 \times 10^{18}}{T_r}(P_a)_i\right)^2\left\{(E_P^2 + E_v^2)(V_d^2 + \{\frac{T_r}{T_a}\}V_a^2) + 2E_P^2 V_d V_a(\frac{T_r}{T_a})^{\frac{1}{2}}\right\}\right]^{\frac{1}{2}}.$$

II.14.

By choosing typical values for the apparatus parameters (Appendix 2) equations II.13. and II.14. become respectively,

$$\partial(n_a)_i = 10^{18}\left[2{\cdot}6\left\{\sum_{j=1}^{i}(P_c)_j - \sum_{j=1}^{i}(P_a)_j\right\}^2\right.$$

$$\left. + 10\left[\sum_{j=1}^{i}\{(P_c)_j\}^2 + \sum_{j=1}^{i}\{(P_a)_j\}^2\right] + 100\{(P_a)_i\}^2\right]^{\frac{1}{2}} \qquad \text{II.15.}$$

and

$$\partial(n_a)_i = 10^{14}\left[1{\cdot}443\left(\sum_{j=1}^{i}(P_R)_j t_j\right)^2 + 2{\cdot}56\sum_{j=1}^{i}\left[(P_R)_j t_j\right]^2\right.$$

$$\left. + 64\sum_{j=1}^{i}\{(P_R)_j\}^2 + 1{\cdot}046 \times 10^{10}\{(P_a)_i\}^2\right]^{\frac{1}{2}} \qquad \text{II.16.}$$

The Dubinin and Radushkevich adsorption isotherm (equation I.32) was used with the constants of Hobson and Armstrong for the system nitrogen adsorbed on glass to calculate a set of values of $(n_a)_i$. Values of $\partial(n_a)_i$ were calculated using equations II.15. and II.16. The relative error

$$\partial(n_a)_i \Big/ (n_a)_i$$

was found to be fairly constant at about 0·2 for both types of apparatus in the pressure range up to 10^{-4} torr after which the error increased rapidly for both methods (see Table II.1.). This indicated that neither type of apparatus is preferable on the basis of precision.

TABLE II.1.

TRUE EQUILIBRIUM PRESSURE	$(n_a)_i$	$\partial(n_a)_i/(n_a)_i$	$\partial(n_a)_i/(n_a)_i$
TORR	MOLECULES cc^{-1}	PIPETTE METHOD	CAPILLARY METHOD
1×10^{-8}	$9{\cdot}14 \times 10^{14}$	0·22	0·25
3×10^{-8}	$1{\cdot}44 \times 10^{15}$	0·17	0·21
7×10^{-8}	$2{\cdot}03 \times 10^{15}$	0·15	0·19
1×10^{-7}	$2{\cdot}33 \times 10^{15}$	0·16	0·18
3×10^{-7}	$3{\cdot}54 \times 10^{15}$	0·15	0·18
7×10^{-7}	$4{\cdot}80 \times 10^{15}$	0·14	0·17
1×10^{-6}	$5{\cdot}44 \times 10^{15}$	0·13	0·17
3×10^{-6}	$7{\cdot}90 \times 10^{15}$	0·13	0·18
7×10^{-6}	$1{\cdot}04 \times 10^{16}$	0·14	0·18
1×10^{-5}	$1{\cdot}16 \times 10^{16}$	0·13	0·18
3×10^{-5}	$1{\cdot}62 \times 10^{16}$	0·16	0·24
7×10^{-5}	$2{\cdot}05 \times 10^{16}$	0·18	0·24
1×10^{-4}	$2{\cdot}26 \times 10^{16}$	0·20	0·37
3×10^{-4}	$3{\cdot}01 \times 10^{16}$	0·34	0·70
7×10^{-4}	$3{\cdot}70 \times 10^{16}$	0·56	0·57
1×10^{-3}	$4{\cdot}03 \times 10^{16}$	0·71	1·66
3×10^{-3}	$5{\cdot}13 \times 10^{16}$	1·63	3·86
7×10^{-3}	$6{\cdot}10 \times 10^{16}$	3·86	3·49
1×10^{-3}	$6{\cdot}54 \times 10^{16}$	4·11	10·26
3×10^{-2}	$7{\cdot}99 \times 10^{16}$	10·07	25·50
7×10^{-2}	$9{\cdot}20 \times 10^{16}$	18·00	30·22
1×10^{-2}	$9{\cdot}72 \times 10^{17}$	27·50	71·44
3×10^{-1}	$1{\cdot}14 \times 10^{17}$	69·82	135·43
7×10^{-1}	$1{\cdot}27 \times 10^{17}$	145·67	151·97
1×10^{-1}	$1{\cdot}32 \times 10^{17}$	200·00	202·27

At first sight it seemed that the apparatus for method (i) would be the easier to construct and possibly the simpler to operate. However, the apparatus for method (ii) was considered to be more flexible in that it would be possible to vary the size of a dose more easily than for method (i). The quantity of gas admitted by the capillary method depends upon

(a) the length of time for which the valve is opened and

(b) the pressure P_R in the reservoir.

Thus there would be a fine control on the size of the doses. The capillary method has a further advantage in that for certain adsorbate-adsorbent combinations the pipette principle may be applied. This occurs when there is no significant adsorption at room temperature such as with nitrogen on Pyrex. An aliquot of adsorbate is let into the adsorption cell at room temperature and the pressure measured. This gives the number of molecules present. The cell is immersed in coolant whereupon adsorption takes place and the equilibrium pressure gives the number of molecules unadsorbed.

Consideration of the above factors showed the capillary flow method to be the more favourable of the two possible methods because of its greater versatility. Consequently it was this principle which was selected for the ultra-high vacuum apparatus.

II.3. DETAILED DESIGN OF APPARATUS

In determining the amount of gas admitted when the valve is kept open for t seconds it is important that the pressure in the bulb R (Fig.II.1.(b).) does not surge and that it remains constant over the entire period of t seconds. The apparatus necessary to maintain a constant dynamic pressure in R will now be discussed in detail.

Fig.II.2. shows the principle of the system. A constant dynamic pressure is established and maintained in the reservoir by allowing gas to flow into it from an intermediate bulb B through capillary 1 of conductance F_1 and at the same time by pumping through valve 2. The pressure in R must be very much greater than the pressure in the adsorption cell and can be maintained at any desired level either by suitable adjustment of the pressure in B or regulation of the pumping rate through valve 2. This idea is due mainly to Hayward et al[43].

In order to determine suitable dimensions for capillaries 1 and 2 it is necessary to set up expressions relating the pressure in R with the respective flow rates through the two capillaries. The pressure in the reservoir is dependent on the number of moles of gas present therein. This is determined by the amount of gas flowing into R through capillary 1 and the amount of gas flowing out through valve 2 and capillary 2. Thus the rate at which the number of moles of gas in R changes with time is given by the expression,

$$\frac{dn_R}{dt} = \frac{dn_1}{dt} - \frac{dn_v}{dt} - \frac{dn_2}{dt} \quad . \qquad \text{II.17.}$$

The instantaneous number of moles of gas in the reservoir is related to the pressure by the expression,

$$n_R = \frac{P_R V_R}{T} .$$

Differentiating this equation with respect to time and substituting in equation II.17. gives the expression,

$$\frac{dP_R}{dt} = \frac{RT}{V_R} \left(\frac{dn_1}{dt} - \frac{dn_v}{dt} - \frac{dn_2}{dt}\right) \qquad \text{II.18.}$$

Calculation of $\frac{dn_2}{dt}$ and F_2.

The expression for the flow rate of nitrogen at 298^0 K may be obtained from equation II.8. which simplifies to,

$$\nu_f = 3{\cdot}219 \times 10^{21} \times \frac{r^3}{L} \times P_R \text{ molecules.sec.}^{-1} \qquad \text{II.19.}$$

Convenient arbitrary values of 32·2 cm. for L, 0·02 cm. for r and 1×10^{-2} torr for P_R are chosen. Using equation II.19. the flow rate through capillary 2 is given by the expression,

$$\frac{dn_2}{dt} = 8{\cdot}0 \times 10^{12} \text{ molecules.sec.}^{-1} \qquad \text{II.20.}$$

Now, the conductance of a cylindrical tube is defined as[42] the flow rate per unit difference of pressure between the ends of the tube. Thus the conductance, F_2, of capillary 2 is

For P_R to be constant, $\frac{dP_R}{dt} = 0$ and hence,

$$\frac{dn_v}{dt} = 7{\cdot}92 \times 10^{14} \text{ molecules/sec.} \qquad \text{II.25.}$$

Also from equation II.18.,

$$\frac{dn_1}{dt} = \frac{dn_2}{dt} + \frac{dn_v}{dt} \quad \text{when} \quad \frac{dP_R}{dt} = 0 \ .$$

Thus, using equations II.20. and II.25., we have that

$$\frac{dn_1}{dt} = 8{\cdot}0 \times 10^{14} \qquad \text{II.26.}$$

and hence

$$F_1 = 8{\cdot}08 \times 10^{14} \text{ molecules.sec.}^{-1}\text{torr.}^{-1} \qquad \text{II.27.}$$

Thus the conductances F_1 and F_2 (equations II.27. and II.21.) must be equal.

Dimensions of Capillaries.

In determining the conductance of capillary 1 arbitrary values of L(32·2 cm.) and r(0·02 cm.) were chosen for capillary 2. From the definition of conductance and equation II.19. it follows that

$$F \propto \frac{r^3}{L} \qquad \text{II.28.}$$

Hence, clearly, alternative values of L and r may be chosen for capillary 1 if desirable provided the condition,

$$\frac{r^3}{L} = \frac{(0\cdot02)^3}{32\cdot2} \text{ cm.}^2 \qquad \text{II.29.}$$

is satisfied. Since the conductances of both capillaries are to be the same (equations II.21. and II.27.) it follows that the dimensions of capillary 1 must be selected in accordance with equation II.29. Some other convenient values of L and r which satisfy this condition are

r(mm.) :	0·1	0·3	0·4
L(cm.) :	4	108	255.

Final pressure change in B and R.

We now want to calculate whether the pressure in B will drop significantly during the course of an entire adsorption run (say two hours) and the initial pressure surge in R one second after opening valve 3. The values of V_B and V_R are arbitrarily chosen as 1 and 2 litres respectively while the values of P_B and P_R are 1·0 and $1\cdot0 \times 10^{-2}$ torr as in the calculation of F_2 and F_1. The number of moles of gas originally present in B is given by

$$n_B = 0\cdot5379 \times 10^{-4} \text{ moles.}$$

The flow rate through capillary 1 is $8\cdot0 \times 10^{14}$ molecules.sec.$^{-1}$ (equation II.26.)

$\therefore$ number of moles of gas flowing out in 120 min. = $9\cdot566 \times 10^{-6}$

$\therefore$ number of moles of gas left in B after 120 min. = $0\cdot4422 \times 10^{-4}$

The pressure exerted by this residual amount of gas is

$$P_B = 0{\cdot}82 \text{ torr}.$$

The lower flow rate, after two hours, through capillary 1 results in a lower value of the pressure P_R. The decrease in P_R may be calculated as follows. Expressing equation II.18. in terms of pressures we have,

$$\frac{dP_R}{dt} = \frac{RT}{V_R}\left[F_1 (P_B - P_R) - F_2 P_R - F_v P_R\right] . \qquad \text{II.30.}$$

For any value of P_B we require that

$$\frac{dP_R}{dt} = 0.$$

Thus it follows that in general,

$$P_R = \frac{P_B \cdot F_1}{2F_1 + F_v} . \qquad \text{II.31.}$$

It can be seen that P_R is directly proportional to P_B and that any change in P_B will result in the same percentage change for P_R.

When $P_B = 1$ torr, $P_R = 10^{-2}$ torr. Thus after two hours the decrease in P_B to 0·82 torr as deduced above results in a decrease in P_R to $0{\cdot}82 \times 10^{-2}$ torr. Thus a drop in P_B from 1 to 0·82 torr results in a drop of pressure from 1×10^{-2} to $0{\cdot}82 \times 10^{-2}$ torr in R.

II.4. DESCRIPTION OF THE APPARATUS

Achievement of ultra-high vacuum conditions involve extensions of normal vacuum practice. The ultimate pressure in any vacuum system is dictated by the competition between two processes. These are firstly, the rate of removal of gas by the pumps and secondly the rate at which gas is introduced into the system either by evaporation from the interior walls or by permeation through them. Thus, ultra-high vacuum pressures may be attained if Ehrlich's[44] "golden" rule is follwed: minimize gas evolution, maximize pumping. A decrease in gas influx rate can be attained by baking the apparatus since the rate of all the processes controlling gas influx (diffusion, desorption, outgassing) varies exponentially with temperature. Sources of gas such as vacuum greases must be precluded. Bakeable metal valves must be used instead of conventional stop-cocks. All connections must consist of glass blown seals as no greased joints may be used.

Fig. II.3. is a flow diagram of the apparatus. The area enclosed by the dotted lines represents the bakeout section. The apparatus is pumped by two ultra-high vacuum diffusion pumps, (20G and EMG), each one pumping from one end of capillary 2 (CAP 2). These two pumps are backed by an oil diffusion pump (10 W) which in turn is backed by a rotary pump (RP). Each pump is seperated from the other by a liquid nitrogen trap (LNT). Back streaming of vapours from the ultra-high vacuum pumps, one of which is an oil diffusion pump (20G) and the other a mercury diffusion pump (EMG) is minimized by one liquid nitrogen trap (LNT 1) directly above 20G and by two bakeable liquid nitrogen traps (VTG) in series directly above EMG. LNT 1 is kept constantly filled with

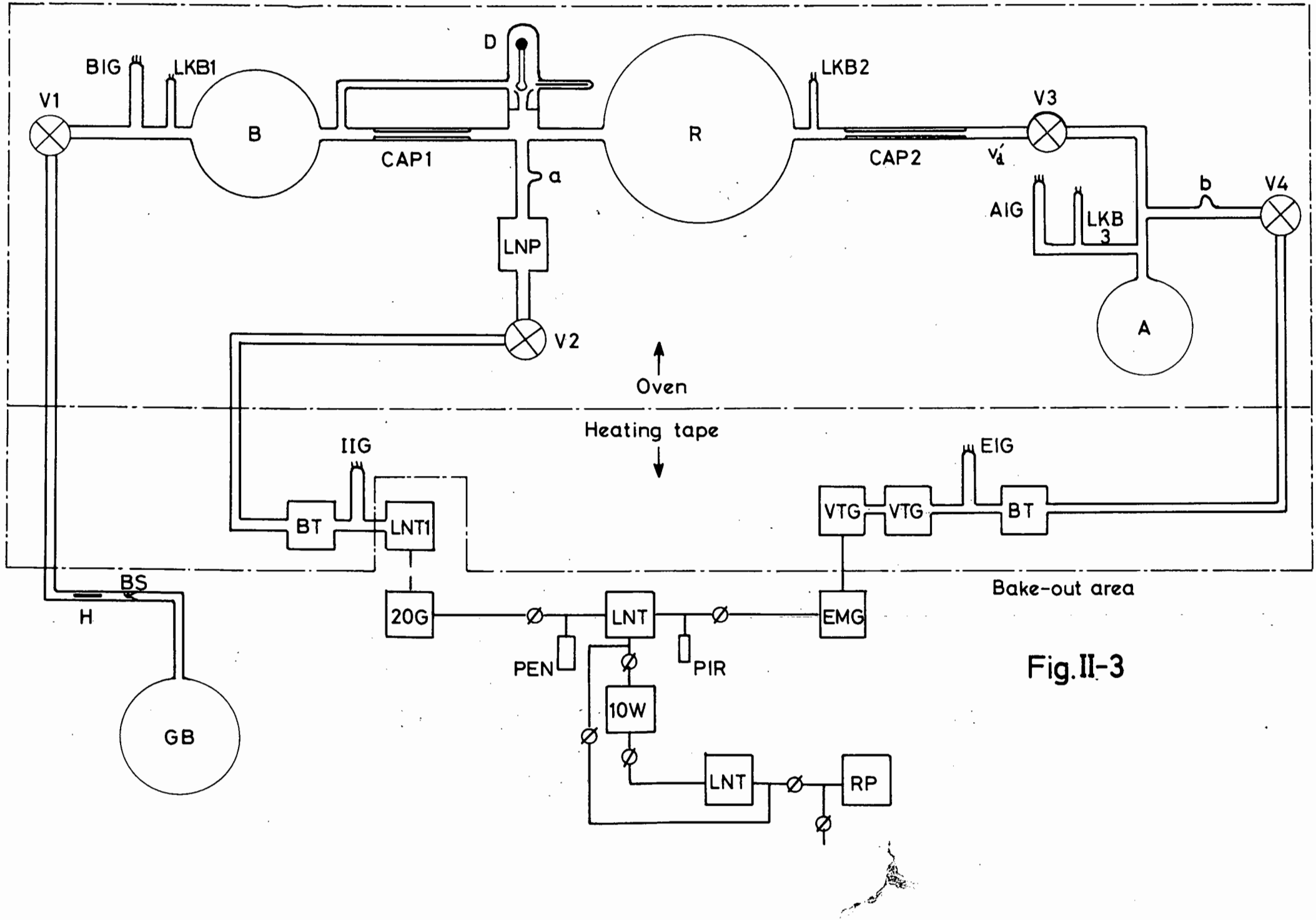
BIG
LKB1
V1
B
D
CAP1
a
LNP
V2
R
LKB2
V3
CAP2
V'1
AIG
LKB 3
b
V4
A
Oven
Heating tape
IIG
BT
LNT1
EIG
VTG
VTG
BT
BS
H
GB
20G
LNT
EMG
PEN
PIR
10W
LNT
RP
Bake-out area

Fig. II-3

liquid nitrogen by means of an automatic device which is described in detail later in this section. It is necessary for this trap to be kept constantly charged in order to minimize creep of the oil along the glass walls. Two Biondi[45] traps (see Fig.II.4.(a).) are used as a further precaution. Each is situated in the pumping line just before valves V2 and V4. The adsorption volume is defined as that bounded by valves V3 and V4. The sample cell (A) is a spherical Pyrex flask which is positioned so that it can be easily removed and replaced by another cell of any particular size or design by glass blowing. Pressures here are measured on a bakeable ionization gauge head (AIG) and a bakeable Pirani-type gauge head (LKB 3). The apparatus to the left of capillary 2 is pumped through valve V2 by 20G. Interposed between the valve and the pump is a large capacity bakeable liquid nitrogen trap (LNP) which is used as a pump. In order to maximize the pumping speed to the left of capillary 1 (CAP 1) a valve of the Decker[46] type (D) is used to by-pass CAP 1. Pressures in B are measured by means of an ionization gauge head (BIG) and a Pirani gauge head (LKB 1) while pressures in R are measured on a Pirani gauge head only (LKB 2). Valve V1 controls the inflow of gas from the gas bottle (GB). Pressures on the high vacuum side of 20G and EMG are measured on two ionization gauge heads (I.IG and E.IG respectively) which are placed outside the area enclosed by the oven thereby enabling pressure measurements to be made during a bakeout. These gauge heads together with other parts of the ultra-high vacuum line which are not enclosed by the oven are heated to bakeout temperatures by heating tapes. Pressures on the high vacuum side of 10 W are measured on a Pirani gauge head (PIR) and a Penning gauge head (PEN).

All interconnecting tubulation is of large bore so as to have high conductance to the pumps. Suitable connection points are provided at a and b for temporary apparatus such as a McLeod gauge for the calibration of the pressure gauges and a gas burette system for the calibration of the adsorption volume.

The various components of the apparatus are now described in greater detail.

Pumps.

The mercury vapour two-stage diffusion pump (EMG) was supplied by Edwards High Vacuum Ltd, Sussex and was charged with 60 ml. of triple distilled mercury. The pump was supplied with two bakeable liquid nitrogen traps (VTG) which were fitted in series with the pump. Special procedures, specified by Edwards, in the bakeout and cooling down of the traps and their subsequent filling with liquid nitrogen were followed. Although the manufacturers claim that pressures of the order of 10^{-13} torr can be achieved, the best vacuum attained in this work was 5×10^{-9} while 5×10^{-8} was attained routinely. The pump has a nominal speed of 3 litres.sec.$^{-1}$ at the upper trap inlet.

The 20G ultra-high vacuum oil diffusion pump was supplied by Balzers of Liechtenstein. It is a two stage pump fitted with a water cooled baffle. A laboratory made liquid nitrogen trap was glass blown to the throat of this baffle. The nominal speed is 4 litres.sec.$^{-1}$. The pump was charged with 150 ml. of DC 705 oil supplied by Midland Silicones Ltd., Glamorgan. Pressures down to $1{\cdot}0 \times 10^{-8}$ torr could be attained regularly after degassing and bakeout.

The DC 705 oil was chosen in preference to the DC 704 oil because of its superior properties with regard to back streaming. However, after the project was well under way it was realized that the DC 705 oil was in fact an unwise choice since the thermal power required for optimum functioning was beyond the capacity of the heaters of the 20G. Consequently the pump did not produce as good a vacuum as it might have done with DC 704 oil.

The backing diffusion pump, the Diff. 10 W was supplied by Balzers. Its nominal pumping speed at 10^{-4} torr is 6·5 litres sec.$^{-1}$ and pressures down to $1{\cdot}0 \times 10^{-6}$ torr were attained regularly. The pump was charged with 15 cc of DC 704 oil supplied by Midland Silicones Ltd. This pump was backed by a two stage Speedivac rotary oil pump (Type 2SC20A) from Edwards.

Valves.

The bakeable valves (V1, V2, V3, V4) were Type C supplied by the Granville-Phillips Company, Colorado, U.S.A. They are precision, all metal valves designed to withstand repeated bakeout cycles at temperatures up to 450^{0}C. They have good leak control properties. The leakage conductance may be adjusted smoothly from about 1 litre.sec.$^{-1}$ to less than 1×10^{-14} litres.sec.$^{-1}$ by means of a torque wrench. Their limitation lies in the fact that they may be baked at temperatures greater than 250^{0}C only when in the open position. The driver must be removed and the valve held open by a bakeout clamp. They may however be baked in the closed position at temperatures up to 250^{0}C for periods up to 8 hours. Longer bakeouts at higher temperatures while closed tend to produce diffusion welding of the seal. The valves must be rigidly

mounted to withstand the torques required to open and close them. Because of this and the fact that other portions of the apparatus are also rigidly mounted high stresses may be developed in and around the glass-to-metal seals during baking. This necessitates the fitting of glass bellows on the inlet and outlet tubes.

The Decker-type valve[46], D, was supplied by Leybold's Nachvolger, Germany. It is a ball and socket valve, the ball being part of a capsule containing magnetic powder. The valve is operated by means of an electro-magnet which fits snugly over the neck of the valve. A magnetic rod, held in a side-arm, can be brought into position between the ball and the socket thereby keeping the valve open.

Biondi Trap[45].

This is a bakeable, non refrigerated isolation trap of high conductance (see Fig. II.4.(a).). Two of these traps were used and each were charged with molecular sieve type 5A (aluminium calcium silicate) manufactured by Linde Air Products Company, a division of Union Carbide and Carbon Corporation. Before the traps and contents were actually sealed into the line they were pumped by a rotary pump to remove any fine powder or sediment which would otherwise have been dispersed over the apparatus. After a few bakeout and degassing cycles it was found that ultra-high vacuum pressures could not be attained. This was at first attributed to the high degassing rate of the molecular sieve and consequently it was decided to remove the traps from the line. Subsequently however the fault was thought to have been due to a leak but it was inconvenient to re-install the traps.

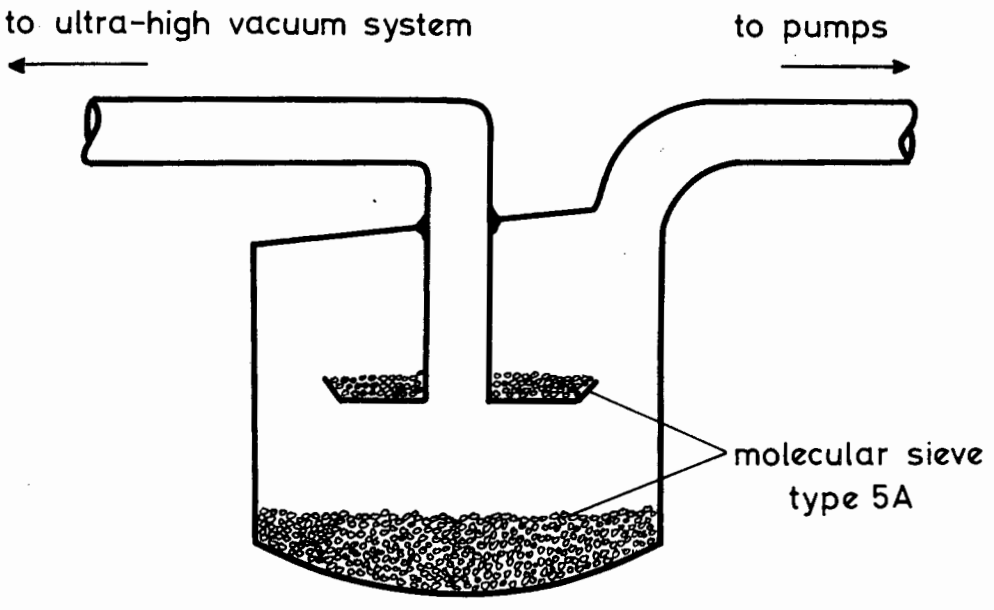

(a) BIONDI TRAP

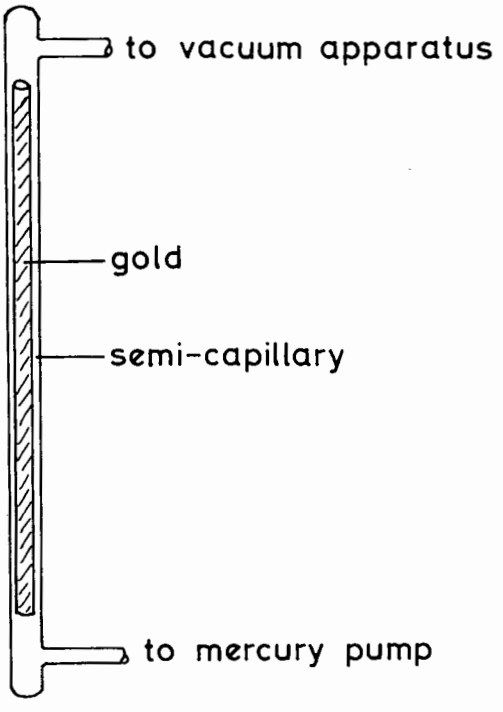

(b) GOLD TRAP

Fig. II-4

In the Bayard-Alpert design of gauge head the ion collector is in the form of a fine wire so as to reduce its surface thereby minimizing the liability of being struck by X-rays generated by electron bombardment of the grid. The collector is positioned in the centre of the grid helix so that there is a good probability of ions reaching it. The filament is mounted outside the grid helix.

The useful pressure range is from 5×10^{-11} torr to 1×10^{-3} torr. Baking temperatures must not exceed 450^{0}C. The control unit used in conjunction with the gauge heads was manufactured by Varian Vacuum Products, California.

(b) Pirani gauge.

The principle of the gauge is as follows. A change in the pressure brings about a rise or fall in the number of gas molecules per unit volume and hence a rise or fall in the thermal conductivity of the gas in a vacuum apparatus. As the thermal conductivity of the gas varies so will the heat loss of a constant voltage electrically heated filament in the apparatus. The Pirani gauge head filament has a high resistance temperature coefficient so that in a vacuum slight changes in pressure bring about large changes in the filament resistance. The filament forms one arm of a Wheatstone bridge and the changing resistance results in an out of balance current which can be read as pressure on a meter.

Two different types of Pirani gauge were used. The one with bakeable heads is the LKB Autovac Vacuum Gauge supplied by LKB Produkter, Sweden. The useful measuring

range starts at about 70 torr and goes down to 1×10^{-3} torr. The LKB gauge head must be calibrated against a McLeod gauge or another previously calibrated LKB gauge head.

The Pirani gauge used on the non bakeable section of the apparatus (PIR, Fig. II.3.) is a "Speedivac" model supplied by Edwards High Vacuum Ltd. Its pressure range is from 1 torr to 10^{-3} torr.

(c) Penning Gauge.

A high voltage discharge between the electrodes of the Penning gauge head ionizes the gas molecules in a vacuum. The pressure in the apparatus determines the number of molecules per unit volume and therefore the ionization current which is read as pressure on the meter scale. The gauge head consists of a glass tube containing two electrodes, an anode in the form of a rectangular wire loop and a cylindrical plate cathode. The tube is enclosed in a strong magnetic field by two permanent magnets. Electrons emitted from the cathode are at first accelerated through the anode loop to the opposite side of the cathode from which they are repelled. This results in the electrons oscillating backwards and forwards until they are collected by the anode. Positive ions are produced by collision between the electrons and the gas molecules. These are attracted to the cathode and form the current. The mean free path of the electrons is increased by the influence of the magnetic field which causes them to follow helical trajectories thereby greatly increasing the probability of ionization by collision and therefore the sensitivity of the gauge head. The pressure

range is from 1 x 10^{-2} to 1 x 10^{-5} torr. The gauge was supplied by Edwards High Vacuum.

Automatic Liquid Nitrogen Filler.

A diagram of the apparatus is shown in Fig. II.5. The top of a 10 litre Dewar flask is sealed with a tight fitting rubber bung (RB). A small heater, (h), consisting of a few turns of nichrome wire wound on a short length (4 inches) of quartz rod is suspended in the flask by its leads which pass through the bung. The external circuit is completed with a step-down transformer, (T), and electronic timer, (ET). A threaded tube, (Tu), of comparatively large diameter passing through the bung facilitates charging the vessel. Tu may be sealed with a tight fitting screw cap. The outlet tube consists of two sections, one of copper (Cu) and one of Tygon (Ty). The low thermal conductivity of the latter minimizes freezing of the rubber bung.

The timer, (ET), controls the time between each switching on of the current and also the period for which the current passes. When the heater is on the pressure increase due to the boiling liquid nitrogen forces the liquid through the outlet tube. The optimum settings on the timer are determined empirically.

Gas-handling System.

The adsorbate gases were research grade purity and were supplied by Air Products. The gas is stored in a 1 litre Pyrex glass bulb under a pressure of about one atmosphere. The gas may be released after a glass seal (BS in Fig.II.3.) is broken. This is done with a magnetic hammer (H) which must be coated with glass since the bare metal is a serious

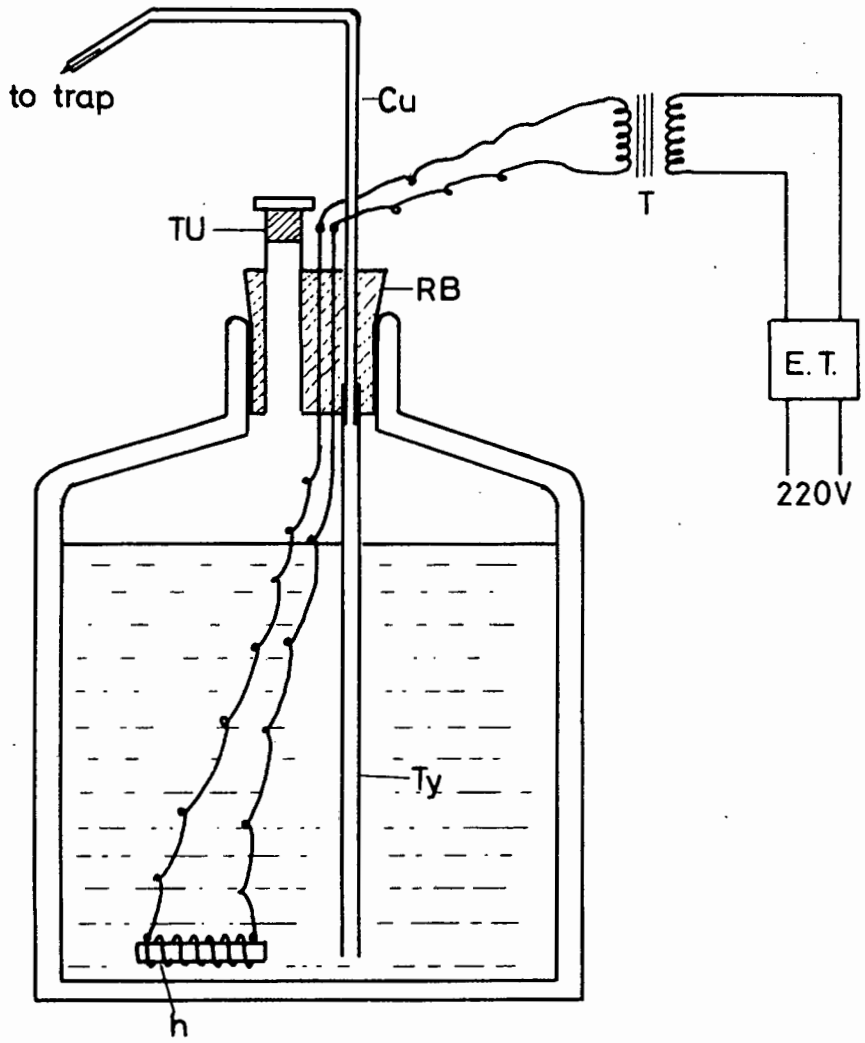

Fig. II-5

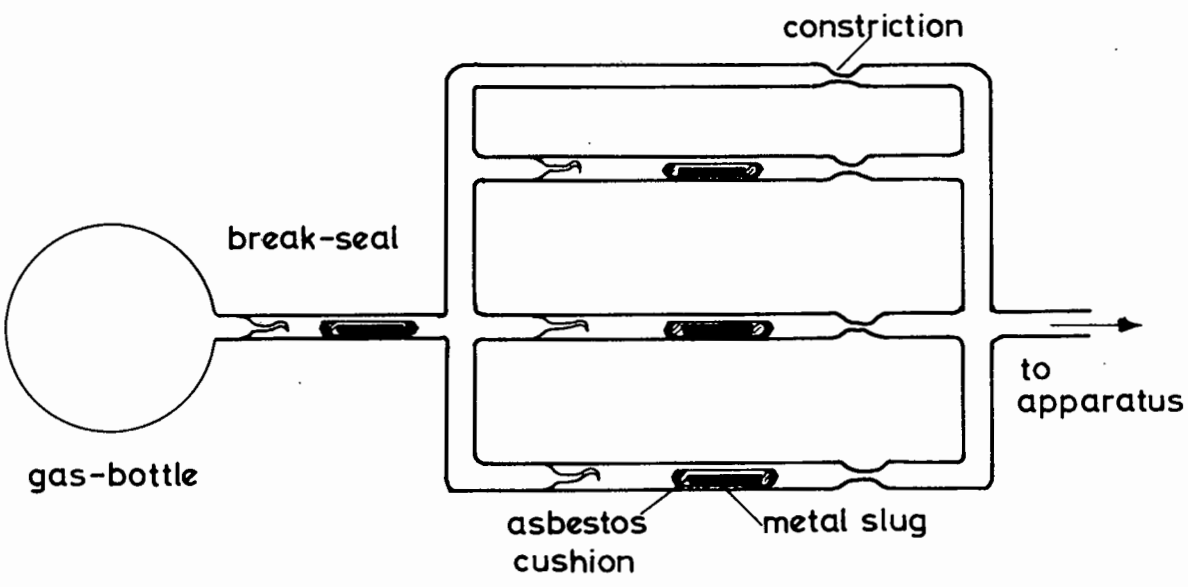

Fig. II-6

source of contamination. It was found that a hammer in cylindrical form was the most suitable since with ball-bearings the protective glass coating tended to crack when the seal was broken. As an extra precaution a small cushion of asbestos paper was packed between the ends of the metal slug and the glass coating.

Once an adsorption run has been completed the system must be pumped down and rebaked. However, as mentioned earlier, the Granville-Phillips valves may be baked at high temperatures only when open. This of course cannot be done with valve V1 once the seal has been broken since this would result in the loss of all the gas. To overcome this difficulty the gas bottle must be connected to a network of three or four arms, each one having its own break seal and hammer. In addition each arm has a thick walled constriction (see Fig. II.6.) which may be sealed by glass blowing. Valve V1 may now be opened and the apparatus baked.

Bakeout Apparatus.

The oven used was supplied by Bálzers and consisted of four u-shaped modules, each fitted with 10 amp. elements. Two side closing lids completed the structure.

Hotfoil flat element heating tapes were used to bake those parts of the apparatus not enclosed by the oven. Temperatures were controlled by means of Variacs.

Because high temperature bakeouts for prolonged periods were necessary the apparatus was sometimes left unattended. It was thus desirable to incorporate safety devices to trip the current should the temperature rise to too high a level. A Sauter thermostat with temperature control

over the range 50 to 800^{0}C was consequently included in the element circuit. As a further precaution a thermistor which was set to trip at a higher temperature than that at which the thermostat was set was also incorporated. The electronic circuit is shown in Fig. II.7.

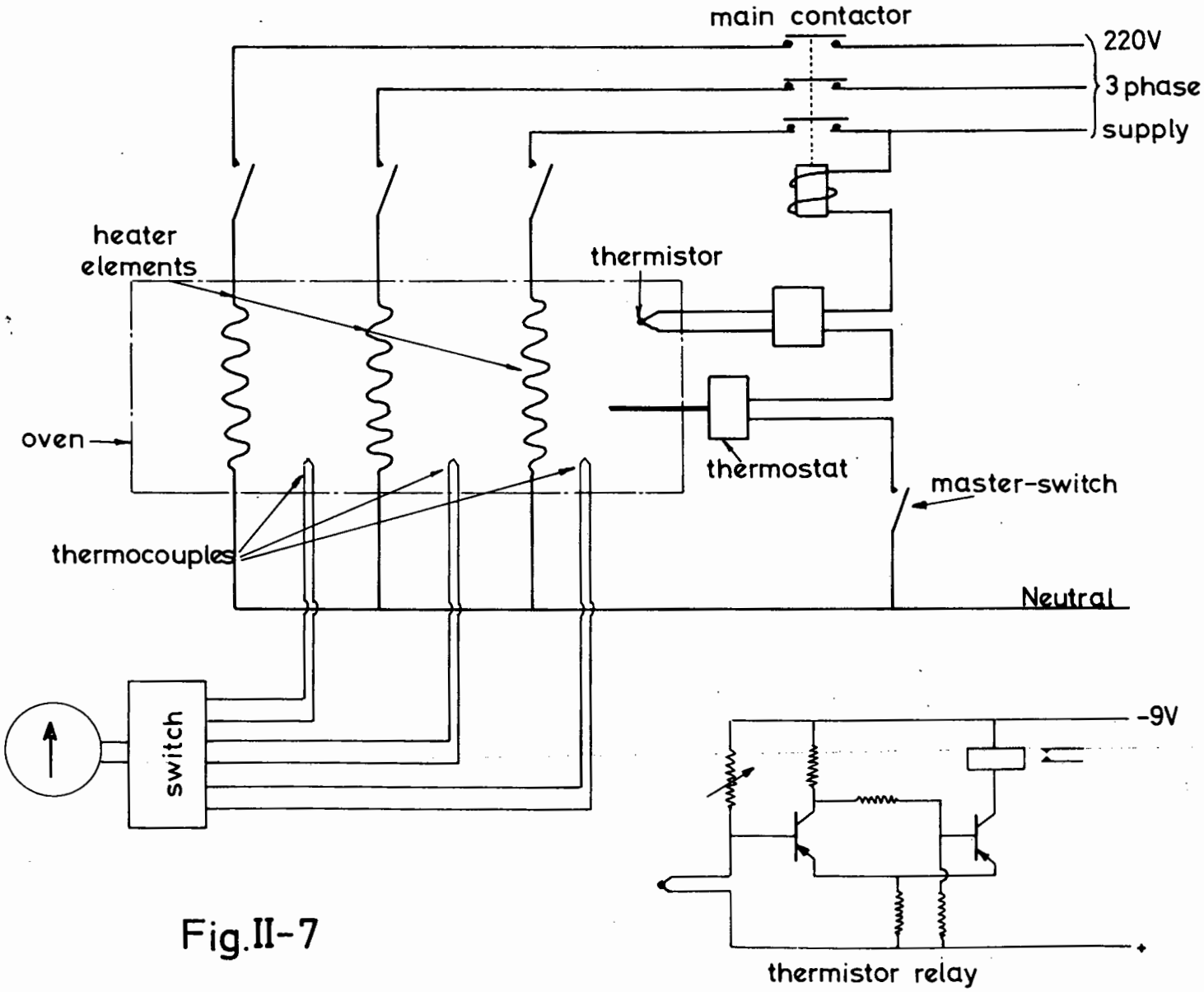
main contactor
220V
3 phase
supply
heater
elements
thermistor
oven
thermostat
master-switch
thermocouples
Neutral
switch
-9V
thermistor relay

Fig.II-7

system was estimated to be about 1500 cc. Accordingly a gas burette was constructed from three bulbs of volumes 500 cc, 1000 cc and 1000 cc joined in series. (See Fig.II.8.). The volumes between successive marks etched on the necks were carefully determined before the burette was assembled. It was obviously impractical to use mercury in the gas burette and thus di-n-butyl phthalate $[C_6H_4(COO.C_4H_9)_2]$ was selected instead. It has a vapour pressure[42] of about 2×10^{-2} torr.

In order to ensure that no di-butyl phthalate vapour diffused into the adsorption apparatus and contaminated the glass a trap was included in the line. It consisted of a Pyrex glass tube, about 1.5 inches in diameter and 12 inches in length, packed with Raschig rings, and positioned such that a flask of liquid nitrogen could be placed around it.

Pressures were measured on a mercury manometer. Helium was admitted to the gas burette via a drying tube.

The calibrating apparatus was joined to the adsorption apparatus at point b (Fig. II.3.). A constriction in the line enabled the burette to be seperated from the main apparatus once the measurements had been completed.

LKB Pirani Gauges.

A McLeod gauge was designed in order that the LKB Pirani gauges could be calibrated in the pressure range 1×10^{-3} to 1 torr. The requirement of the McLeod gauge was that when pressures in this range were being measured the difference in heights of the mercury levels in the two capillaries of the gauge should preferably be greater than about 5 mm. Using the expression,

$$P = \frac{(\text{difference in heights})(\pi r^2 h')}{\ell}$$

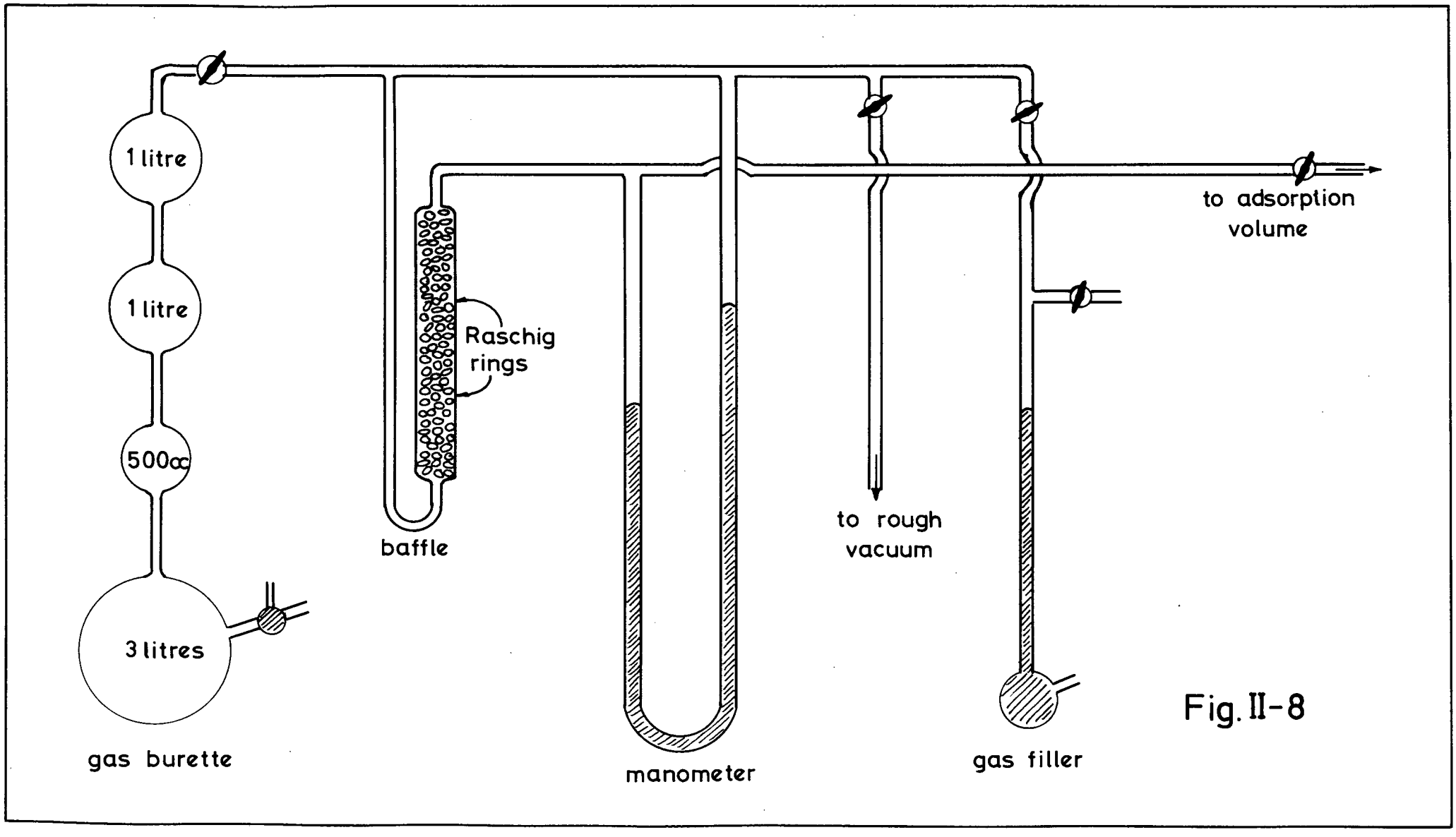
1 litre
1 litre
500cc
3 litres
gas burette
baffle
Raschig rings
manometer
to rough vacuum
to adsorption volume
gas filler

Fig. II-8

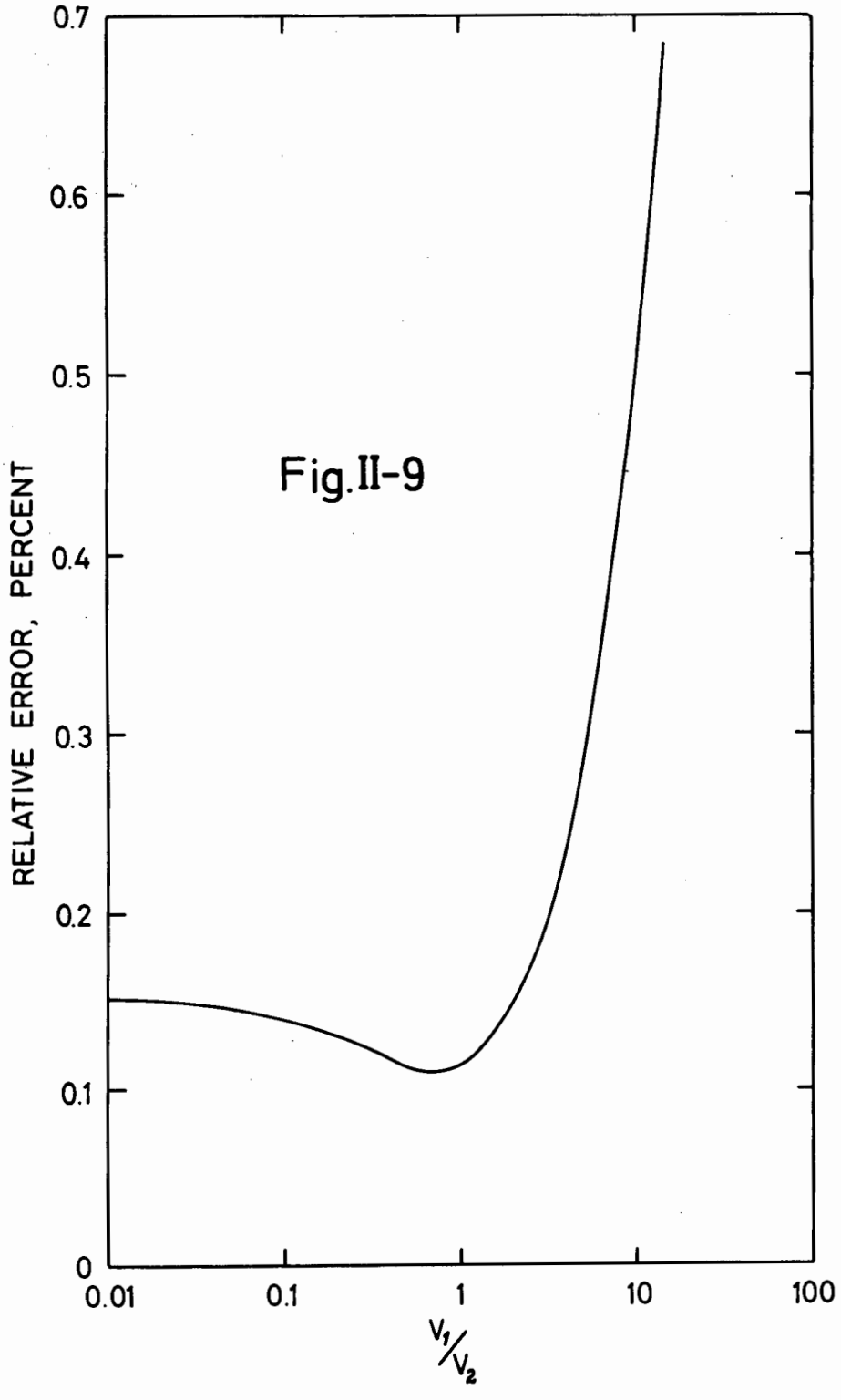
0.7
0.6
0.5
0.4
0.3
0.2
0.1
0
RELATIVE ERROR, PERCENT
0.01
0.1
1
10
100
V1/V2

Fig.II-9

it was determined that the dimensions of a McLeod which satisfied the above requirement was one with a volume of 100 cc and with a capillary radius of 1 mm.

The McLeod was connected to point a, (Fig. II.3.) for the calibration of LKB 1 and LKB 2. For LKB 3 it was connected at point b.

II.6. METHODS OF OPERATION OF THE ADSORPTION APPARATUS

It was found that the value of the number of molecules admitted for each dose obtained from pressure measurements in the cell at room temperature (when no adsorption occurred) was significantly greater than that obtained using the flow equation II.9. It was realized that this error arose from the fact that there is a dead volume V'_d between the end of the capillary and valve V3, as can be seen in Fig. II.3. With V3 shut adsorbate flows from R into V'_d until, if V3 is kept closed for long enough the pressures in V'_d and R will equalize. On opening the valve the gas trapped in V'_d enters the cell and is immediately followed by gas flowing through the capillary from R. If the valve is closed after t seconds and this value of t is used in the flow equation II.9. to calculate the amount of gas let into the cell, a quantity which is less than the true amount will be obtained since the gas originally trapped in V'_d was not taken into account.

In the design of the apparatus this shortcoming of the capillary method had not been foreseen. This is discussed further in Chapter VI . Consequently it was necessary to adapt the method of operation to overcome this difficulty. Before opening V3 the number of molecules present in V'_d must be determined. This may be done by leaving V3 closed for a long enough time for the pressure in V'_d to reach P_R, in which case if V'_d is accurately known, n'_d may be obtained from the expression,

$$n'_d = 3{\cdot}24 \times 10^{16} \times P_R \times V'_d \text{ molecules.} \qquad \text{II.33.}$$

II.7. PERFORMANCE OF THE CONSTANT DYNAMIC PRESSURE SECTION OF THE APPARATUS

The apparatus was tested to determine whether a dynamic equilibrium could in fact be set up and maintained in R (see Fig. II.3.). Nitrogen was let into bulb B until a pressure of about 1 torr was registered on LKB 1. The valves D, V2 and V3 were kept closed while gas leaked through CAP 1 into R. When the pressure here had reached about 1×10^{-2} torr the driver on valve V2 was manipulated so that P_R remained constant. On opening V3, P_R was found not to surge and to remain constant. The pressure in R could be increased or decreased by suitable adjustment of P_B and/or the conductance of V2.

Once the correct setting for the conductance of V2 had been found a further refinement in technique was adopted. Before letting gas into B via V1, the conductance of V2 was set to the predetermined torque. With D open gas was allowed into B and R until a pressure of 10^{-2} torr was registered on LKB 1. D was then closed and P_B allowed to increase to about 1 torr. In this way a good deal of time was saved and the second of the two alternative methods of operation discussed on page 65 could be applied.

II.8. CALIBRATION OF CAPILLARY 2

From equation II.9. it can be seen that the number of molecules of a given gas at a fixed temperature admitted through a capillary is given by the term

$$\text{constant} \times P_R \times t \qquad \text{II.37.}$$

Once the adsorption cell volume and the LKB Pirani gauges had been calibrated the value of this constant for capillary 2 was determined empirically. Nitrogen was allowed to flow from R into the adsorption cell for measured times t_1, t_2, etc. at a fixed value of P_R. The amount of gas admitted for each dose was determined from pressure measurements in the cell at room temperature and a knowledge of the volume of the adsorption cell system. The constant was found to have a value of $1{\cdot}10 \times 10^{15}$ for nitrogen at 298^0 K.

II.9. ACHIEVEMENT OF HIGH VACUUM

The techniques which were used are essentially those described by Redhead et al[48]. Initially the apparatus was pumped down from atmospheric pressure to about 5×10^{-3} torr by the rotary pump. With the 10 W oil diffusion pump the pressure dropped to about 1×10^{-6} torr. Pressures of about 1×10^{-7} torr were reached with the two ultra-high vacuum diffusion pumps. The oven and heating tapes were placed around the respective sections of the apparatus as indicated in Fig. II.3. The temperature of the heating tapes enclosing the two VTG traps was allowed to rise to about 280^{0}C. At the same time the temperature of all other bakeout sections was brought to 350^{0}C over a period of about 5 hours. It was necessary for the oven to be baked at a higher temperature than the VTG traps as this minimized the tendency for mercury vapour to diffuse into the hotter sections of the apparatus. Bakeouts were usually continued for a further 16 hours.

A special cooling down procedure was followed. The heating tape on the lower of the two VTG traps was switched off first and after this had cooled to about 80^{0}C (usually about 1 hour) the heating tape on the second VTG trap as well as the oven heaters were switched off. The oven was left in position and the first VTG trap was filled with liquid nitrogen over a period of about 60 minutes by which time filling of the second VTG trap had begun. The oven was removed after the temperature had reached about 60^{0}C.

The valves were degassed by opening and closing them repeatedly until no rise in pressure was detected during this operation. The ionization gauge head electrodes were degassed

by means of the circuit shown in Fig. II.10, in two stages:

(i) the filament alone by resistive heating and

(ii) grid and collector together by electron bombardment.

In the first stage the filament current was increased slowly over a period of about one hour to a maximum current of 7 amps at which point it was left for about 40 minutes. Thereafter the current was decreased slowly at the same rate. For the electron bombardment the grid and ion collector were interconnected and the filament current was increased slowly to 160 ma maximum and left at this level for about one hour. The current was decreased over an hour.

As soon as degassing of the gauge heads was completed the baking cycle was repeated. It was found that several cycles of degassing and baking were necessary as is stated by Ehrlich[44]. This was especially the case when the system had been allowed to rise to atmospheric pressure due to a leak or because glassblowing had been necessary.

It was found that once the apparatus had been thoroughly baked and degassed it was easier to achieve a good vacuum. Moreover after the apparatus had been flushed with pure nitrogen a good vacuum could be achieved by baking at temperatures as low as 200^0 C for short periods such as 8 hours.

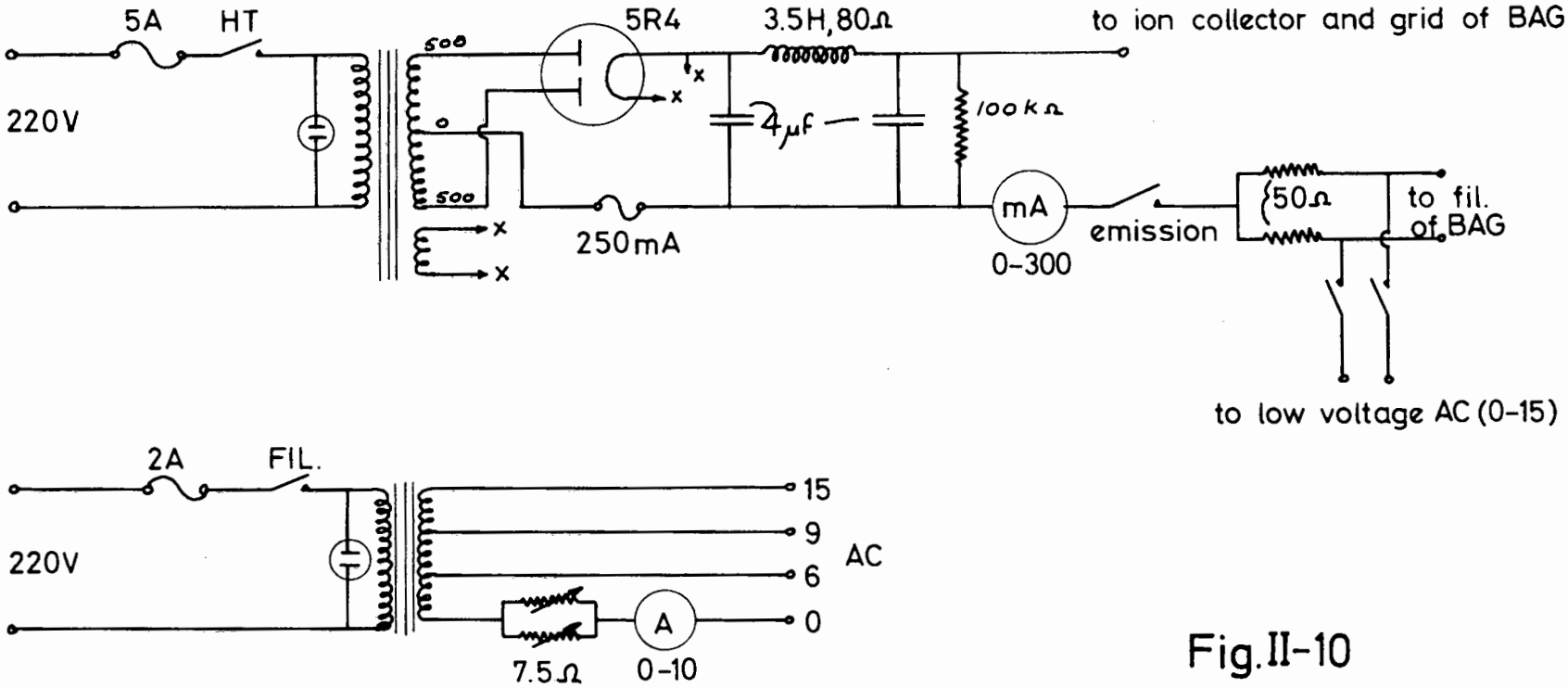

Fig.II-10

CIRCUIT DIAGRAM OF DEGASSING UNIT

C H A P T E R III.

ADSORPTION OF NITROGEN BY PYREX.

III.1. EXPERIMENTAL

Once pressures of the order of 10^{-8} torr had been obtained routinely and the apparatus established as leak proof, adsorption isotherms of nitrogen on Pyrex were measured. The adsorbing surface was the interior of a standard 0·5 litre spherical flask which had not been treated with solvents of any kind.

Preliminary experiments showed that equilibrium was not attained instantaneously and that adsorption was not significant at room temperature. Hence the method described on page 42 involving the adaptation of the pipette principle was used. Nitrogen was admitted to the adsorption volume through valve V3 until a desired pressure P_1, as observed on the ionization gauge (AIG Fig. II.3.) was attained. Valve V3 was then closed. The total number of molecules admitted to the adsorption volume was easily calculated from P_1. The adsorption flask was then immersed in coolant and the pressure fell to an observed value of P_2. The pressure in the cooled flask P_2' was obtained by correcting P_2 for thermomolecular flow (see Appendix 1). From P_2 and P_2' the number of molecules in the gas phase $n_2 + n_2'$ was obtained. The difference $n_1 - (n_2 + n_2')$ represented the number of molecules adsorbed.

As soon as equilibrium had been reached the coolant was removed and the flask was warmed to room temperature and the pressure P_1' measured. Comparison with P_1 showed that adsorption was reversible. The whole procedure was then repeated for aliquot 2.

Hobson[34] operated the ionization gauges continuously. The resulting ionic pumping gave a measurable time dependence

to the results and it was concluded that physical adsorption equilibrium was probably not achieved. Hobson and Armstrong[36] minimized this pumping action by operating the gauges intermittently. In the work described in this thesis the gauge was switched on every quarter hour and the pressure read after 30 seconds. Successive pressure readings which agreed were assumed to be the equilibrium pressure.

Adsorption isotherms were determined at 77^0K and 90^0K and heats of adsorption were calculated by using the Clausius-Clapeyron equation.

III.2. RESULTS AND DISCUSSION

Three adsorption runs at 77°K and three at 90°K were determined for nitrogen on Pyrex. The results of all the runs at both temperatures yielded straight lines when plotted in the co-ordinates of the Dubinin-Radushkevich adsorption isotherm equation. A typical set of results for each temperature is shown in Fig. III.1. The values of the constants of the six Dubinin-Raduskevich plots are given in Tables III.1. and III.2. together with those of Hobson and Armstrong[36] and Hobson.[35]

TABLE III.1.

		THIS WORK		HOBSON AND ARMSTRONG[36]	
TEMP.	RUN	B	σ_M	B	σ_M
77°K	1	$3{\cdot}62 \times 10^{-7}$	$6{\cdot}76 \times 10^{14}$	$3{\cdot}56 \times 10^{-7}$	$(5{\cdot}3 \text{ to } 6{\cdot}4) \times 10^{14}$
	2	$5{\cdot}97 \times 10^{-7}$	$6{\cdot}30 \times 10^{14}$		
	3	$4{\cdot}08 \times 10^{-7}$	$4{\cdot}47 \times 10^{14}$		

TABLE III.2.

		THIS WORK		HOBSON[35]	
TEMP.	RUN	B	σ_M	B	σ_M
90°K	1	$3{\cdot}28 \times 10^{-7}$	$3{\cdot}80 \times 10^{14}$	$3{\cdot}62 \times 10^{-7}$	$6{\cdot}4 \times 10^{14}$
	2	$4{\cdot}49 \times 10^{-7}$	$3{\cdot}72 \times 10^{15}$		
	3	$5{\cdot}45 \times 10^{-7}$	$4{\cdot}46 \times 10^{15}$		

Heats of adsorption were calculated at different coverages (see Table III.3.) and the variation of the heat of adsorption with coverage is shown in Fig. III.2.

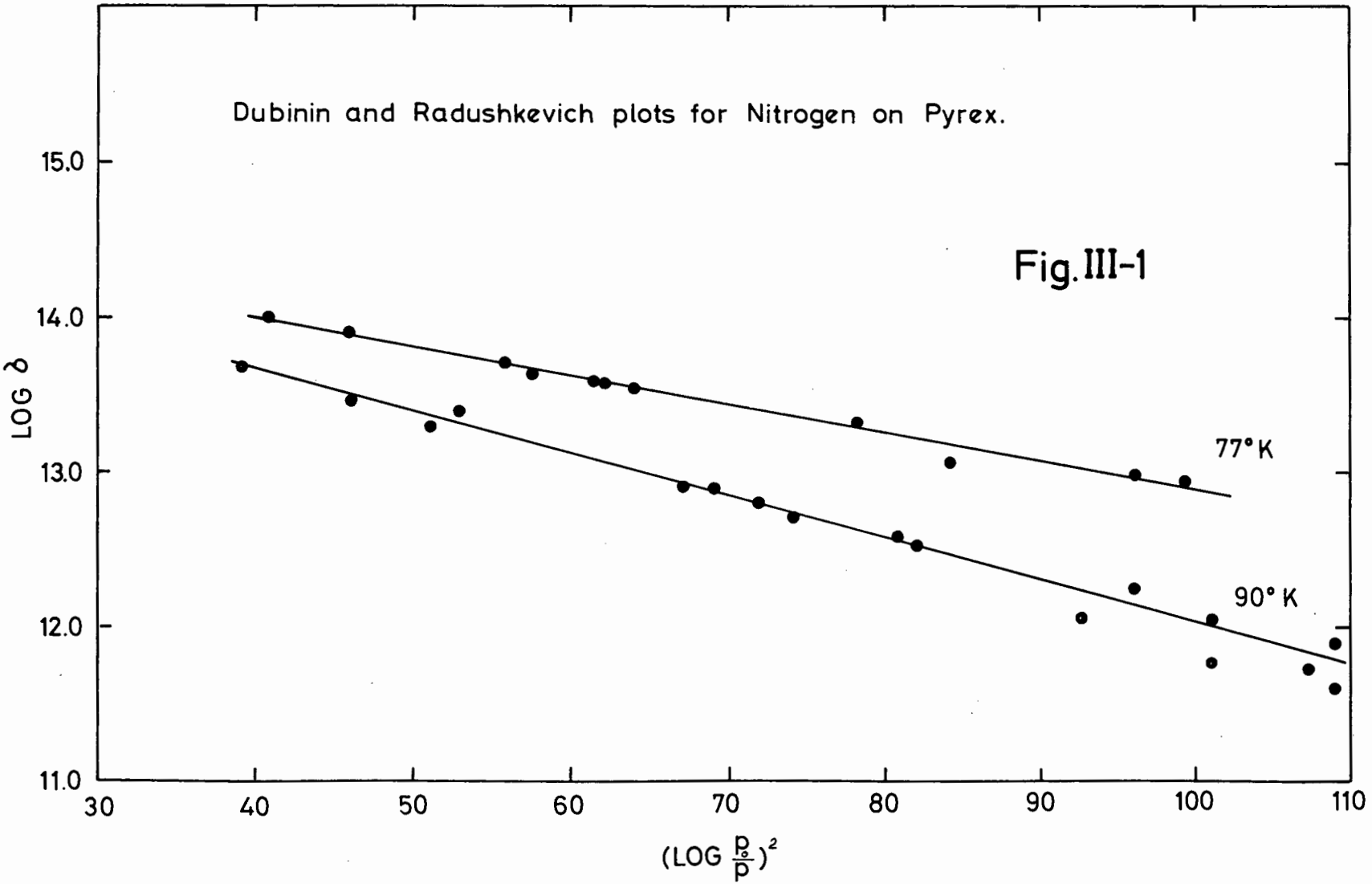
Dubinin and Radushkevich plots for Nitrogen on Pyrex.
Fig. III-1
LOG δ
15.0
14.0
13.0
12.0
11.0
30
40
50
60
70
80
90
100
110
77° K
90° K
(LOG $\frac{p_0}{p}$)^2

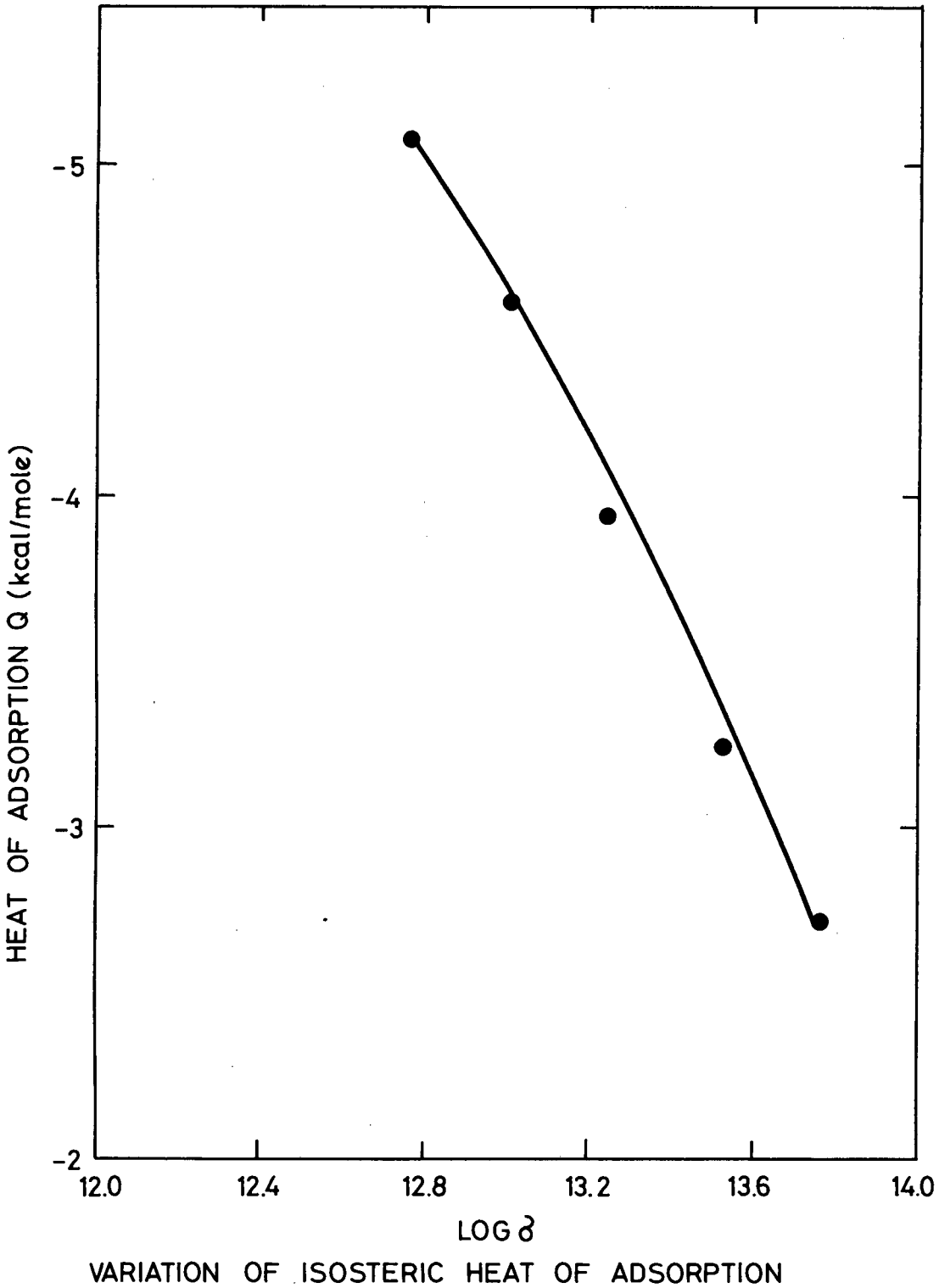

VARIATION OF ISOSTERIC HEAT OF ADSORPTION WITH COVERAGE FOR NITROGEN ON PYREX

Fig. III-2

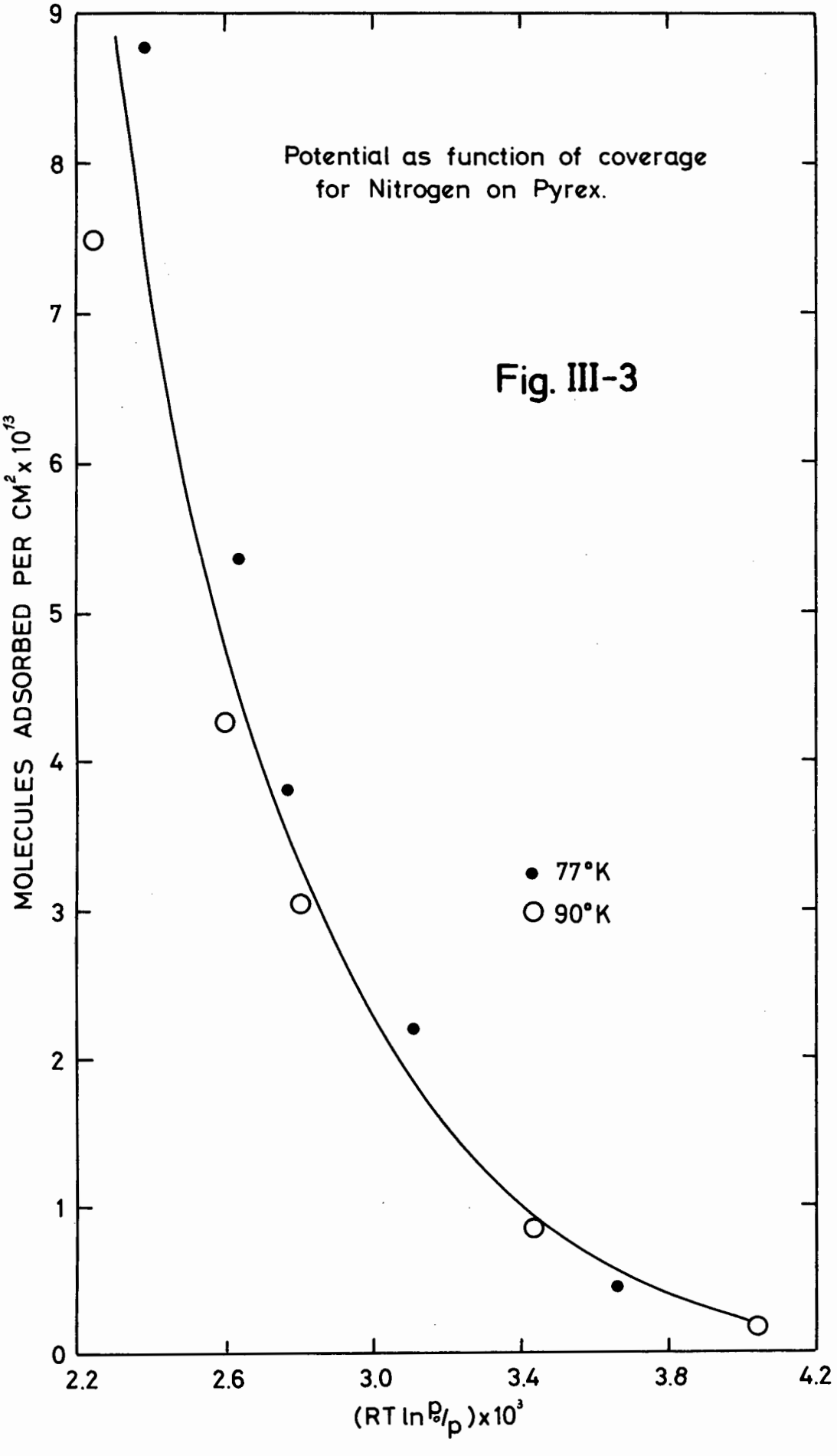
Potential as function of coverage
for Nitrogen on Pyrex.
Fig. III-3
MOLECULES ADSORBED PER CM² x 10¹³
(RT ln P₀/P) x 10³
77°K
90°K
0
1
2
3
4
5
6
7
8
9
2.2
2.6
3.0
3.4
3.8
4.2

C H A P T E R IV.

PREPARATION OF EVAPORATED FILMS OF ALKALI HALIDES.

IV.1. INTRODUCTION

Any experiment designed to study the physical or chemical properties of a surface whose composition is representative of the bulk material requires the preparation of a surface as free from contamination (in the form of any alien particles) as possible and the maintenance of this cleanliness for the duration of the experiment.

An atomically clean surface is "one free from all but a few percent of a single monolayer of foreign atoms, either adsorbed on or substitutionally replacing surface atoms of the parent lattice".[49]

Methods which have been used to generate clean surfaces include high temperature heating of the bulk material, cleaving of a crystal, bombardment (sputtering) of the substrate by noble gas ions and evaporation onto a substrate. These are now discussed briefly.

High Temperature Heating of Bulk Material.

Refractory metals such as tungsten, molybdenum, rhenium, tantalum, niobium, platinium and nickel as well as silicon and germanium may be cleaned by heating ribbons or wires of the desired material to a high temperature in an ultra-high vacuum. Such surfaces may be readily recleaned by merely flashing to a high temperature at very low pressures and may therefore be used for many experiments.

Cleaving of Single Crystals.

By cleaving a single crystal in a high vacuum, it is possible to expose a new surface which should be free from foreign contaminants. The method is limited to those materials which are brittle and easily fractured. A big

advantage of this technique is that clean surfaces may be prepared at room temperatures thus reducing the possibility of lattice deformation which may occur if the sputtering technique is used. The technique has been successfully applied to the semi-conductors InSb, GaAs, Bi_2Te_3, germanium[50] and silicon[51] as well as to a number of alkali halides[52].

Sputtering.

In this technique positive ions are accelerated at high velocity in a vacuum to a target surface (cathode) of the desired material thereby causing ejection of the surface atoms. These ejected particles travel in the vacuum and can be condensed onto a substrate in a similar way to that of evaporated atoms.

Many different types of sputtering apparatus have been developed for investigating the mechanism of sputtering but for the production of thin films two main types of sputtering principle may be distinguished.

(i) Diode sputtering: a discharge is formed in a gas at a pressure between 10^{-1} and 10^{-3} torr. This discharge supplies the high energy ions that are needed for the ejection.

(ii) Ion beams: here an ion beam is formed and is allowed to impinge on the target. The beam itself may be produced in a number of ways one of which involves the injection of electrons at 10^{-4} torr into a strong magnetic field causing the electrons to spiral. Ionization occurs and the resulting ions are attracted to the target.

Because of the relatively high pressures used and the high number of charged particles present the possibilities of contamination are very high. Thus the modern technique is to start with an ultra-high vacuum and subsequently to introduce a highly purified gas to the working pressure.

The method is generally useful with a large number of materials and it is also possible to deposit alloys of known composition.

Evaporation.

Perhaps the simplest method of producing a clean surface is by heating the material to its boiling or sublimation point in an ultra-high vacuum and causing the vapour to condense on a suitable substrate (eg. the walls of the adsorption cell). A vast number of metals and non-metals can be evaporated in vacuo. The technique has received considerable attention from Holland[53], Powell et al[54] and Anderson[55]. In addition to being a method that works well with many types of material, evaporation can be used to produce surface films of a large area.

In general, evaporated films consist of a random array of small crystallites. However by suitable experimental conditions, films of definite crystallographic faces can be prepared. In order to keep the evaporated film free from contamination the pressure in the apparatus must be kept very low (of the order of 10^{-9} torr)[49].

Among the several substances that have been successfully evaporated in vacuo are the alkali halides. Hall and Tompkins[56] prepared potassium chloride films in a residual gas pressure of 10^{-6} torr and Granville and Hall[22,23] prepared evaporated

films of lithium chloride, sodium chloride, potassium chloride and caesium chloride. Since clean alkali halide films have been successfully prepared by the evaporation technique the method was selected for this project. The technique is now discussed in detail.

IV.2. THE EVAPORATION TECHNIQUE

Source.

The source is really the fundamental component of an evaporation apparatus and is the point from which evaporation occurs. The configuration of the evaporator depends upon the nature of the material to be evaporated and may be divided into two main groups:

(i) those made from wire, such as helices or conical baskets as shown in Fig. IV.1.(a).

(ii) those constructed from foil bent into the form of troughs as in Fig. IV.1.(b).

Metals which can be used for filament heaters are those which have a high melting point and low volatility. They are, in decreasing order of their melting points, tungsten, tantalum, molybdenum, columbium, platinum, iron, nickel and chromel. Of these, tungsten, molybdenum and platinum are the most widely used.

Tungsten wire must be heated to about 100^0C if in the polycrystalline form and to 400^0C if highly annealed, before being wound into any particular shape of filament. Tantalum and molybdenum are easier to work with than tungsten, but tantalum is much more expensive. All three become brittle after being degassed at high temperatures in vacuo. Because of this Granville and Hall[22] used a platinum source.

The filament is made of several strands of wire since this provides more surface for the evaporant to wet. Surface tension prevents the molten evaporant from flowing out between the closely spaced turns. The open wound helix

(v) The evaporant must not form an alloy with the heater which has a melting point below the temperature of evaporation.

Preparation of the Substrate.

Prior to evaporation it is important that the walls of the adsorption cell on which the film is to be deposited be free from such contaminants as grease, oil and adsorbed water. The degree of durability and adhesion is dependent primarily on this basic requirement. Various chemical methods have been devised for cleaning glass surfaces prior to evaporation. Modern detergents such as Teepol can be used with success[53]. The glass surface can be cleaned further with cotton wool dipped in iso-propyl alcohol[56]. Holland[57] has found iso-propyl alcohol to be a more effective degreasing solvent than the chlorinated hydrocarbons. Final cleaning may be accomplished by baking the surface in vacuo or by high velocity ion bombardment.

Degassing of the Source and Contents.

This aspect of the evaporation technique is crucial for the successful preparation of a clean film. Most authors merely state that prior to evaporation the source, material to be evaporated and leads must be thoroughly degassed but only a few give detailed accounts of how this is to be done.

Several workers interpret the change in the pressure during evaporation as an indication of the cleanliness of evaporated films. Hickmott and Ehrlich[58] in the preparation of tungsten films found a pressure rise from 5×10^{-10} to 4×10^{-8} torr indicating that their films had been contaminated. These films were discarded and the next evaporation was carried out in short bursts. This time they found that there was

no noticeable rise in pressure during evaporation. Hayward[43] prepared tungsten films in a background pressure of (2 to 5) x 10^{-10} torr and rejected any films for which the pressure rose to 10^{-8} torr during evaporation.

A commonly used method of degassing is described, amongst others, by Brennan and Graham[59] who prepared a number of evaporated metal films. All metals were thoroughly degassed, sometimes over a period of several days by heating to just below the evaporation temperature and periodically flashing to a temperature at which some evaporation occurs. Anderson and Baker[60] prepared tungsten films in a cell which had been baked to 350°C for 15 hours the last hour of which the filament was degassed by resistive heating. For nickel films the cell was baked to 350°C for 15 hours during the whole time of which the filament was heated. Anderson's technique was recommended by Granville[61] for the preparation of alkali halide films using platinum filaments.

After a film has been prepared the adsorption cell should be baked before adsorption measurements are made. This is necessary since most evaporated films are porous with a high surface area to weight ratio. If formed at low temperatures they may be somewhat unstable owing to their high surface energy and should therefore be sintered at a temperature above that reached in any subsequent part of the experiment.

Hall and Tompkins[56] prepared potassium chloride films (ca. 0.3 g.) by passing a current through a conical basket of molybdenum and containing a pellet of the A.R. chloride. Granville and Hall[22,23] prepared films of potassium, sodium,

caesium and lithium chloride using a basket constructed of 26 s.w.g. platinum wire instead of molybdenum as the latter became brittle on heating. Films of about 0.3 to 0.5 grams were deposited using a current of 5 amps. for 70 minutes.

Fig. Ⅳ-2

(a)

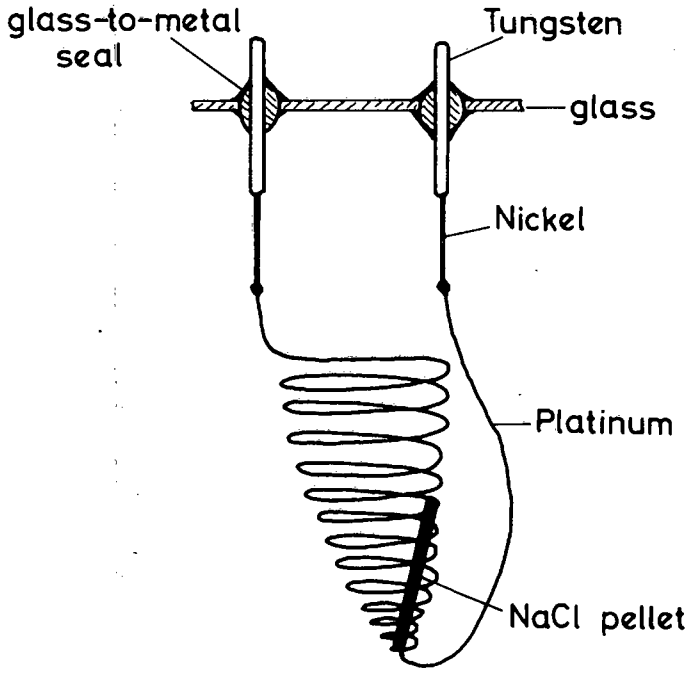
glass-to-metal seal
Tungsten
glass
Nickel
Platinum
NaCl pellet

(b)

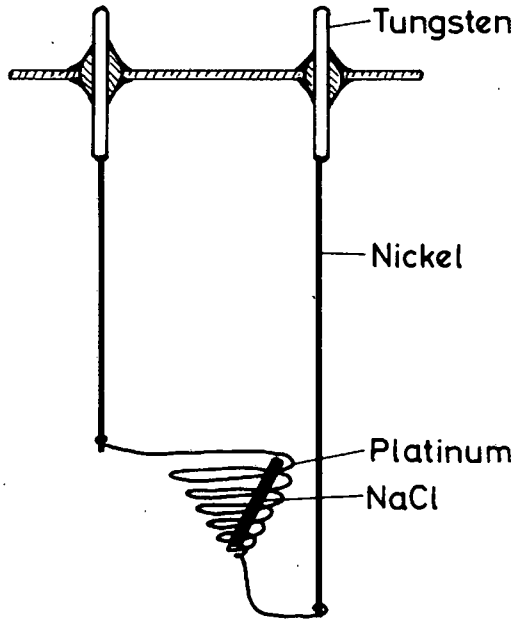
Tungsten
Nickel
Platinum
NaCl

The literature does not give much detail on the actual dimensions of evaporation sources although a fair idea might be obtained from the photographs given by Dushman[42]. Granville gave the following information, in private correspondence, concerning the size of the basket used in his experiments[23]. The diameter at the top of the cone was 13 mm, the height 7 mm and it consisted of 4 turns of 26 s.w.g. platinum wire.

For the second attempt a basket similar to Granville's was constructed. The length of wire used was a portion of that used for the first filament since it had previously had a high current passed through it and was consequently very soft, it was hoped that further resistive heating would not cause significant buckling. Before actually sealing the basket into the cell two precautionary measures were adopted. Firstly, a high current was applied to the filament to test whether any sagging would take place. Secondly, a pellet of sodium chloride was placed in the basket and a gradually increasing current passed through it. In this way it was possible to test:

(a) whether the sodium chloride could in fact be evaporated;

(b) whether the coils were closely spaced enough for the liquid sodium chloride to be held by surface tension and

(c) to see what current was required to cause the sodium chloride to evaporate.

In fact, a knowledge of (c) is very useful since the platinum coil and sodium chloride may be degassed in vacuo, prior to evaporation, by applying a slightly lower current.

The second design of conical basket and reaction cell is shown in Fig. IV.2(b). Comparison with the first design (Fig. IV.2(a).) reveals the following improvements.

(i) The basket is supported from underneath by a length of nickel and not by the platinum itself.

(ii) The height and number of turns of wire are just sufficient to encase the pellet thereby reducing the overall weight of the basket and the likelihood of its sagging when heated.

It has been necessary to discuss this part of the evaporation technique in detail since the literature is rather vague on this aspect of the work.

Subsequently two films of sodium chloride were successfully prepared and adsorption measurements made on them. (The preparation of the films is discussed later in this section while the adsorption measurements are described in Chapter V).

After determining low coverage isotherms on the third film the latter was transferred to another apparatus in order that additional measurements might be made. (The reasons are discussed in Chapter V). To facilitate the transfer and at the same time to avoid contaminating the film the features shown in Fig IV.3. were incorporated in the cell design. A double walled constriction was included in the tubulation connecting the cell to the rest of the apparatus. A break seal of the type discussed on page 59 and shown in Fig. II.6. was incorporated into an arm parallel to the interconnecting tube.

Experimental.

Pellets of A.R. sodium chloride from The British Drug Houses Ltd., England, were prepared in a hydraulic press under 300 Kg cm^{-2} pressure (cf Granville[23]). The weights of the pellets used were between 0·1 and 0·4g.

In the preparation of the first sodium chloride film it was found, prior to sealing the basket into the cell, that a current of ca 3 amps. was needed to evaporate the sodium chloride. The filament was degassed for ca 3 hours by passing a current of 2·5 amps. through it at a pressure of about 10^{-7} torr. Thereafter the entire apparatus was baked at 250°C for about 12 hours. At the commencement of the evaporation a background pressure of 5×10^{-8} torr was recorded. The film was deposited by passing a current of 3 amps. through the coil for about 70 minutes with the adsorption cell held at 0°C. However the pressure rose to 2×10^{-4} torr and the film was thus rejected. The degassing had thus been inadequate.

For the second pellet (0·16 g.) a more rigorous degassing procedure was followed. This time a current of 2 amps. was passed through the coil for several hours while the whole adsorption apparatus was baked at 250°C. The filament was occassionally flashed for a second or two to 4 amps. After degassing the coil in this manner the apparatus was baked for a further 15 hours at 250°C. During the deposition of this film, A, the pressure did not rise above $5{\cdot}0 \times 10^{-7}$ torr. Adsorption runs were subsequently carried out with this film.

The next film, B (0·44 g.), was prepared in the same manner and a number of runs at different temperatures were

TRANSFERABLE REACTION CELL

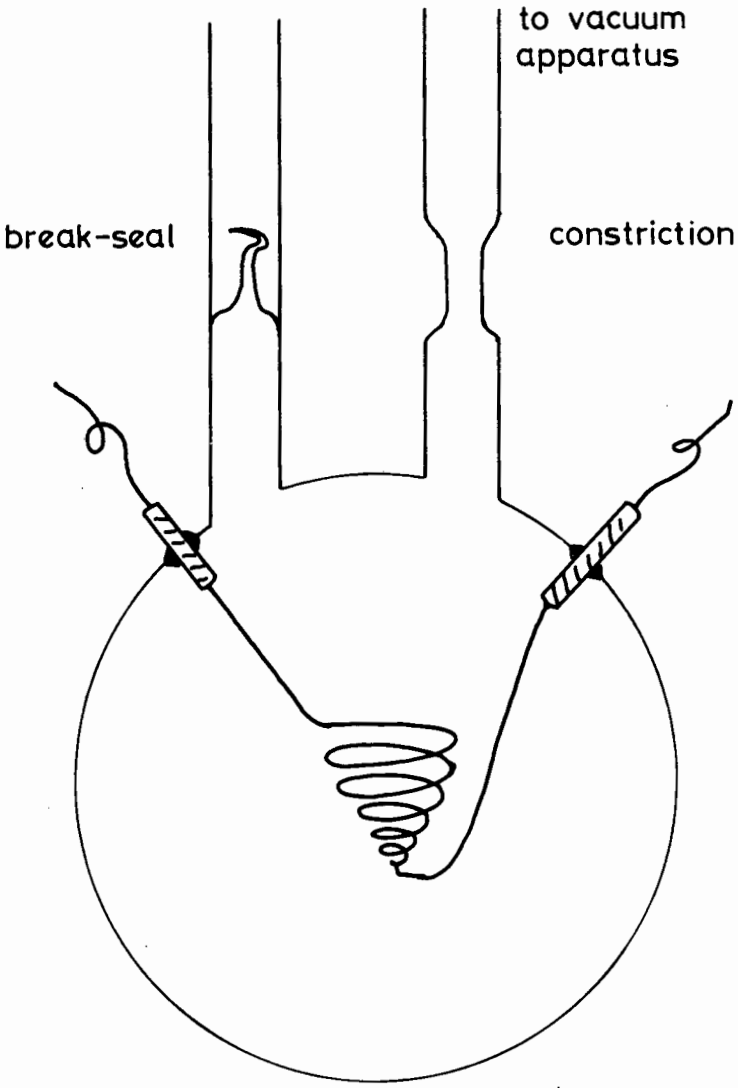

Fig. Ⅳ-3

carried out.

Film C (0.43 g.) was prepared in the transferable adsorption cell (Fig. IV.3.) under similar conditions to those used for films A and B. After adsorption measurements had been made on the ultra-high vacuum apparatus the film was successfully transferred to another apparatus where more measurements were made.

IV.4. DISCUSSION

In using the evaporation technique there is a danger of contaminating the film with impurities arising from the metal of which the heating coil is constructed. No matter how well the filament is degassed, gases sorbed by it will be set free when evaporation is carried out since the current used for evaporation is higher than that used for degassing. Since metals tend to sorb particularly large quantities of gas very tenaciously the degassing process is time consuming and tedious. The glass - to - metal seals necessary for making electrical connections to the heating basket are very fragile and prone to develop leaks.

Because of the above disadvantages the following novel and simple ideas are suggested. Instead of using the conical basket method the pellet could be placed in a small side-arm made of silica which is joined to the Pyrex sample bulb by means of a glass - to - silica seal (see Fig. IV.4.(a).). After degassing the side-arm and contents by means of a heating mantle, heating tape or flame, the sample bulb is surrounded by a suitable refrigerant and the temperature of the side-arm raised sufficiently to vapourize the pellet. The vapour then condenses on the cooled walls of the sample bulb. The side-arm must be of silica since the very high temperatures required to vapourize the pellet would cause Pyrex glass to melt. With this arrangement there is no longer the problem of degassing the filament. There are no foreign metals present in the cell and no glass - to - metal seals. The glass - to - silica seal is probably less likely to develop leaks. Yet another advantage lies in the fact that it is very simple to construct.

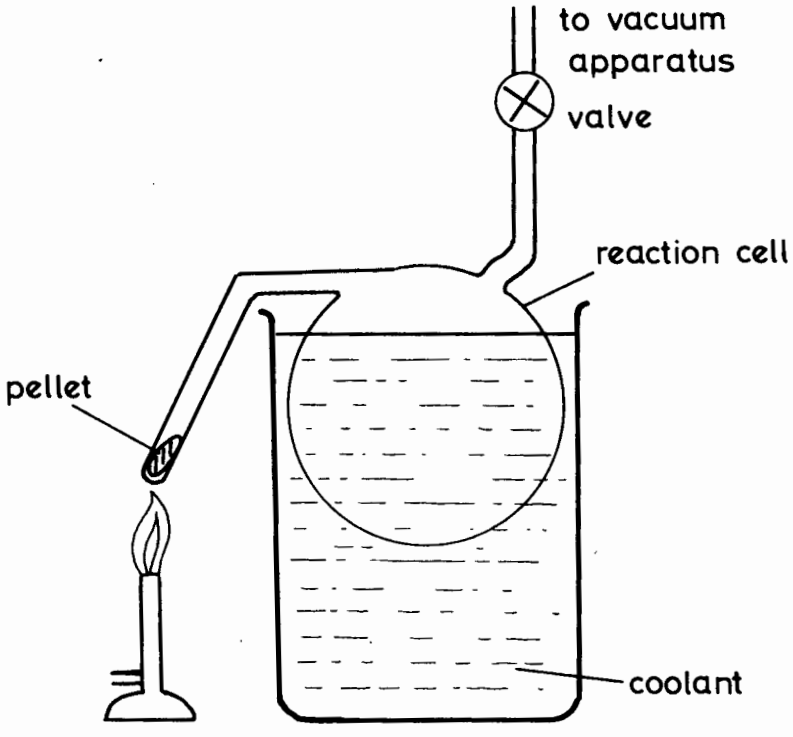
to vacuum
apparatus
valve
reaction cell
pellet
coolant

(a)

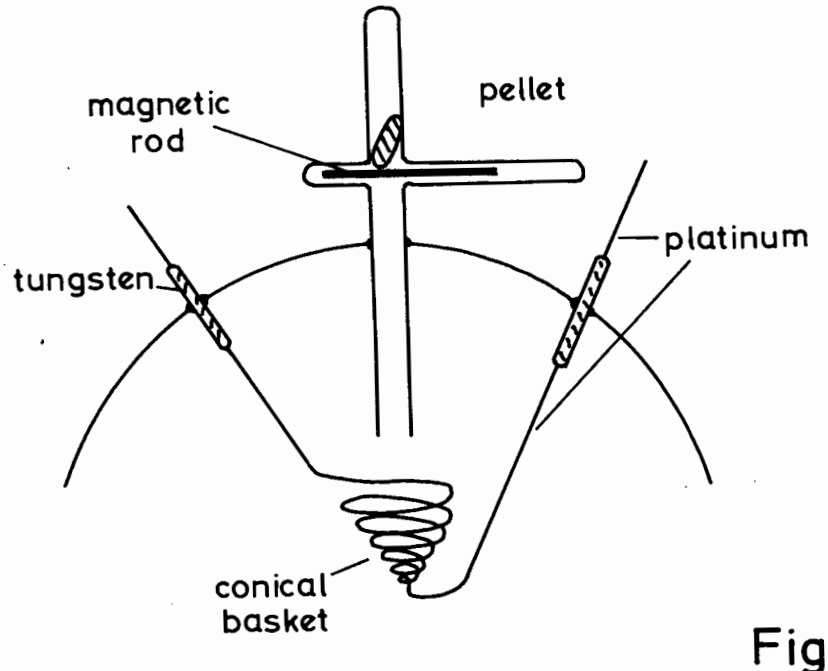
magnetic
rod
pellet
platinum
tungsten
conical
basket

(b)

Fig. Ⅳ-4

Fig. IV.4.(b). shows a second suggested arrangement which will enable the heating basket to be thoroughly degassed. The pellet is held by means of a magnetic rod, in a narrow tube which extends vertically into the cell to a point just above the mouth of the conical basket. The rod may be moved into a side-arm by means of a magnet thereby allowing the pellet to drop down the tube which directs it into the evaporator.

After film C had been transferred to the second apparatus and several adsorption runs determined, it became necessary to regrease the stop-cock used to admit adsorbate to the adsorption cell (see Fig. A.1.). Because this would have required exposing the film to the atmosphere it could not be done. Consequently, after a few more adsorption runs the stop-cock developed a serious leak and the film had to be discarded. This could have been avoided if two stop-cocks in series had been present in the tubulation leading to the adsorption cell. The one furthest from the cell is used to admit adsorbate. When it requires a regrease, the stopcock below it is closed. In this way the film will not be exposed to the atmosphere.

C H A P T E R V.

ADSORPTION OF NITROGEN AND ARGON BY EVAPORATED FILMS OF SODIUM CHLORIDE.

V.1. EXPERIMENTAL

Once the films had been prepared preliminary experiments were carried out to determine how rapidly equilibrium was attained. Aliquots of nitrogen were admitted to the adsorption cell system. The cell itself was immersed in coolant. After Valve V3 was closed the pressure as read on AIG (see Fig. II.3.) did not drop significantly showing that equilibrium was virtually instantaneous.

To determine adsorption isotherms, it was found best to use the second of the procedures described in section II.6. on page 65. The measured pressures were corrected for thermal transpiration effects (see Appendix 1) using equations A.1.(8). and A.1.(9). for the very high pressures and equation A.1.(1). for the lower pressures.

The adsorption of nitrogen by all three films was investigated and in addition a few measurements of the adsorption of argon by film B were made. Nitrogen isotherms on films A and C were determined at 77^0K (liquid nitrogen) and 90^0K (liquid oxygen). For film B measurements were also made at 81^0K (liquid air mixture) and 87^0K (liquid argon). For the argon isotherms measurements were made at 77^0K, 81^0K and 87^0K. The temperature of the liquid air mixture was measured with an iron-constantan thermo-couple which had been calibrated against nitrogen and liquid oxygen. The temperature of the liquid air did not remain constant for very long and consequently only a few results could be obtained at this temperature.

The liquid argon was obtained by passing the gas from a cylinder into a 2 litre spherical pyrex flask immersed in a large Dewar filled with liquid nitrogen.

V.2. RESULTS.

Only a few measurements were made of the adsorption of nitrogen by film A (0·16 g) at 77° K and 90° K since a leak developed in the apparatus and the film had to be discarded. However, the results obtained gave a straight line when plotted in the co-ordinates of the Freundlich adsorption isotherm

$$\log N = {}^{1}/_{F'} \log P + \log K. \qquad \text{V.1.}$$

The values of ${}^{1}/_{F'}$ and log K are given in Table V.1. together with those obtained for films B and C.

The results for the adsorption of nitrogen by film B (0·44 g) at 77° K, 81° K, 87° K and 90° K are given in Fig. V.1. and the Freundlich plots are given in Fig. V.2.
The straight lines drawn through the points were determined by simple linear regression analysis. The curves in Fig. V.1. have been obtained directly from the four straight lines in Fig. V.2. by using the respective constants of these lines (Table V.1.) in the Freundlich equation to calculate the theoretical curve. Not many results were obtained at 81° K owing to difficulties in keeping the temperature constant.

The adsorption of argon by film B is shown in Fig. V.3. and the Freundlich plots in Fig. V.4. The values of ${}^{1}/_{F'}$ and K are given in Table V.2. The straight lines drawn through the points in Fig. V.4. were determined by simple linear regression analysis and the curves as in Fig. V.5. were calculated using the constants of the straight lines.

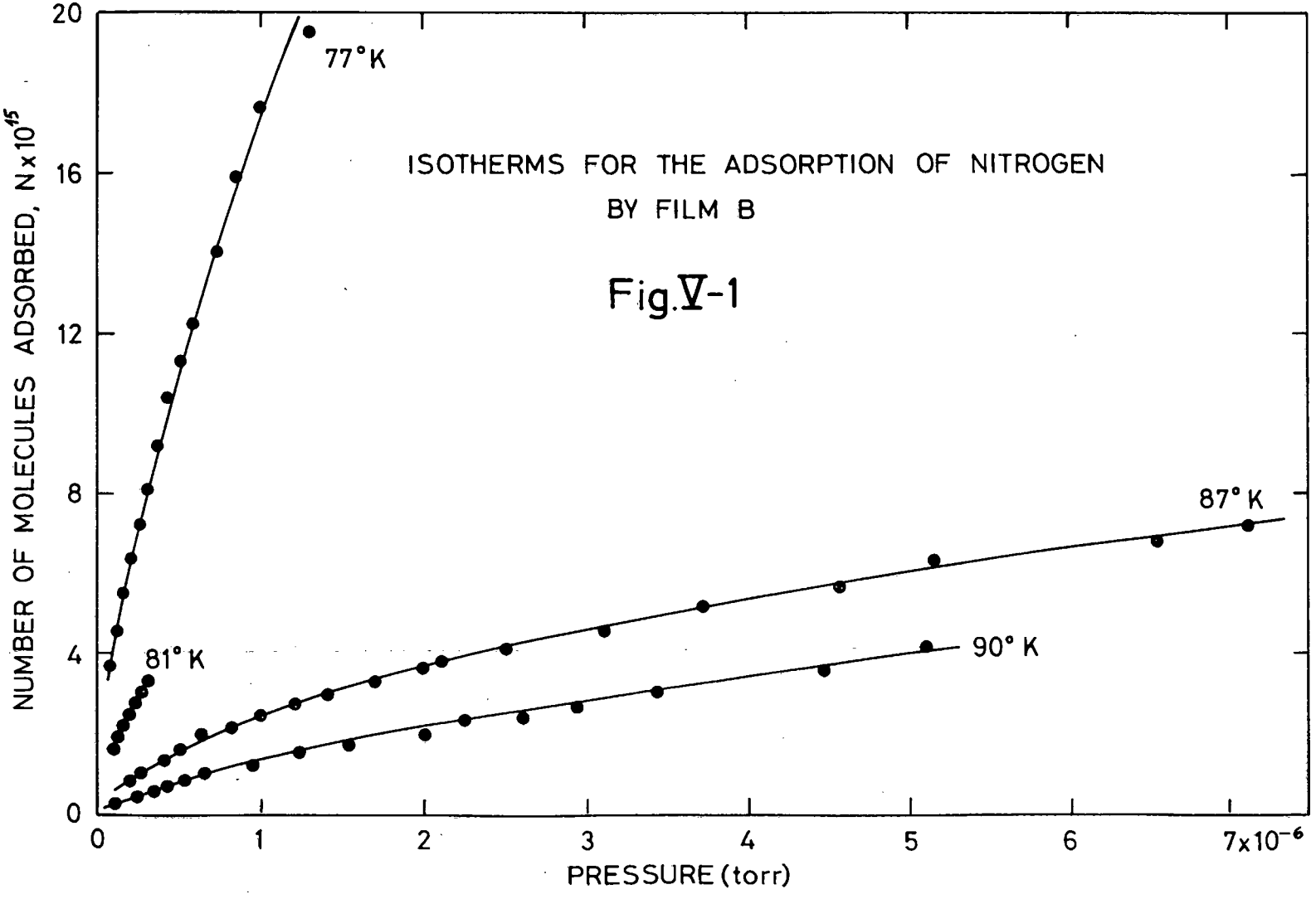
ISOTHERMS FOR THE ADSORPTION OF NITROGEN
BY FILM B
Fig.V-1
NUMBER OF MOLECULES ADSORBED, N x 10^15
PRESSURE (torr)
77° K
81° K
87° K
90° K
0
4
8
12
16
20
1
2
3
4
5
6
7x10^-6

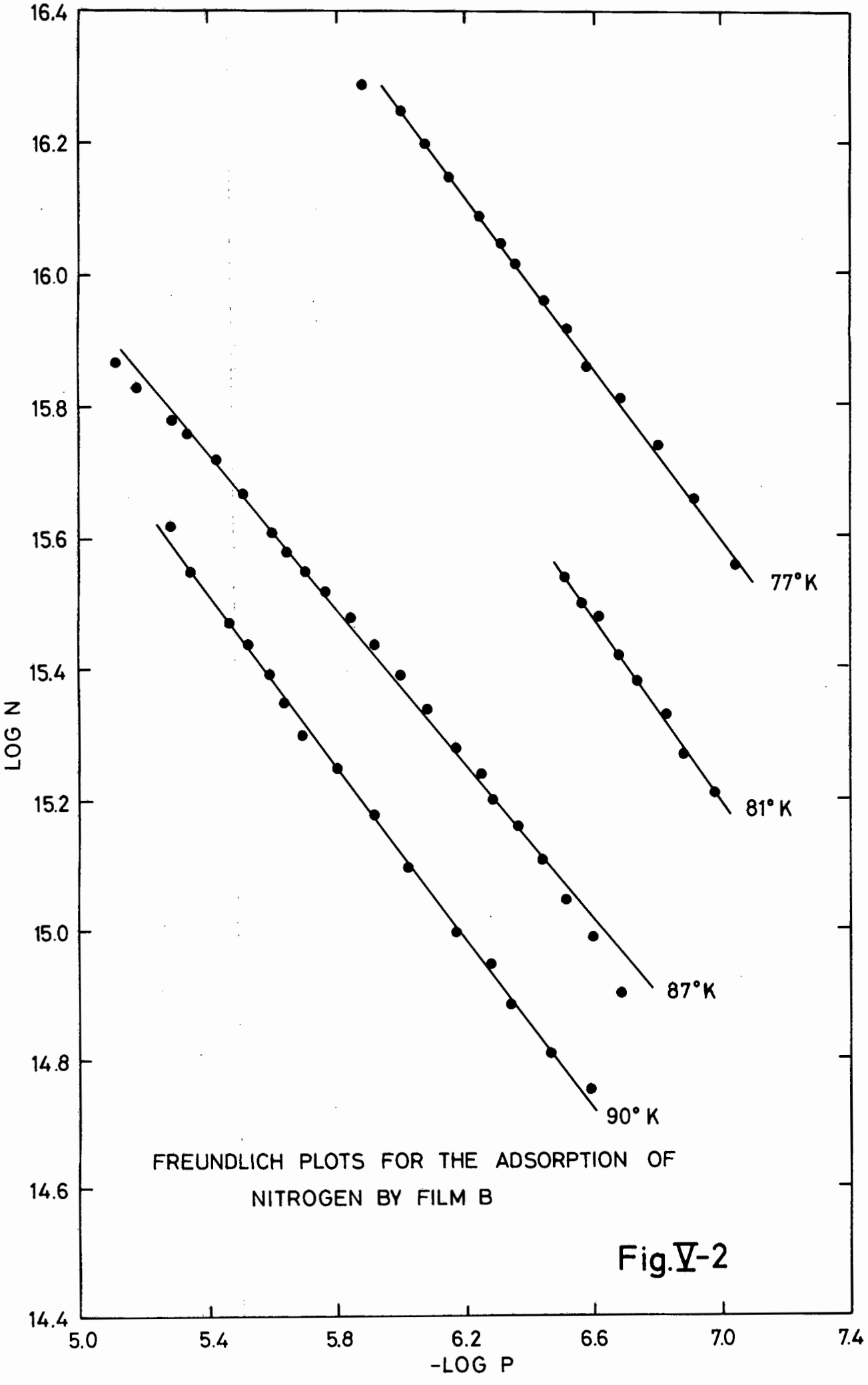

FREUNDLICH PLOTS FOR THE ADSORPTION OF NITROGEN BY FILM B

Fig.V-2

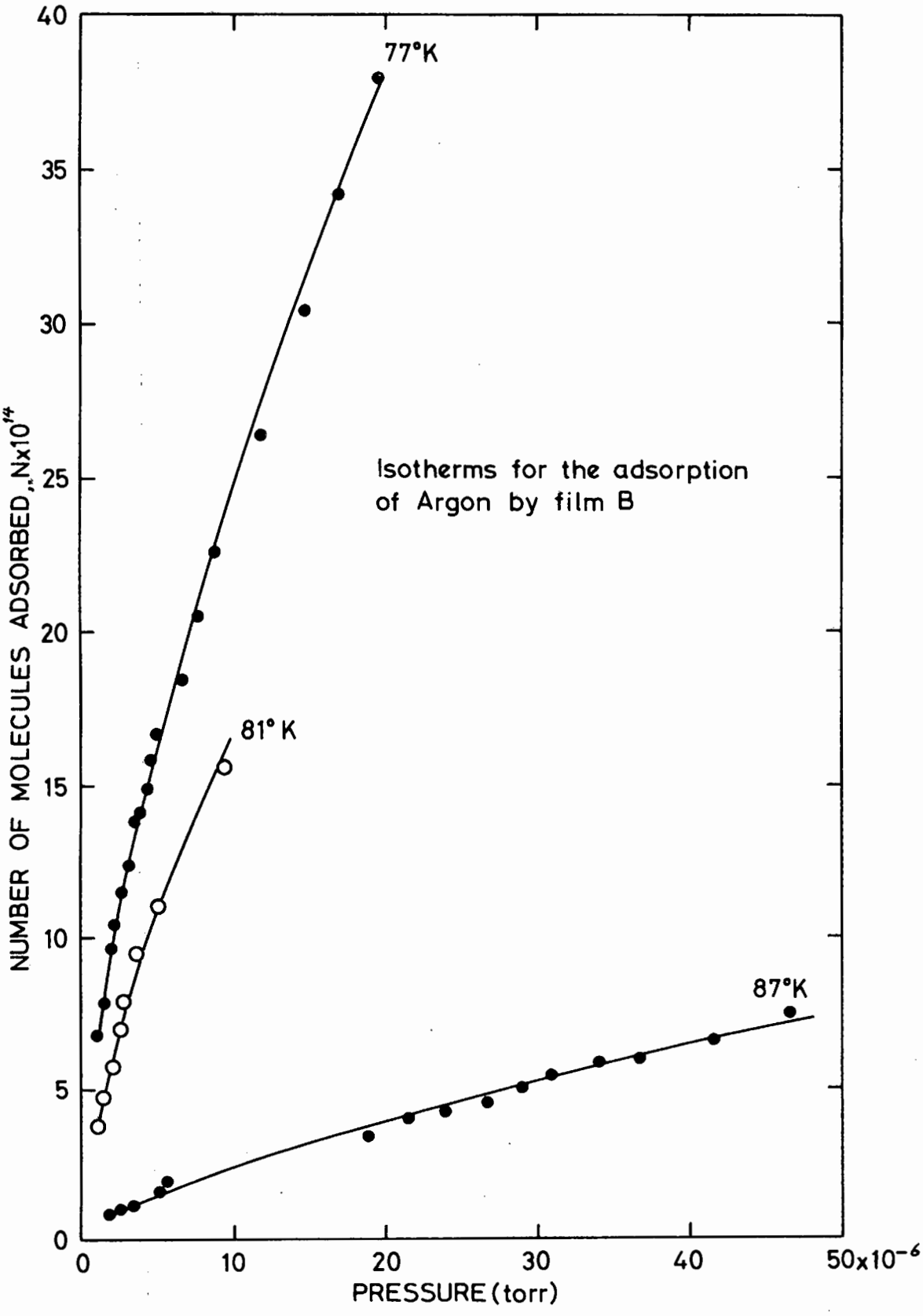
77°K
81° K
87°K
Isotherms for the adsorption
of Argon by film B
NUMBER OF MOLECULES ADSORBED, N x10^14
PRESSURE (torr)
0
5
10
15
20
25
30
35
40
0
10
20
30
40
50x10^-6

Fig. V-3

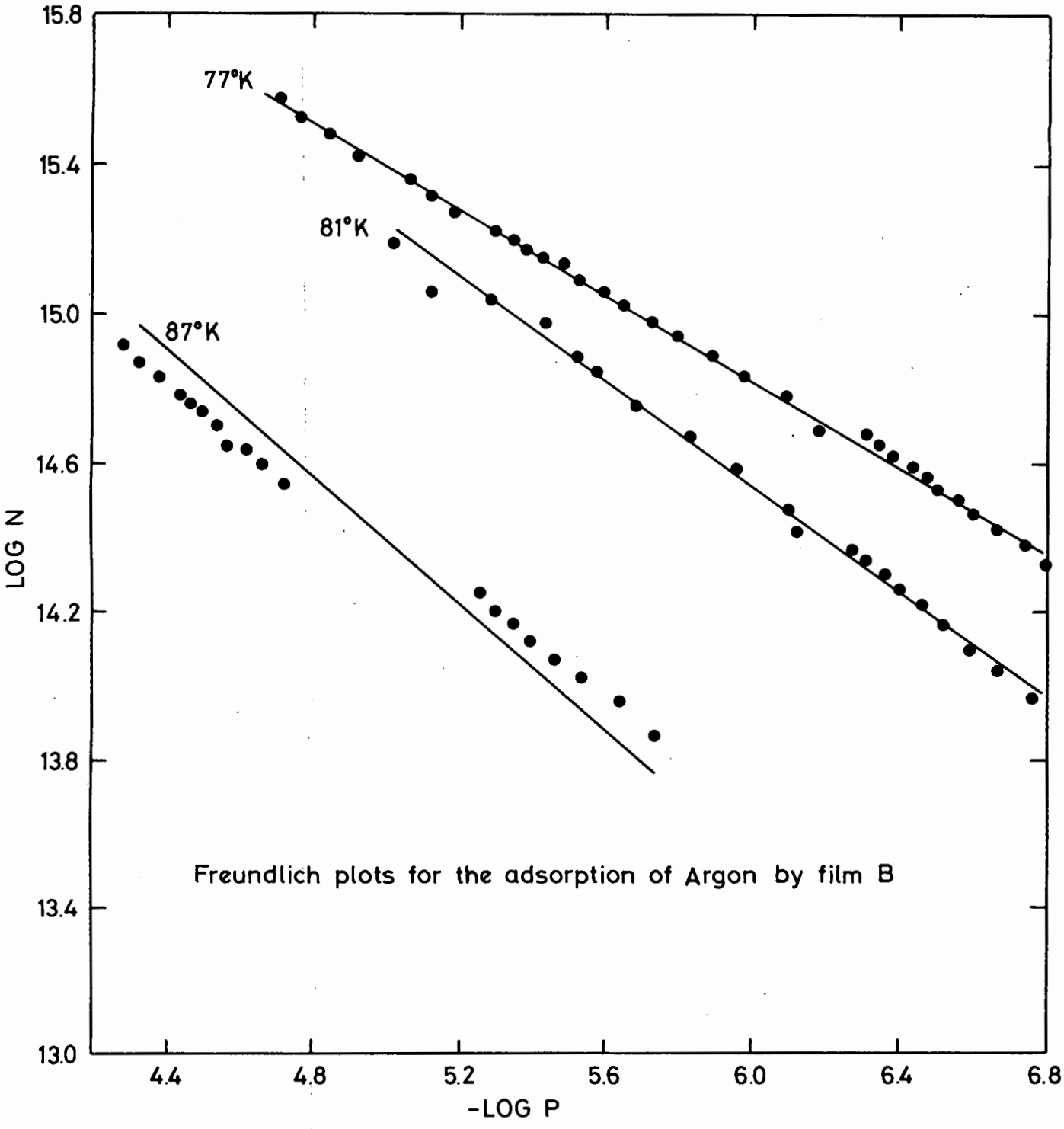

Freundlich plots for the adsorption of Argon by film B

Fig. V-4

TABLE V.1.

	FREUNDLICH CONSTANTS FOR NITROGEN				
	TEMP. ^{0} K	77	81	87	90
FILM A	$1/F'$	0.54			0.65
	log K	19.5			18.9
FILM B	$1/F'$	0.63	0.69	0.60	0.70
	log K	20.0	20.0	19.0	19.3
FILM C	$1/F'$	0.71			0.74
	log K	19.9			18.8

TABLE V.2.

	FREUNDLICH CONSTANTS FOR ARGON ON FILM B		
	77	81	87
$1/F'$	0.58	0.68	0.68
log K	18.3	18.7	17.8

The isosteric heats (equation I.15) and entropies (equation I.18) of adsorption for nitrogen and argon are given in Table V.3. and V.4. respectively.

Fig. V.5. shows the variation of the heats and entropies with coverage for argon. The initial heat of adsorption, obtained by extrapolation of the heat curve for argon (Fig.V.5.) to zero coverage is -2.9 k.cal.mole^{-1}. From Table V.3. it can be seen that the heats for nitrogen were found to be constant over the range of coverage investigated.

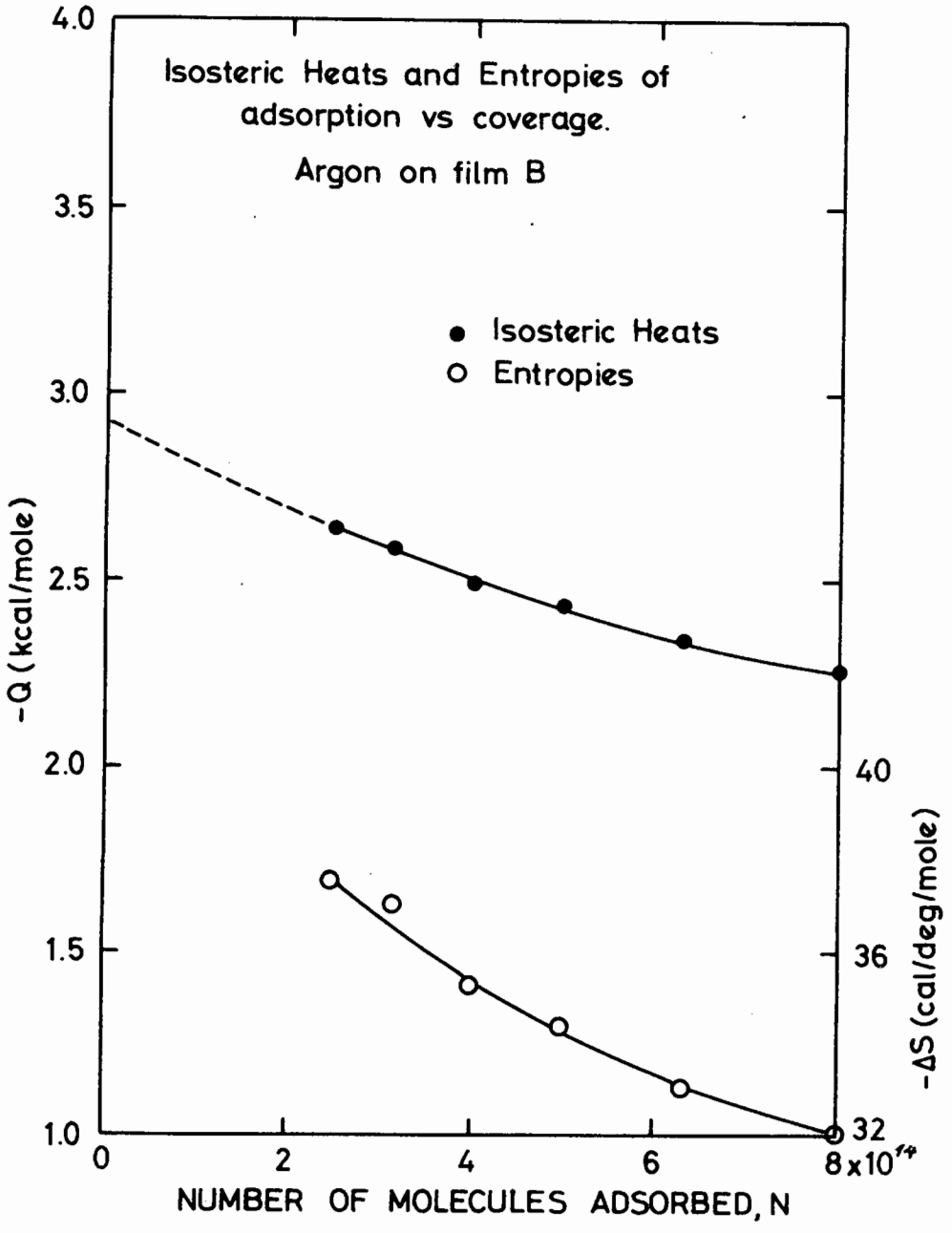
Isosteric Heats and Entropies of adsorption vs coverage.
Argon on film B
Isosteric Heats
Entropies
-Q (kcal/mole)
-ΔS (cal/deg/mole)
4.0
3.5
3.0
2.5
2.0
1.5
1.0
40
36
32
0
2
4
6
8x10^14
NUMBER OF MOLECULES ADSORBED, N

Fig.V-5

vacuum apparatus it was necessary to devise a means of transferring the film to the apparatus described in Appendix 3 where the high coverage measurements could be made. The reaction cell has already been described. (section IV.3., Fig. IV.3.). Film C (0·43 g) was prepared in this cell and the Freundlich plots at 77^0K and 90^0K over the entire range of coverage investigated are shown in Fig. V.6. The isotherm plots, N against P over the range $17{\cdot}5 \leqslant \log N \leqslant 18{\cdot}6$, obtained with the apparatus shown in Fig. A.1. (Appendix 3) are shown in Fig. V.7. The curve drawn through the points at 90^0K was calculated from the least squares slope and intercept for log N vs. log P values in the same range. The curve through the points at 77^0K was obtained by inspection. Isosteric heats and entropies of adsorption in this range were determined from the curves shown in Fig. V.7. In the lower coverage range ($15{\cdot}5 \leqslant \log N \leqslant 17{\cdot}5$) isosteric heats and entropies were determined from the straight lines shown in Fig. V.6. which were obtained by inspection. The values are given in Table V.5. and the variation with coverage is shown in Fig. V.8. The values of the fractional coverage θ were obtained by determining the surface area of film C from Krypton adsorption measurements and applying the BET theory (Appendix 4.) The cross sectional area of Krypton[23] was taken as 19·5 Å^2 which yielded a value for the surface area of 3·89 m^2. From the latter the monolayer coverage, N_m, for nitrogen was deduced to be $2{\cdot}40 \times 10^{19}$ molecules. The cross sectional area of one closely packed nitrogen molecule was taken to be 16·2 Å^2.

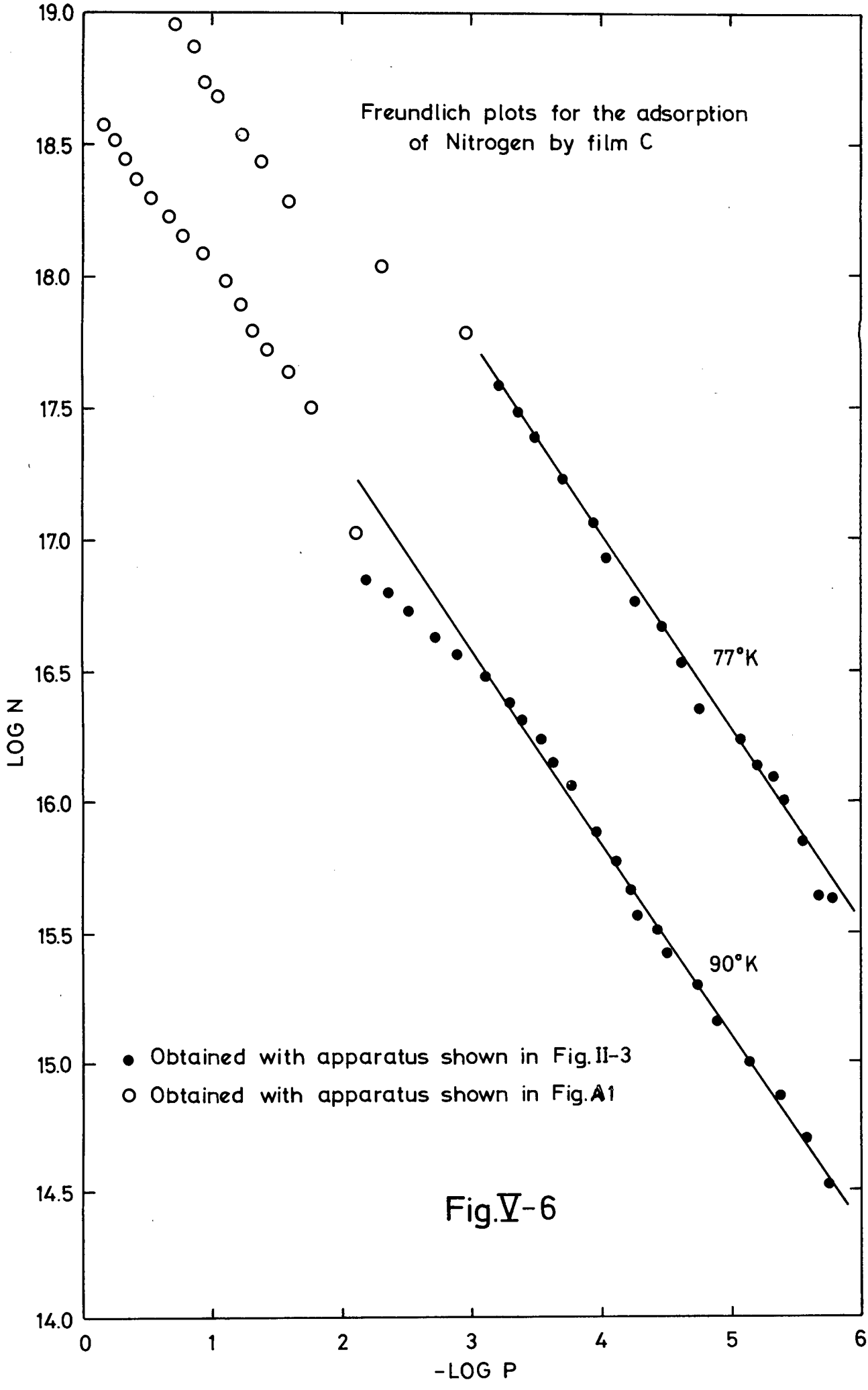
Freundlich plots for the adsorption
of Nitrogen by film C
77°K
90°K
● Obtained with apparatus shown in Fig. II-3
○ Obtained with apparatus shown in Fig. A1
LOG N
-LOG P
19.0
18.5
18.0
17.5
17.0
16.5
16.0
15.5
15.0
14.5
14.0
0
1
2
3
4
5
6

Fig. V-6

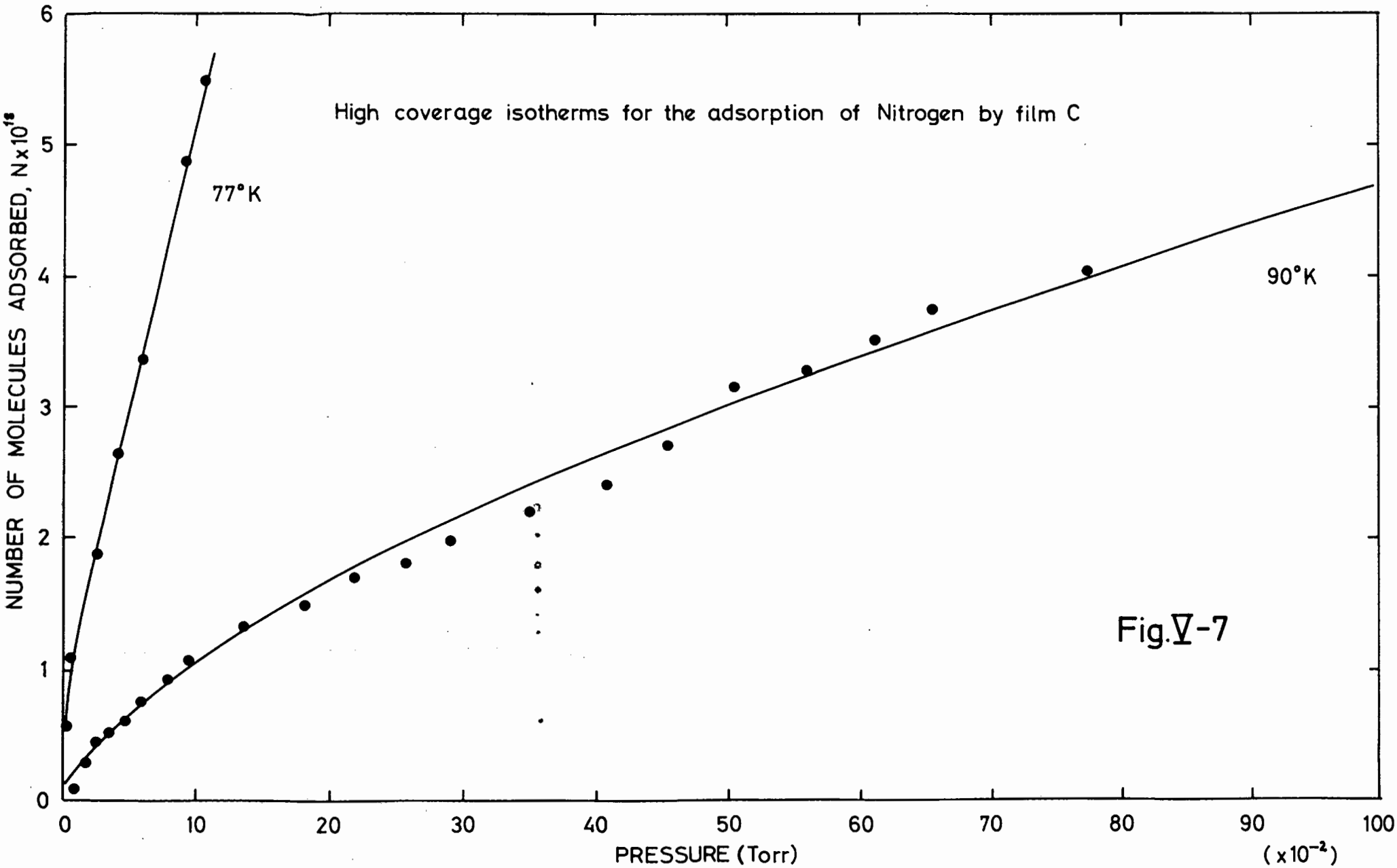
High coverage isotherms for the adsorption of Nitrogen by film C
77°K
90°K
NUMBER OF MOLECULES ADSORBED, N x 10^15
PRESSURE (Torr)
(x 10^-2)
0
1
2
3
4
5
6
0
10
20
30
40
50
60
70
80
90
100

Fig.V-7

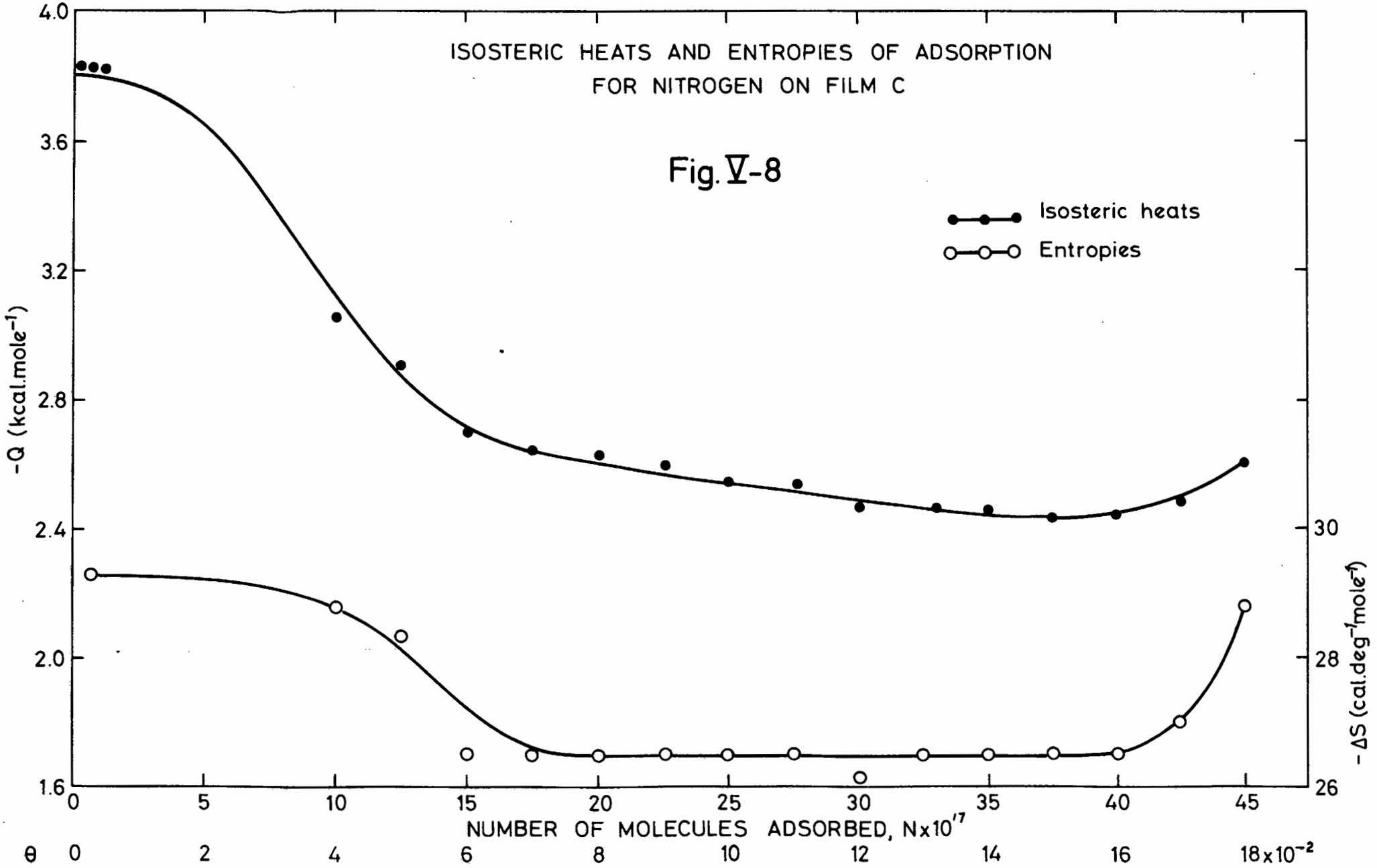
ISOSTERIC HEATS AND ENTROPIES OF ADSORPTION
FOR NITROGEN ON FILM C
Fig. V-8
Isosteric heats
Entropies
-Q (kcal.mole⁻¹)
-ΔS (cal.deg⁻¹mole⁻¹)
NUMBER OF MOLECULES ADSORBED, Nx10¹⁷
θ
4.0
3.6
3.2
2.8
2.4
2.0
1.6
30
28
26
0
5
10
15
20
25
30
35
40
45
2
4
6
8
10
12
14
16
18x10⁻²

V.3. DISCUSSION.

The general shapes of the isotherms for the different films were concave to the pressure axis as shown in Figs. V.1., V.3. and V.7. and are thus similar to those obtained by Hayakawa[16] on cubic sodium chloride crystals. That the results are well represented by the Freundlich isotherm is shown by the good fit of the calculated curves to the experimental points although in the latter case (Fig. V.7.) the curve was only calculated for the results at 90^0 K. In general[42] the value of K in the Freundlich isotherm equation decreases with increase in the temperature while the value of $^1/F'$ increases. An examination of Table V.1. shows this to hold for the results obtained in this work but in the cases of nitrogen at 87^0K and argon at 81^0K on film B these trends are not obvious. The respective values of the constants vary somewhat for the different films but seem to be of comparable magnitude.

Roughly speaking, the intercept of the Freundlich plots gives a measure of the adsorbent capacity. For film C the average value of the intercept is log K = 19·4 (Table V.1.). Hence $N_m = 2.5 \times 10^{19}$ for nitrogen molecules. This is in good agreement with the value of $2{\cdot}40 \times 10^{19}$ determined from the krypton surface area measurements. The Freundlich intercept, log K, for film B has an average value of 19·6 (Table V.1.) which corresponds to a nitrogen monolayer coverage of about $N_m = 4 \times 10^{19}$ molecules. Thus the θ values corresponding to the N values in Table V.3. range from 4×10^{-5} to $1{\cdot}6 \times 10^{-4}$. For argon log K was found to have an average value of 18·3 (Table V.2.) corresponding to $N_m = 2 \times 10^{18}$ molecules.

The coverages in Table V.4., therefore, cover the range of θ from about 1×10^{-4} to 4×10^{-4}.

The isosteric heats of adsorption for films B and C were found to be constant over the ranges $4 \times 10^{-5} \leqslant \theta \leqslant 1{\cdot}6 \times 10^{-4}$ (Table V.3.) and $1{\cdot}3 \times 10^{-4} \leqslant \theta \leqslant 2{\cdot}3 \times 10^{-3}$ (Table V.5.) respectively. For film B results at higher coverages were not obtained but the results for film C show that in the range of coverage $\theta > 2{\cdot}3 \times 10^{-3}$ the heats of adsorption decreased as the coverage increased (Fig. V.8.). There are indications of a minimum in the heat of adsorption of about 2·5 k. cal $mole^{-1}$ in the region $\theta = 1{\cdot}5 \times 10^{-1}$. The results however, do not extend to a sufficiently high enough coverage for this to be conclusive. Nevertheless the indicated minimum is close to Hayakawa's[16] value of 2·25 k. cal $mole^{-1}$. An untimely leak in the vacuum apparatus precluded any further measurements on film C. Time did not permit the preparation of another film and hence investigations over a more extensive range of θ.

The values of the initial heat of adsorption for nitrogen on films B and C (3·9 and 4·2 k. cal $mole^{-1}$) are in agreement but are far in excess of Hayakawa's experimental (2·67 k. cal $mole^{-1}$) and theoretical value (2·40 k. cal $mole^{-1}$).

The initial heat of adsorption for argon (2·9 k. cal $mole^{-1}$) in this work is however in better agreement with Hayakawa's experimental value (2·19 k. cal $mole^{-1}$) although the calculated value[16] is 1·98 k.cal $mole^{-1}$.

The high heat of adsorption found for nitrogen compared with argon is attributed to the quadrupole interaction of the nitrogen molecules with the surface.

The discrepancy between the experimentally found heat for nitrogen and Hayakawa's theoretical value can be accounted

for by the fact that Hayakawa's theoretical value includes an uncertain calculation of the quadrupole interaction energy of nitrogen. However this quadrupole interaction energy is unlikely to be of such a large magnitude as the difference between the experimental and theoretical heats. The discrepancy may however be explained in the same way in which Granville and Hall[23] explained the discrepancies which they found in the calculated and experimentally determined heats of adsorption for krypton and nitric oxide on the 100 face of sodium chloride. They point out that Hayakawa's[16] results are for the (100) plane of sodium chloride whereas their sample might have been exposing some other crystalline face. This may indeed be the case for film C especially since Schulz[25] has observed the predominance of the (110) plane in evaporated films of sodium chloride. The latter has a more open structure than the (100) plane and so it is reasonable to expect a higher interaction on the (110) plane.

A comparison of the initial heat of adsorption of argon as determined experimentally in this work may be made with the heat for krypton experimentally determined by Granville and Hall[23] ($3{\cdot}6$ k.cal.mole^{-1}). This can be done on the approximate basis mentioned on page 14, using the intermolecular energy parameters for these adsorbates. The equilibrium separation energies for argon and krypton are[24] $1{\cdot}46 \times 10^{14}$ and $1{\cdot}97 \times 10^{14}$ ergs respectively. These are in the ratio $0{\cdot}71$. Thus the heat for argon should be $0{\cdot}71 \times 3{\cdot}6$ k.cal.mole^{-1}. The resulting value of $2{\cdot}6$ k.cal.mole^{-1} is in good agreement with the value $2{\cdot}9$ k.cal.mole^{-1} found in this work. This indicates the possibility of Granville and Hall's[23] sodium chloride film being of the same crystal orientation as film B.

A constant heat of adsorption with increasing coverage is often interpreted as a compensation effect between surface heterogeneity and mutual attractions. The former gives rise to decreasing heats while the latter results in an increase in the heats of adsorption. If both effects are equally present the resultant heat of adsorption would be constant. However, a simple calculation shows for films B and C that the average spacing between adsorbed nitrogen molecules at a coverage of about $\Theta = 1 \times 10^{-4}$ is of the order of several hundred Å at which separation van der Waals attractions are certainly negligible. It appears therefore that adsorption has occurred on the most active sites which have been exposed owing to the rigorously clean conditions under which the films were deposited. These sites evidently form a group of uniform adsorptive activity and heterogeneity only becomes apparent at coverages of about $\Theta = 2 \times 10^{-3}$ (Table V.5., Fig. V.8.).

The results for argon on the other hand (Table V.4., Fig. V.5.) indicate a trend of decreasing heats of adsorption with increasing coverage over the range $1 \times 10^{-4} \leqslant \Theta \leqslant 4 \times 10^{-4}$. The results for argon are thus in direct contrast to the interpretation for nitrogen. It was consequently necessary to determine entropies of adsorption so that a deeper insight into the nature of the adsorbed molecules could be made.

The entropies were calculated on the following basis. Two extreme cases were considered;

(i) a mobile non-localized film and

(ii) an immobile localized film.

(i) Mobile non-localized film.

In general the differential entropy change for the transfer of a gas in a standard state of P = 1 atmosphere at T^0K to a mobile adsorbed film in a standard state in which the intermolecular separation[63] is given by $a^0 = 4{\cdot}08T \times 10^{-16}$ cm^2 (coverage θ_s). may be determined from the expression

$$-\Delta\dot{S}_t = \frac{R}{2}\ell n\, M + \frac{R}{2}\ell n\, T + 2{\cdot}30 + R. \qquad V.2.$$

Equation V.2. is obtained[3] from equations I.19. and I.28. and must now be corrected for the transfer of the gas from the adsorbed standard state to a mobile adsorbed film in a state corresponding to a coverage θ. Thus

$$-\Delta\dot{S}_t = \frac{R}{2}\ell n\, M + \frac{R}{2}\ell n\, T + 2{\cdot}30 + R + R\,\ell n\left[\frac{\theta}{1-\theta}\Big/\frac{\theta_s}{1-\theta_s}\right] + R\left[\frac{1}{1-\theta} - \frac{1}{1-\theta_s}\right]. \qquad V.3.$$

The value for $\Delta\dot{S}_t$ obtained from equation V.3. must be compared with $\Delta\dot{S}_\theta$ (from equation I.18.). If they are comparable the implication is that the adsorbed film behaves as a two dimensional gas with translational freedom only.

The rotational entropy contribution may be obtained by using equation I.21. Since nitrogen has only one moment of inertia equation I.21. becomes

$$-S_r = R\,\ell n\,\frac{1}{\pi\sigma'}\left[\frac{8\pi^3.A^*.k.T.}{h^2}\right]^{\frac{n^*}{2}} + \frac{Rn^*}{2}. \qquad V.4.$$

The constants for the nitrogen molecule are[24] $\sigma' = 2$, $A^* = 13.81 \times 10^{-40}$ g.cm^2. For 1 degree of freedom, $n^* = 1$. The value of S_r so obtained can be added to $\Delta\dot{S}_t$ (equation V.3.) and compared with $\Delta\dot{S}_\theta$ (equation I.18.). If there is good agreement the implication is that the adsorbed film is a two dimensional gas with two translational and one rotational degree of freedom.

(ii) Immobile localized film.

In this case the standard state cannot be selected in the same way as that for the mobile adsorbed film:[3] the distance of closest approach of two adsorbed molecules is determined by the spacing of the adsorption sites and not solely by the molecular dimensions of the adsorbate. The standard state can therefore be selected for convenience of calculation and is chosen as $\theta_s = 0.5$. Differentiation of equation I.26. and combination with equation I.28 yields

$$\Delta\dot{S}_c = -\left[\frac{3}{2} R \ln M + \frac{5}{2} R \ln T - 2.31 + R \ln \frac{\theta}{1-\theta}\right] \quad \text{V.5.}$$

This represents the differential entropy change associated with the transfer of a gas in a standard state of 1 atmosphere to an adsorbed localized film in a standard state corresponding to $\theta = 0.5$. If $\Delta\dot{S}_c$ and $\Delta\dot{S}_\theta$ are comparable the implication is that the adsorbed film is localized and immobile with no rotational or vibrational freedom.

Using equations V.3., V.4., and V.5. the respective entropies were calculated. These, together with the experimental values, are shown in Tables V.6. (nitrogen on film B), V.7. (argon on film B) and V.8. (nitrogen on film C).

TABLE V.6.

ENTROPIES OF ADSORPTION - NITROGEN ON FILM B.

$N \times 10^{15}$	θ	$-\Delta\dot{S}_\theta$ EXPERIMENTAL	$-\Delta\dot{S}_t$	$-\Delta\dot{S}_t - S_r$	$-\Delta\dot{S}_c$	$-\Delta\dot{S}_c - S_r$
1.59	3.99×10^{-5}	19.8	-2.28	-0.46	9.48	11.29
1.78	4.47×10^{-5}	19.8	-2.05	-0.24	9.70	11.52
2.00	5.02×10^{-5}	20.8	-1.82	-0.01	9.94	11.75
2.24	5.63×10^{-5}	20.3	-1.59	0.22	10.16	11.98
2.51	6.31×10^{-5}	20.8	-1.37	0.45	10.39	12.20
2.82	7.08×10^{-5}	21.3	-1.14	0.67	10.62	12.43
3.16	7.94×10^{-5}	20.8	-0.91	0.90	10.85	12.66
3.55	8.92×10^{-5}	22.9	-0.68	1.13	11.08	12.89
3.98	1.00×10^{-4}	21.0	-0.45	1.36	11.30	13.12
4.47	1.12×10^{-4}	21.5	-0.23	1.59	11.53	13.34
5.01	1.26×10^{-4}	22.9	0.01	1.82	11.76	13.58
5.62	1.41×10^{-4}	24.3	0.23	2.04	11.99	13.80
6.31	1.51×10^{-4}	24.3	0.37	2.18	12.12	13.94

TABLE V.7.

ENTROPIES OF ADSORPTION - ARGON ON FILM B.

$N \times 10^{14}$	θ	$-\Delta\dot{S}_\theta$ EXPERIMENTAL	$-\Delta\dot{S}_t$	$-\Delta\dot{S}_c$
2.51	1.26×10^{-4}	37.52	0.33	12.74
3.16	1.58×10^{-4}	37.07	0.78	13.19
3.98	2.00×10^{-4}	35.24	1.25	13.65
5.01	2.51×10^{-4}	34.32	1.70	14.10
6.31	3.16×10^{-4}	32.95	2.16	14.56
7.94	3.98×10^{-4}	32.03	2.62	15.02

TABLE V.8.

ENTROPIES OF ADSORPTION - NITROGEN ON FILM C.

θ	$-\Delta\dot{S}_\theta$ EXPERIMENTAL	$-\Delta\dot{S}_t$	$-\Delta\dot{S}_t - S_r$	$-\Delta\dot{S}_c$	$-\Delta\dot{S}_c - S_r$
1.31×10^{-4}	22.88	0.09	1.90	11.84	13.65
7.42×10^{-4}	26.08	3.53	5.34	15.29	17.10
2.34×10^{-3}	29.29	5.83	7.64	17.58	19.39
5.21×10^{-2}	28.37	12.20	14.01	23.84	25.66
7.29×10^{-2}	26.54	12.96	14.77	24.56	26.37
9.38×10^{-2}	26.54	13.55	15.36	25.10	26.91
1.15×10^{-1}	26.54	14.06	15.87	25.55	27.37
1.35×10^{-1}	26.54	14.47	16.28	25.92	27.73
1.56×10^{-1}	26.54	14.86	16.68	26.25	28.07
1.77×10^{-1}	27.00	15.23	17.04	26.56	28.37

From Table V.6. it can be seen that neither of the two extreme models considered gives good agreement with the experimental entropies. However it appears that the immobile localized model gives better agreement although quite obviously other effects such as vibration must be significant to account for the discrepancies between the experimental and theoretical values. Hayakawa[16] on the other hand found that the vibrational entropy contribution of nitrogen on cubic sodium chloride was negligible. For argon the immobile localized model is again favoured but the differences between $\Delta\dot{S}_\theta$ and $\Delta\dot{S}_c$ are much greater than for nitrogen. This indicates that the nature of the adsorption for argon may be different from that for nitrogen. Possibly the argon molecules are occupying a different set of sites from the nitrogen. From Table V.8.

for film C it can be seen that there is very good agreement between the values of $\Delta\dot{S}_\theta$ and $\Delta\dot{S}_c$ especially at coverages $\theta > 5{\cdot}2 \times 10^{-2}$. On the other hand the values of $\Delta\dot{S}_t$ are not even remotely close to the values of $\Delta\dot{S}_\theta$ and seem to tend toward zero at the lower coverages. Thus it appears that the nitrogen molecules adsorbed on film C are strongly localized. Furthermore, rotational as well as vibrational contributions seem to be significant since the discrepancy between $-\Delta\dot{S}_c$ and $-\Delta\dot{S}_\theta$ becomes greater towards the lower coverages.

The appearance of negative values for $-\Delta\dot{S}_t$ (Table V.6.) may at first sight seem surprizing as this indicates an increase in the entropy upon adsorption. However, this may be explained as follows. Simple calculations show that at $83{\cdot}5^0$K and under 1 atmosphere pressure the seperation between molecules in the gas phase is $2{\cdot}2 \times 10^{-7}$ cm. When $\theta \leqslant 1{\cdot}1 \times 10^{-4}$, $-\Delta\dot{S}_t$ is negative. The separation between the adsorbed molecules, when $\theta = 1{\cdot}1 \times 10^{-4}$, may be shown to be $3{\cdot}8 \times 10^{-6}$ cm. Since this separation is over 10 times greater than that of the free gas, the latter in becoming adsorbed has undergone an effective expansion. Now the isothermal expansion of a gas is accompanied by an increase in the entropy. Hence $\Delta\dot{S}_t$ is negative because the entropy increase associated with this 'expansion' overrides the entropy decrease associated with the loss of translational freedom. From Table V.8. it can be seen that the entropy approaches zero with decreasing coverages and had measurements been made on film C at lower coverages, $-\Delta\dot{S}_t$ would no doubt have become negative.

The discrepancy that occurs between $\Delta\dot{S}_c$ and $\Delta\dot{S}_\theta$ towards lower coverages presumably must be attributed in part to the increase in entropy associated with the effective expansion of the gas.

In the light of the above considerations it appears that both adsorbed nitrogen and argon may be reasonably well described in terms of the localized model.

CHAPTER VI.

GENERAL DISCUSSION

VI. GENERAL DISCUSSION

Owing to the fact that a considerable amount of time was spent on commissioning the apparatus, objectives (c) and (d) outlined on page 30 were not completely met. Perhaps the most frustrating aspect of vacuum work is the detection of leaks. In this work no leak detector was available and hence the methods used to find a particular leak were rather unsophisticated and very time consuming. Because of its very large overall size and the great number of independent component parts it usually took a considerable time to restore the efficient functioning of the apparatus. Consequently it was not possible to extend the adsorption investigations to other alkali halide adsorbents as had been hoped. The work presented here too should have been extended to include wider ranges of coverage and temperature so that more conclusive interpretations could have been obtained. Nevertheless the results obtained in this work have been rigorously treated and much has been derived from them.

Ehrlich[44] states that one of the golden rules of attaining ultra high vacuum pressures is to maximize the pumping speed. The author would like to add a corollary, namely, that the volume which is to be evacuated must be as small as is practically possible. The total volume of the apparatus used in this project was far too large for the two ultra high vacuum diffusion pumps to handle and consequently pressures of only 10^{-8} torr could be obtained routinely. The excess volume arose from the glass bellows which had to be connected to each valve and also from interconnecting tubulation. Although these are very necessary components of the vacuum line the author feels that if the resultant slow pumping speed had been foreseen, greater care would have been taken to construct the apparatus

more compactly with a minimum wastage of dead volume.

A serious limitation in the construction of the apparatus was the absence of an ionization gauge head at R in addition to LKB 2. Although in the design of the apparatus it had been decided to keep the pressure in R constant at a level of 1×10^{-2} torr it was experimentally found that this value of P_R resulted in the initial equilibrium pressure increase being larger than was desirable. With an ionization gauge at R it would have been possible to read much lower values of P_R than with the LKB Pirani gauge only.

The error in the determination of the amount of gas entering the adsorption cell owing to the volume V'_d between the end of capillary 2 and valve V3 has already been mentioned (see page 64). This of course seriously limits the versatility of the apparatus since once the run has been commenced valve V3 must remain open. It cannot be closed since an unknown amount of gas will collect in V'_d. Thus only adsorbents such as sodium chloride which attain instantaneous equilibrium with the adsorbate may be studied. The fact that valve V3 must remain open for the duration of the run means that P_R cannot be increased at any stage. The latter becomes necessary when the adsorption pressure rises to such a level that the condition $P_R \geq 1000\ P_a$ (set on page 37) is no longer satisfied. Consequently the range of equilibrium pressures followed in any particular run was small and therefore several runs had to be carried out, each with an increased value for P_R, so that a wide range of P_a values could be obtained.

The error owing to V'_d could in principle be minimized by making it negligibly small. However this is impractical because metal valves require a means of relieving the stress,

owing to expansion of the glass tubing, on the glass - to - metal seals. Glass valves cannot be used in the present type of application because they have finite conductance when in the closed position. Thus for ultra-high vacuum work, where bakeable metal valves are required, the volume V'_d cannot be made negligibly small and hence the pipette method discussed on page 33 would seem to be the more suitable design principle.

Despite the shortcomings of the apparatus, very low pressures (1×10^{-8} torr) were obtained routinely. The evaporated films which were prepared must certainly have been cleaner than Hayakawa's[16] crystals and were probably somewhat less contaminated than Granville and Hall's[22,23] films.

The range of coverage investigated in this work was very much lower than that investigated in the above work. The heats of adsorption at very low values of θ were found to be independent of coverage which was not reported by Hayakawa. Granville and Hall[23] however, found that the heat of adsorption for krypton on caesium chloride was independant of coverage in the range $0{\cdot}1 < \theta < 0{\cdot}35$ but, they do not comment on this. The constant heat of adsorption found in this work for nitrogen is attributed to the presence of certain active sites which, in Hayakawa's samples, were not available owing to contamination of the surface. The initial heat of adsorption obtained by extrapolating the heat curves to zero-coverage were 3·9 and 4·2 k.cal mole^{-1} for nitrogen on films B and C respectively and 2·9 k.cal mole^{-1} for argon on film B. The values for nitrogen so obtained are perhaps more reliable than Hayakawa's value (2·67 k.cal mole^{-1}) since the extrapolation of a horizontal line can be carried out with greater confidence than the extra-

owing to expansion of the glass tubing, on the glass - to - metal seals. Glass valves cannot be used in the present type of application because they have finite conductance when in the closed position. Thus for ultra-high vacuum work, where bakeable metal valves are required, the volume V'_d cannot be made negligibly small and hence the pipette method discussed on page 33 would seem to be the more suitable design principle.

Despite the shortcomings of the apparatus, very low pressures (1×10^{-8} torr) were obtained routinely. The evaporated films which were prepared must certainly have been cleaner than Hayakawa's[16] crystals and were probably somewhat less contaminated than Granville and Hall's[22,23] films.

The range of coverage investigated in this work was very much lower than that investigated in the above work. The heats of adsorption at very low values of θ were found to be independent of coverage which was not reported by Hayakawa. Granville and Hall[23] however, found that the heat of adsorption for krypton on caesium chloride was independant of coverage in the range $0{\cdot}1 < \theta < 0{\cdot}35$ but, they do not comment on this. The constant heat of adsorption found in this work for nitrogen is attributed to the presence of certain active sites which, in Hayakawa's samples, were not available owing to contamination of the surface. The initial heat of adsorption obtained by extrapolating the heat curves to zero-coverage were 3·9 and 4·2 k.cal mole^{-1} for nitrogen on films B and C respectively and 2·9 k.cal mole^{-1} for argon on film B. The values for nitrogen so obtained are perhaps more reliable than Hayakawa's value (2·67 k.cal mole^{-1}) since the extrapolation of a horizontal line can be carried out with greater confidence than the extra-

polation of a curve. The close agreement of the heats for nitrogen on the two films B and C indicates good reproducibility. For argon however, only a limited set of results was obtained for film B. Ideally many more measurements for both adsorbates on both films should have been made.

The large discrepancy found between the experimental values of 3·9 and 4·1 k.cal mole^{-1} and Hayakawa's theoretical value of 2·40 k.cal mole^{-1} is attributed to:

(a) uncertainty in calculating the quadrupole interaction of the nitrogen molecules with the surface in Hayakawa's theoretical heat of adsorption.

(b) the possibility of the surface prepared in this work exposing different crystallographic features.

The influence of the crystallographic face on the heats of adsorption may be determined by investigating the adsorption by films which have been prepared with deliberately oriented faces. Corresponding theoretical values are required but there exists the difficulty of the accurate determination of the quadrupole interaction energy.

The power of entropy as a tool for determining the nature of the adsorbed film has been well illustrated. Theoretical entropies, corresponding to two extreme models - that of the mobile non-localized film and that of the immobile localized film - were calculated. Translational and rotational entropies as well as a configurational entropy, associated with the localized model, were taken into account. Vibrational entropies were not considered since Hayakawa found them to be

insignificant. The comparison of experimental and theoretical values indicate that adsorbed nitrogen and argon modecules are fairly well represented by the immobile localized model. This is not really surprising since the temperatures at which measurements were made were very low (70 to 90^0 K). Nevertheless the discrepancies between the calculated and theoretical values show that the true nature of the adsorbed films is somewhat more complicated than that described by the simple model. Presumably some rotation and vibration may be involved.

The preparation of evaporated films by the distillation of the solid from a silica side arm (page 88) could prove to be an efficient technique, and may well produce cleaner films than have been obtained in this work.

With a new apparatus, based on the pipette principle, it would be very worthwhile to investigate other adsorbate - alkali halide combinations. Measurements on these rigorously cleaned surfaces at very low coverages would be of great interest since the various postulates of this thesis could be investigated thoroughly.

A P P E N D I C E S

APPENDIX 1.

THERMAL TRANSPIRATION.

The phenomenon of thermal transpiration occurs when a pressure reading is obtained from a gauge that is at a different temperature from that of the sample.[3] The gas tends to pass from the cooler to the warmer region and a steady state is reached when the pressure difference between the two regions is sufficient to balance this thermal transpiration. In other words, thermal transpiration is the phenomenon whereby a pressure gradient results from a temperature gradient.

In the determination of an adsorption isotherm, thermal transpiration results in the measured equilibrium pressure being greater or less than the true value, according as to whether the temperature of the adsorbent is lower or higher than the temperature of the pressure measuring device.

Knudsen has shown that[41] when the mean free path of the gas molecules is very much greater than the diameter of the connecting tube that is subject to the temperature gradient the following relationship holds:

$$\frac{P_A}{P_r} = \left(\frac{T_A}{T_r}\right)^{\frac{1}{2}} \qquad \text{A.1.(1)}$$

As the pressure increases, so the mean free path decreases and equation A.1.(1) becomes invalid. Similarly if the diameter of the connecting tube is increased equation A.1.(1) again becomes invalid. The failure of equation A.1.(1) occurs when the mean free path is less than about 20 times the diameter of the tube. In practice, this restricts the

use of the equation to pressures below a few microns.

The mean free path of air at room temperature[41] is given by

$$\lambda = \frac{5}{10^3 P} \text{ cm} \qquad \text{A.1.(2).}$$

If the diameter of the tubing which is subject to the thermal transpiration effect is 1 cm., for equation A.1.(1). to hold

$$\lambda \geq 20 \text{ cm.}$$

Substituting $\lambda = 20$ cm in equation A.1.(2) yields

$$P = 2{\cdot}5 \times 10^{-4} \text{ torr.}$$

as the maximum pressure at which the equation holds.

The glass tubing used to construct adsorption apparatuses usually has an inside diameter of several millimetres to allow rapid diffusion of gas and hence short pump out times. Nevertheless the adsorption isotherm may extend into the high equilibrium pressure region beyond the scope of equation A.1.(1).

Liang[64] introduced the following equation for applying thermal transpiration corrections to the higher pressures.

$$R_T = \frac{P_A}{P_r} = \frac{\left[\alpha_{He}(\phi_g X)^2 + \beta_{He}(\phi_g X) + T^*\right]}{\left[\alpha_{He}(\phi_g X)^2 + \beta_{He}(\phi_g X) + 1\right]} \qquad \text{A.1.(3).}$$

Bennett and Tompkins[65] give the following equations for α_{He} and β_{He}

$$\alpha_{He} = 3{\cdot}70\ (1{\cdot}70 - 2{\cdot}6 \times 10^{-3}\ \Delta T)^{-2} \qquad \text{A.1.(4).}$$

$$\beta_{He} = 7{\cdot}88\ (1 - T^*) \quad \text{for } T^* \leqslant 1 \qquad \text{A.1.(5).}$$

Values of ϕ_g for a number of different gases are given. Bennett and Tompkins suggest that a more accurate correction can be obtained throughout the pressure range by introducing a factor f = 1·22 which must be inserted into equation A.(1).3. when the diameter of the tubing exceeds a value of 1 cm. For tubing of diameter less than 1 cm., f = 1. The modified form of Liang's equation which can be used for pressures up to 3 torr is

$$R_T = \frac{\left[\alpha_{He}(f\phi_g X)^2 + \beta_{He}(f\phi_g X) + T^*\right]}{\left[\alpha_{He}(f\phi_g X)^2 + \beta_{He}(f\phi_g X) + 1\right]}. \qquad \text{A.1.(6).}$$

The Takaishi-Sensui[66] equation is yet another modification of Liang's formula. This equation may be written in the form

$$\frac{\left(P_A/P_r\right) - 1}{\left(T_A/T_r\right)^{\frac{1}{2}} - 1} = (\bar{A}\bar{X}^2 + \bar{B}\bar{X} + \bar{C}\bar{X}^{\frac{1}{2}})^{-1} \qquad \text{A.1.(7).}$$

Values of the constants for different gases are listed and equations for their calculation are also given.

Equations A.1.(1), A.1.(3), A.1.(6) and A.1.(7) have been examined by other authors. For example references 22, 34, 36, 37, 67, 68.. It appears that the particular correction formula to be applied depends upon the nature of

the system under investigation.

The sensitivity of the results to the correction consequently depends strongly on the gas, coverage and pressure in question. In this work, for the adsorption of nitrogen on both Pyrex and evaporated films of sodium chloride, the Bennet and Tompkins formula (equation A.1.(6). with equations A.1.(4). and A.1.(5).) was used for pressures up to 5×10^{-5} torr and the simpler Knudsen formula (equation A.1.(1).) for lower pressures. Equation A.1.(1). was also used for the argon measurements.

The Bennett and Tompkins expressions for nitrogen reduced to the following

(a) at 77^0K :

$\alpha_{He} = 2{\cdot}8814.$

The diameter d of the tubing was 15 mm.

Thus $f = 1{\cdot}22$; $\phi_{N_2} = 3{\cdot}53$

$\therefore \beta_{He} = 3.8541.$

$$f\phi_g X = 64{\cdot}599 \times P \quad ; \quad (f\phi_g X)^2 = 4{\cdot}1730 \times 10^3 \times P^2.$$

A.1.(8).

$$\therefore \text{P corrected} = \text{P measured} \times \frac{(1{\cdot}2024\times10^4 \times P^2) + (2{\cdot}4897\times10^2 P) + 0{\cdot}5109}{(1{\cdot}2024\times10^2 \times P^2) + (2{\cdot}4897\times10^2 \times P) + 1}$$

(b) at 90^0K:

Similarly at 90^0K, the equation is A.1.(9).

$$\text{P corrected} = \text{P measured} \times \frac{(1.0992\times10^4 \times P^2) + (2.2333\times10^2 \times P) + 0{\cdot}5590}{(1{\cdot}0992\times10^4 \times P^2) + (2.2333\times10^2 \times P) + 1}$$

For krypton (surface area measurements).

$\phi_{Kr} = 3{\cdot}90$ A.1.(10).

$$\text{P corrected} = \text{P measured} \times \frac{(1.4677\times10^4 \times P^2) + (2{\cdot}7507\times10^2 \times P) + 0.5109}{(1{\cdot}4677\times10^4 \times P^2) + (2{\cdot}7507\times10^2 \times P) + 1}$$

APPENDIX 2.

DEVELOPMENT OF ERROR EXPRESSIONS.

According to Pantony[69], when measurements x, y, z.... are combined in a formula to give an overall figure Q where

$$Q = f(x, y, z \ldots)$$

the absolute error in Q is given by

$$\delta Q = \left[\left(\frac{\partial Q}{\partial x}\right)^2 \delta^2 x + \left(\frac{\partial Q}{\partial y}\right)^2 \delta^2 y \ldots .\right]^{\frac{1}{2}} \qquad \text{A.2.(1).}$$

This expression was applied to equations II.5. and II.12. in order to calculate the absolute error in $(n_a)_i$ for both the pipette and capillary methods. In the simplification of the resulting expressions the fractional errors in pressures and volumes were assumed to be constant and for the capillary method all time values were assumed to have the same absolute error. Using this treatment equations II.13 and II.14 were developed.

The following typical set of values for the parameters were chosen.

Pipette Method:

V_c = 500 cc	T_r = 298·2°K	E_v = 0·1
V_d = 50 cc	T_a = 77·4°K	E_p = 0·2
V_a = 500 cc		

Capillary Method:

V_d = 500 cc	T_r = 298·2°K	r = 0·02 cm.
V_a = 500 cc	T_a = 77·4°K	L = 32.2 cm.
E_p = 0.2	δ_r = 0.001 cm.	
E_v = 0.1	δ_L = 0.2 cm.	δ_t = 1 sec.

APPENDIX 3.

ADSORPTION APPARATUS FOR THE PRESSURE RANGE 10^{-4} TO 1 TORR.

The apparatus to which film C was transferred (pages 85 and 94/95) is shown in Fig. A.1. It was of the conventional volumetric type incorporating a gas burette, doser and McLeod gauge. Pressures of about 1 x 10^{-6} torr were attained by means of an Edwards "Speedivac" oil diffusion pump, model 203B which was backed by a two stage Edwards "Speedivac" rotary high vacuum pump.

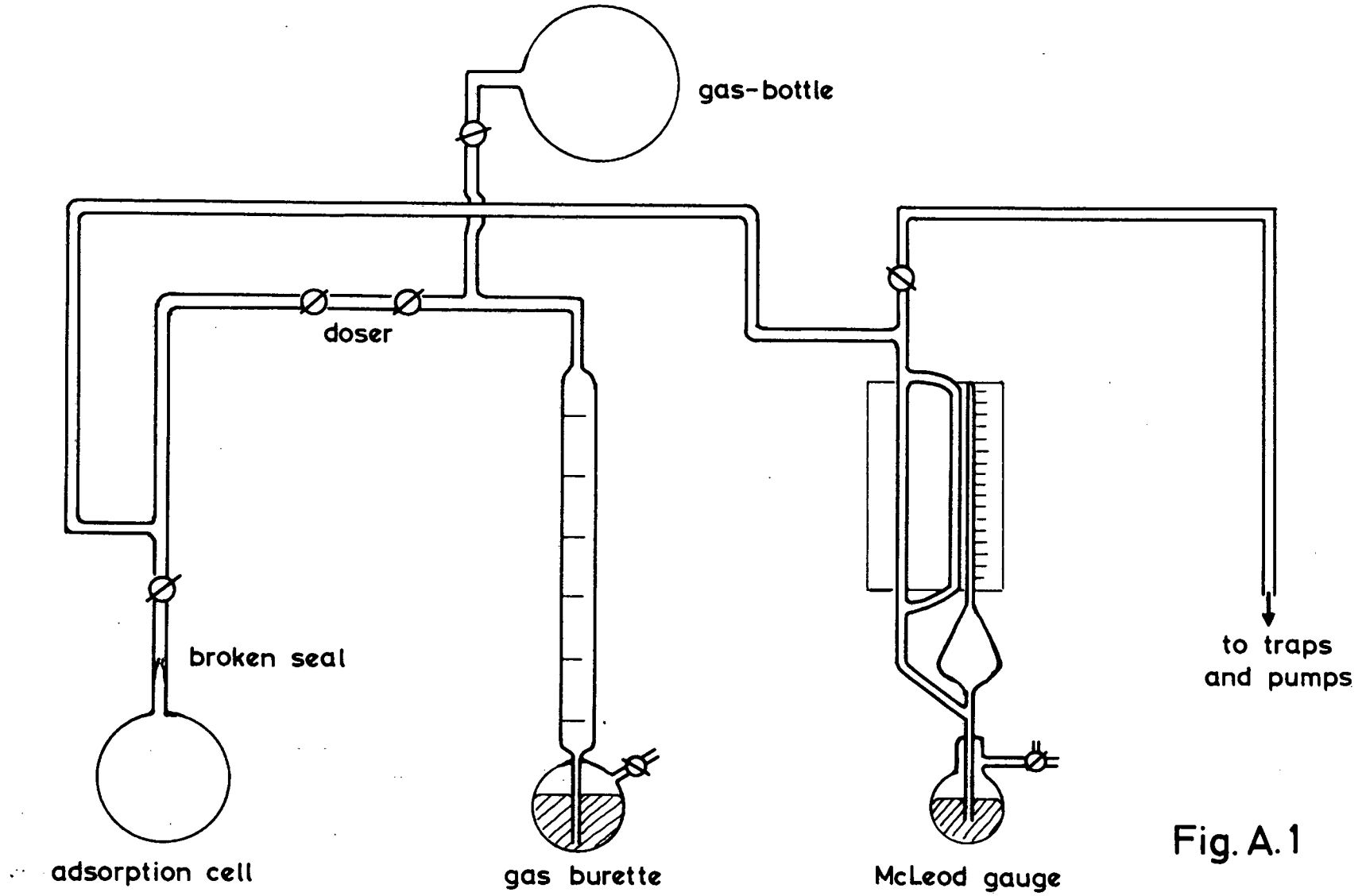
gas-bottle
doser
broken seal
adsorption cell
gas burette
McLeod gauge
to traps
and pumps

Fig. A.1

APPENDIX 4.

SURFACE AREA DETERMINATION[70]

If the number of adsorbate molecules required to form a unimolecular layer on a particular adsorbent can be determined, and if the area occupied by each adsorbed molecule is known, the surface area available to the adsorbate molecules may be calculated.

A value for the monolayer coverage can be obtained from the B.E.T. theory. From this theory, the adsorption of a gas on a solid may be represented by the equation

$$\frac{P}{N(P_0 - P)} = \frac{1}{N_m C} + \frac{(C - 1)P}{N_m C . P_0 .} \qquad \text{A.4.(1).}$$

If a set of experimental results plotted as $\frac{P}{N(P_0 - P)}$ against $\frac{P}{P_0}$ is found to be linear over the range of relative pressures 0·05 to 0·35 the value of N_m for the system under investigation may be determined from the slope and intercept.

In the measurement of low surface areas only a small fraction of the gas in the system is adsorbed. This quantity cannot be determined with great confidence since it represents the small difference between two large quantities namely the amount of gas originally admitted to the system and the amount left in the gas phase at equilibrium. However, it can be determined accurately if these two quantities are of unlike magnitude. This occurs at low relative pressures where virtually all the gas admitted is adsorbed and the amount not adsorbed is virtually negligible. As the relative pressure increases the amount adsorbed does not increase and so the amount unadsorbed tends toward the amount of gas admitted.

Thus the method is less sensitive at high relative pressures particularly with adsorbents having low surface areas. In other words the adsorption should be carried out at temperatures where the saturation vapour pressure of the adsorbate is so low that the range of validity of the B.E.T. equation is reduced from the order of 10 cm. of Hg to a millimetre or less.

Krypton is generally used as the adsorbate since at 77^0K its vapour pressure is 2 torr. Thus since the B.E.T. equation is applied in the range of relative pressure $0{\cdot}05 \leqslant P/P_0 \leqslant 0{\cdot}35$, the range of equilibrium pressures for krypton will be $0{\cdot}1 \leqslant P \leqslant 0{\cdot}6$ torr. This is a convenient range for measurements by means of McLeod gauges.

The surface area is the product of N_m and the area occupied by one molecule. Faeth[70] gives for krypton that

$$A_M = 19{\cdot}6 \text{ Å}^2 .$$

Thus, having determined the value of N_m for krypton from the B.E.T. plot, the surface area may be easily determined. To calculate the corresponding monolayer coverage for nitrogen the surface area (in square Å units) must be divided by the area occupied by one nitrogen molecule ($16{\cdot}2$ Å^2).

APPENDIX 5.

LIST OF SYMBOLS.

A_M	:	cross sectional area of one molecule.
A_r	:	cross sectional area of tube (equation II.6).
A*, B* ....G*	:	moments of inertia of a molecule and its individually rotating parts (equation I.21).
$\bar{A}$, $\bar{B}$ ...	:	temperature independent constants specific to the gas concerned.
B'	:	constant in repulsive energy equation I.5.
B	:	constant in Dubinin and Radushkevich isotherm equation, characteristic of the adsorbent-adsorbate combination.
C	:	constant in B.E.T. equation.
C'	:	constant in dispersion energy equation I.3. dependent on energy levels of atoms.
E	:	potential at points other than the centre of an atom (equation I.9).
E_c	:	potential at the centre of an atom due to a crystalline field (equation I.9).
E_D	:	dispersion energy.
E_i	:	induced attractive potential energy.
E_L	:	potential of an inhomogeneous electric field.
E_p	:	fractional error in measurement of pressure.
E_Q	:	quadrupole interaction energy.
E_R	:	repulsive energy.
E_s	:	equilibrium separation energy.
E_v	:	fractional error in measurement of volume.

LIST OF SYMBOLS cont ....

F_1, F_2	:	conductances of capillaries 1 and 2, (see Fig. II.3).
F_e	:	electric field intensity due to a crystal.
F_v	:	conductance of value.
F'	:	constant in Freundlich expression dependent on adsorbent and adsorbate as well as temperature.
G	:	free energy.
G_m	:	mass of gas in flow rate expression II.6.
J	:	characteristic energy of an adsorbed atom.
K	:	constant in Freundlich expression dependent on adsorbent and adsorbate as well as temperature.
K'	:	dimensionless constant used in mass flow rate expression II.6.
L	:	length of capillary.
M	:	molar mass.
N	:	number of molecules adsorbed.
N_m	:	number of molecules adsorbed in a complete monolayer.
$\mathcal{N}$	:	Avogadro number.

LIST OF SYMBOLS cont ....

T	:	absolute temperature
T_A	:	temperature of adsorbent.
T_a	:	temperature of adsorbent.
T_r	:	room temperature.
T^*	:	$(\frac{T_A}{T_r})^{\frac{1}{2}}$
U	:	adsorptive potential between a gas molecule and any point on a solid surface (Fig. I.1).
V	:	volume
V_B	:	volume of intermediate bulb B. (Fig.II.3).
V_R	:	volume of constant pressure reservoir R. (Fig. II.3).
V_a	:	volume of adsorption cell at temperature T_a.
V_c	:	dosing volume (Fig. II.1(a)).
V_d	:	volume of adsorption cell at room temperature T_r (Fig. II.1).
V'_d	:	dead volume between end of capillary 2 and valve V3 (Fig.II.3).
W	:	distance along axis of symmetry of quadrupole, (equation I.11).
W'	:	thermodynamic probability.
X	:	P_r x d (pressure as read on gauge at room temperature x internal diameter of tube).
$\bar{X}$	:	$2 P_r d / (T_A + T_r)$

LIST OF SYMBOLS cont ....

a	:	constant in repulsive energy equation I.3.
a', b'...	:	rotational degrees of freedom associated with the corresponding moments of inertia A*, B*.
a_0	:	standard state intermolecular separation of adsorbed molecules.
b	:	perimeter of cross section of tube. (equation II.6).
c	:	velocity of light.
d	:	internal diameter of tube over which thermal transpiration effect is experienced
f	:	pressure correction factor (equation A.1(6)).
h	:	Planck constant.
h'	:	height of gas trapped in closed limb of McLeod gauge.
k	:	Boltzmann constant.
ℓ	:	volume of McLeod gauge.
m	:	mass of a single molecule
m'	:	mass of an electron.
n	:	number of molecules
n_B	:	number of molecules in intermediate bulb B.
n_R	:	number of molecules in reservoir R.

LIST OF SYMBOLS cont ....

n_a	:	number of molecules adsorbed.
n_c	:	number of molecules in V_c
n_d	:	number of molecules in V_d
n'_d	:	number of molecules in V'_d
n_0	:	number of adsorption sites.
n_r	:	residual number of molecules after adsorption.
n*	:	total number of rotational degrees of freedom.
r	:	radius of capillary.
r'	:	interatomic distance
r*	:	radial polar co-ordinate
t	:	time
t'	:	time for which gas flows through capillary 2 into V'_d.
u	:	constant in equation I.12, I.13.
x	:	magnetic susceptibility.

α	:	empirical constant in thermal transpiration equation A.1.(3).
α'	:	polarizability
α^*	:	condensation coefficient
β	:	empirical constant in thermal transpiration equation A.1.(3).
δ	:	error
ε	:	adsorption potential
η	:	quadrupole moment
θ	:	fraction of the surface covered with adsorbed molecules.
θ^*	:	angular polar co-ordinate
λ	:	mean free path
ν	:	frequency of vibration (equation I.20)
ν_f	:	volumetric flow rate
ρ	:	atomic electron density.
σ	:	number of molecules adsorbed per cm^2
σ_M	:	number of molecules adsorbed per cm^2 in a complete monolayer
σ'	:	symmetry number [30] defined as the number of indistinguishable permutations produced by rotation of a molecule or its parts (equation I.21).

τ	:	residence time
τ_0	:	property of a solid surface related to the frequency of vibration of the atoms of the solid.
ϕ_g	:	pressure shifting factor (equation A.1.(3)) defined such that $\phi_{He} \equiv 1$.
χ	:	height of energy barrier between adjacent sites (Fig. I.1.).

REFERENCES

REFERENCES

1. D.M. Young and A.D. Crowell, "Physical Adsorption of Gases", Butterworths and Company, Ltd. 1962.
2. J.R. Dacey, Industrial and Engineering Chemistry 57, 27(6), (1965).
3. S. Ross and J. Olivier, "On Physical Adsorption", Interscience 1964.
4. W.A. Steele, Advances in Colloid and Interface Science, 1, (1) (1967).
5. S. Glasstone and D. Lewis, "Elements of Physical Chemistry", D. van Nostrand and Company, Inc., 1962.
6. A. Müller, Proc. Roy. Soc. A154, 624, (1936).
7. E. Mason and W. Rice, J.Chem. Phys. 22, 522, (1954).
8. S. Gregg and K. Sing, "Adsorption, Surface Area and Porosity", Academic Press 1967.
9. L.E. Drain, Trans. Far. Soc. 49, 650, (1953).
10. C. Greenhow and W. Smith, J. Chem. Phys. 19, 1298, (1951).
11. F. Lenel, Z.phys. Chem. B23, 379, (1933).
12. W. Orr, Trans. Far. Soc. 35, 1247, (1939).
13. W. Orr, Proc. Roy. Soc. A173, 349, (1939).
14. F.C. Tompkins and D.M. Young, Trans. Far. Soc. 47, 77, (1951).
15. D. Young, Trans. Far. Soc. 48, 548, (1952).
16. T. Hayakawa, Bull. chem. Soc. Japan. 30, 124, (1957).
17. T. Hayakawa, Bull. chem. Soc. Japan. 30, 243, (1957).
18. T. Hayakawa, Bull. chem. Soc. Japan. 30, 337, (1957).
19. T. Hayakawa, Bull. chem. Soc. Japan. 30, 343, (1957).
20. T. Hayakawa, Bull. chem. Soc. Japan. 30, 236, (1957).
21. T. Hayakawa, Bull. chem. Soc. Japan. 30, 332, (1957).
22. A. Granville and P.G. Hall, J. Phys. Chem. 70, 937, (1966).
23. A. Granville and P.G. Hall, Trans. Far. Soc. 63, 701, 1967.
24. E. Moelwyn-Hughes, "Physical Chemistry", 2nd Edition, Pergamon Press, Ltd., London. 1965.

25. L. Schulz, J.Chem. Phys. 17, 1153, (1949).

26. G.P. Dube. Proc. Cambr. Phil. Soc. 34, 587, (1938).

27. S. Brunauer, L. Deming, W. Deming and E. Teller. J.Amer.Chem. Soc. 62, 1723, (1940).

28. S.J. Gregg, "The Surface Chemistry of Solids", 2nd Edition, Chapman and Hall Ltd., 1961.

29. C. Kemball, Proc. Roy. Soc. A187, 73, 1946.

30. J.O. Halford, J. Chem. Phys. 2, 694, (1934).

31. T. Hill, J. Chem. Phys. 16, 181, (1948).

32. J.M. Drain and J.O. Morrison, Trans. Far. Soc. 48, 316 (1952).

33. S. Glasstone, "Textbook of Physical Chemistry", MacMillan and Co. Ltd., p861, (1960).

34. J.P. Hobson, Can.J.Phys. 37, 1105, (1959).

35. J.P. Hobson, J. Chem. Phys. 34, 1850, (1961).

36. J.P. Hobson and R.A. Armstrong, J. Phys. Chem., 67, 2000, (1963).

37. F. Ricca, R. Medana and A. Bellardo, J. Phys. Chem. 52, 276, (1967).

38. J. Ross and M. Roberts, Journal of Catalysis, 4, 620, (1965).

39. S. Wagener, Brit. J. Appl. Phys. 1, 225, (1950).

40. S. Wagener, Instit. of Electrical Engineers (London) 99(iii), 135, (1952).

41. A. Turnbull, R. Barton, J. Riviere, "An Introduction to Vacuum Technique", George Newnes, 1962.

42. S. Dushman, "Scientific Foundations of Vacuum Technique", John Wiley and Sons, 1962.

43. D. Hayward, D. King and F. Tompkins, Proc. Roy Soc. Lond. A297, 305, (1967).

44. G. Ehrlich, Advances in Catalysis, 14, 394, (1963).

45. M.A. Biondi, Rev. Sci. Instr. 30, 831, (1959).

46. R. Decker, J. Appl. Phys. 25, 1441, (1954).

47. B. Lambert and C. Phillips. Phil. Trans. Roy. Soc. Lond. A242, 427, (1950).

48. P.A. Redhead, E. Kornelsen, J. Hobson. Can. J. Phys. 40, 1814, (1962).

49. R.W. Roberts and T.A. Vanderslice "Ultrahigh Vacuum and its Applications" Prentice-Hall, Inc., 1963.

50. D. Haneman, J. Phys. Chem. Solids, 11, 205, (1959).

51. G. Gobeli and F. Allen, J. Phys. Chem. Solids 14, 23, (1960).

52. T.A. Vanderslice and N.R. Whetten, J. Chem. Phys. 37, 535, (1962).

53. L. Holland, "Vacuum Deposition of Thin Films". John Wiley and Sons Inc., 1960.

54. C.F. Powell, J.H. Oxley and J.M. Blocher, "Vapor Deposition" John Wiley and Sons. Inc., 1966.

55. J.C. Anderson "The Use of Thin Films in Physical Investigations" Academic Press, 1966.

56. P.G. Hall and F.C. Tompkins. J. Phys. Chem. 66, 2260, (1962).

57. L. Holland, Le Vide, 97, 83, (1962).

58. T.W. Hickmott and G. Ehrlich, J. Phys. Chem. Solids 5, 47, 1958.

59. D. Brennan and M. Graham. Phil. Trans. Roy. Soc. Lond. 258A, 325, (1965).

60. J. Anderson and B. Baker, J. Phys. Chem. 66, 482, (1962).

61. A. Granville, Private correspondence, June-July 1969.

62. A.W. Adamson, "The Physical Chemistry of Surfaces," Interscience, 1967.

63. J.H. de Boer, "The Dynamical Character of Adsorption", Clarendon Press, 1953, p 112.

64. S.C. Liang, J. Phys. Chem. 57, 910, (1953).

65. M.J. Bennett and F.C. Tompkins Trans. Far. Soc. 53, 185, (1957).

66. T. Takaishi and Y. Sensui, Trans. Far. Soc. 59, 2503, (1963).

67. H. Podgurski and F. Davis, J. Phys. Chem. 65, 1343, (1961).

68. B. Baker and P. Fox, Trans. Far. Soc. 61, 2001, (1965).

69. D.A. Pantony, "Statistics, Theory of Error and Design of Experiment", Royal Institute of Chemistry Lecture Series 1961, Number 2.

70. P.A. Faeth, "Adsorption and Vacuum Technique" Instit. Sci. and Tech. Univ. of Michigan 1962.